2007

DETOXIFICATION OF SELECTED CHLORO-ORGANICS BY OXIDATION TECHNIQUE USING CHELATE MODIFIED FENTON REACTION

YongChao Li
University of Kentucky, yli9@uky.edu

ABSTRACT OF DISSERTATION

YongChao Li

The Graduate School

University of Kentucky

2007

DETOXIFICATION OF SELECTED CHLORO-ORGANICS BY OXIDATION TECHNIQUE USING CHELATE MODIFIED FENTON REACTION

ABSTRACT OF DISSERTATION

A dissertation submitted in partial fulfillment of the
Requirements for the degree of Doctor of Philosophy in the
College of Engineering
At the University of Kentucky

By
YongChao Li

Lexington, Kentucky

Director: Dr. Dibakar Bhattacharyya, Alumni Professor of Chemical Engineering

Lexington, Kentucky

2007

ABSTRACT OF DISSERTATION

DETOXIFICATION OF SELECTED CHLORO-ORGANICS BY OXIDATION TECHNIQUE USING CHELATE MODIFIED FENTON REACTION

The use of hydroxyl radical based reaction (Fenton reaction) for the destruction of organic pollutants has been widely reported in the literature. However, the low pH requirement and rapid hydrogen peroxide consumption rate make the application of conventional Fenton reaction difficult for in-situ treatment. In this study, we conducted a modified Fenton reaction by introducing a chelating agent into the reaction system that could prevent $Fe(OH)_3$ (s) precipitation even at a neutral pH condition and reduce the H_2O_2 consumption rate by controlling the Fe^{2+} concentration. A chelating agent (mono-chelate or poly-chelate) combines with Fe^{2+} or Fe^{3+} to form stable metal-chelate complexes in solution. This decreases the concentration of Fe^{2+} in the solution so that reactions can be carried for longer contact times. Experimental results (citrate was the chelating agent) for 2,4,6-trichlorophenol (TCP) showed that TCP degradations were greater than 95% after 2.5 h and 24 h reaction times at fixed pH 5 and 6, respectively. For the same reaction time, the normalized chloride formations were 85% at pH 5 and 88% at pH 6. Several other chlorinated organic compounds were also chosen as the model compounds for detoxification studies because of their chemical structures: trichloroethylene (unsaturated hydrocarbon), carbon tetrachloride (highly oxidized compound), 2,2′-dichlorobiphenyl, and biphenyl (a dual-aromatic ring structure). Poly-chelating agents (such as polyacrylic acid-PAA) provide multiple Fe^{2+}/Fe^{3+} binding sites in the modified Fenton reaction for the oxidation of contaminants (2,2′-dichlorobiphenyl, and biphenyl) at a neutral pH environment. Numerical simulation based on the kinetic model developed from the well known Fenton reaction and iron-chelate chemistry fits experiment data well for both standard and chelate modified Fenton reactions. In this dissertation, it was proven that both monomeric (citrate) and polymeric (PAA) chelate modified Fenton reactions were effective for dechlorination of carbon tetrachloride from aqueous phase by the superoxide radical anion.

On the other hand, PAA (a poly-chelating agent) can also be used for solid surface modification by polymerization of acrylic acid (monomer). The successful degradations of biphenyl and trichloroethylene by the PAA functionalized silica particles/membrane

demonstrate the versatile applications of the chelate modified Fenton reaction.

KEYWORDS: chelating agent, hydroxyl radical, superoxide radical anion, numerical simulation, and kinetic model.

YongChao Li

November 16, 2007

DETOXIFICATION OF SELECTED CHLORO-ORGANICS BY OXIDATION TECHNIQUE USING CHELATE MODIFIED FENTON REACTION

By

YongChao Li

Dr. Dibakar Bhattacharyya
Director of Dissertation

Dr. Barbara Knutson
Director of Graduate Studies

November 16, 2007
Date

RULES FOR THE USE OF DISSERTATIONS

Unpublished dissertations submitted for the Doctor's degree and deposited in the University of Kentucky Library are as a rule open for inspection, but are to be used only with due regard to the rights of the authors. Bibliographical references may be noted, but quotations or summaries of parts may be published only with the permission of the author, and with the usual scholarly acknowledgements.

Extensive copying or publication of the dissertation in whole or in part also requires the consent of the Dean of the Graduate School of the University of Kentucky.

A library that borrows this dissertation for use by its patrons is expected to secure the signature of each user.

Name	Date

DISSERTATION

YongChao Li

The Graduate School

University of Kentucky

2007

DETOXIFICATION OF SELECTED CHLORO-ORGANICS BY OXIDATION TECHNIQUE USING CHELATE MODIFIED FENTON REACTION

DISSERTATION

A dissertation submitted in partial fulfillment of the
Requirements for the degree of Doctor of Philosophy in the
College of Engineering
At the University of Kentucky

By
YongChao Li

Lexington, Kentucky

Directors: Dr. Dibakar Bhattacharyya, Alumni Professor of Chemical Engineering

Lexington, Kentucky

2007

ACKNOWLEDGEMENT

At first, I would like to thank my advisor, Dr. Dibakar Bhattacharyya, for his guidance, encouragement, and support during my Ph.D study. His extensive knowledge and creative ideas inspire and stimulate my desire to think more. I also want to express my gratitude to my Ph.D committee members: Dr. Leonidas G. Bachas, Dr. Barbara Knutson, Dr. Yi Tin Wang, and Dr. Dong-Sheng Yang. I would like to acknowledge the National Institute of Environmental Health Sciences (NIEHS) and the Kentucky Research Consortium for Energy and Environment (KRCEE) for providing funding for my study at the University of Kentucky. I would like to thank John May from the UK Environmental Research and Training Laboratory (ERTL) for his help to set up various analytical procedures. In addition, I want to say thank you to all my lab mates who have cooperated and helped me during my study. Finally, I appreciate and thank the support from my family: my brother-YongLi, my parents, my two angels- LeYi and LeCheng, and my wife-Zeng Feng. I could not have finished my study without their endless support, and this thesis is dedicated to them.

Table of Contents

List of Tables

List of Figures

Chapter 1. Introduction and Objectives

Many organic chemicals are manufactured in a large quantity as needed by industry. Although usage of these chemicals benefited and promoted technology advancement, misuse and improper handling of some chlorinated organic chemicals presented hazardous effects for the environment and human beings. Trichloroethylene (TCE) was widely used as a solvent and metal degreaser in industry, and 2,4,6-trichlorophenol (TCP) was once widely used as a preserve agent. Polychlorinated biphenyls (PCBs) were manufactured to be used as insulating fluid or stabilizing additives for industrial applications. These chlorinated organic compounds are highly toxic chemicals and very difficult for biodegradation. A lot of research indicated that these chlorinated organic compounds could be bioaccumulated and presented health problems for humans and animals. For example, TCE and TCP were identified to have a carcinogenicity effect during animal experiments (Maltoni, et al., 1988; NTP, 1988 and 1990; IARC 1987, and 1999). Unfortunately, many chlorinated organic compounds are present in the environment as pollutants due to the industrial manufacture and usage. According to the EPA-SUPERFUND program, there were 11 mega sediment sites whose cost for remediation exceeded 50 million dollars in 2005. Due to the threat of water source pollution, EPA and government agents implemented many strict regulations about industrial wastewater discharge and set up research funds for contaminated water remediation. Thus, effective and inexpensive remediation techniques are necessary to protect our community and our water resources.

Usually chemical reduction and oxidation technologies are two common and effective in-situ methods used for groundwater remediation. The principle of a reduction or oxidation technique is to weaken the electron stability of pollutants for further decomposition through exchanging electrons with the reducing agent or the oxidizing agent. The main difference between chemical reduction and oxidation is the different final products: non-chlorinated hydrocarbon will be the final product for the reduction technique (e.g., biphenyl for PCBs), while aromatic ring opening products, organic acids, even CO_2 are the final products for the oxidation technique. A brief description of both techniques is provided below.

1.1 Water Remediation by Reduction Technique

Many researchers found that the chemical reduction process was an effective way for detoxification of chlorinated organic compounds in water. The following section will discuss two successful reduction methods for water pollutants remediation: pollutant reduction by using vitamin B_{12} and zerovalent metals.

1.1.1 Pollutant Reduction by Using Vitamin B_{12}

Cobalt (Co (III)) of vitamin B_{12} is a transition metal and can be reduced to Co(I) by a bulk reductant according to the following reactions:

$$M^{n+} \rightarrow M^{(n+2)+} + 2e^- \quad (1.1)$$

$$Co(III) + 2e^- \rightarrow Co(I) \quad (1.2)$$

where M represents the bulk reducing agent.

According to Schrauzer and Deutsh (1968), Co(I) is a strong nucleophile and can provide electrons to degrade chloro-organics as the following reaction:

$$R\text{-}Cl_n + H^+ + 2e^- \rightarrow RH + nCl^- \quad (1.3)$$

Gantzer and Wackett (1991) did experiments for PCE dechlorination by vitamin B_{12} with the bulk reducing agent titanium (III) citrate. Their study confirmed that ethane was the final product of PCE dechlorination as suggested by reaction 1.3. Nonnenberg et al. (2002) also observed that hydrogenolysis reaction would lead to ethane formation as the final product. Ahuja et al. (2004) explored a new method to reduce Co(III) to Co(I): immobilization of vitamin B_{12} in an electropolymerized polypyrrole film, and found that the dechlorination rate of TCE and cis-DCE by using this system was much higher than that of using excessive bulk reductant and vitamin B_{12}. On the other hand, Pratt and Van der Donk (2006) proposed another reaction mechanism for PCE and TCE dechlorination by vitamin B_{12}. They suggested that a nucleophilic attack pathway (organocobalamin formation) was more likely for degradation of PCE and TCE rather than an electron transfer pathway.

1.1.2 Pollutant Reduction by Zerovalent Metals

Zerovalent metals (for example: Fe, Zn, Fe/Pd, and Fe/Ni) can be another effective reduction technique for pollutant dechlorination. Zhang et al. (1998) established the synthesis method of bimetallic nanoparticles for some chlorinated solvents (PCE, TCE, cis-DCE, and vinyl chloride). The successful dechlorination of these contaminants

demonstrated that the bimetallic nanoparticles enhanced the reaction rates by increasing the surface area and surface reactivity. Xu and Bhattacharyya (2005, 2007) established a new way to produce nanoiron particles inside the membrane matrix. They conducted the dechlorination experiments for polychlorinated biphenyls (PCBs) and TCE by using nano-Fe inside a membrane matrix. They found that the reaction rates for PCBs dechlorination were closely related to the amount of the second metal coating (Ni or Pd). The dechlorination rate of the reaction increased if the second metal coating (Ni or Pd) increased up to the optimum level. However, the dechlorination reaction rate declined sharply, if the outer second metal coating isolated the nano-Fe because the dechlorination reaction needed the electrons provided by the corrosion reaction of iron nanoparticles. The degradation of chlorinated organic compounds can be expressed as the following reactions (Liu et al., 2005):

$$n\,Fe^{0} \rightarrow n\,Fe^{2+} + 2n\,e^{-} \quad (1.4)$$

$$R\text{-}Cl_n + n\,e^{-} + n\,H^{+} \rightarrow R\text{-}H + n\,Cl^{-} \quad (1.5)$$

$$2H^{+} + 2\,e^{-} \rightarrow H_2\,(gas) \quad (1.6)$$

Following the reduction mechanism of the nano-iron particle, the final products will be unsaturated or saturated hydrocarbons and chloride ions for a complete dechlorination of the chlorinated organic compounds. Hydrogen gas will also be observed as one of the final products from the reaction.

1.2 Water Remediation by Oxidation Reaction

Oxidation is another highly successful process for in-situ water remediation. There are many effective ways to generate oxidizing agents for pollutant detoxification, for example: Ozone (O_3), permanganate (MnO_4^-), Fenton reaction (Fe^{2+} + H_2O_2), Fenton reaction + UV light, etc. The following section will give some brief description of the ozone and permanganate. Fenton reaction and photo-Fenton reaction will be discussed in Chapter 2.

1.2.1 Ozone

Ozone (O_3) has the power to oxidize many organic pollutants and has been used in the area of wastewater remediation. It has three oxygen atoms and is much more reactive than diatomic oxygen (O_2). The following reactions are considered as the major reactions during the aqueous phase pollutant oxidation by O_3:

$$OH^- + O_3 \rightarrow HO_2\bullet + O_2\bullet^- \quad (1.7)$$

$$HO_2\bullet \leftrightarrow H^+ + O_2\bullet^- \quad (1.8)$$

$$O_2\bullet^- + O_3 \rightarrow O_2 + O_3\bullet^- \quad (1.9)$$

$$H^+ + O_3\bullet^- \rightarrow HO_3\bullet \quad (1.10)$$

$$HO_3\bullet \rightarrow O_2 + OH\bullet \quad (1.11)$$

$$OH\bullet + O_3 \rightarrow O_2 + HO_2\bullet \quad (1.12)$$

OH● generated in the system will attack a pollutant to start the oxidation reaction, and organic acids or even CO_2 will be the final products. The pollutant oxidation reaction can be summarized as:

$$R–Cl_n + OH● \rightarrow \text{intermediates} \quad (1.13)$$

$$\text{Intermediates} + OH● \rightarrow \text{organic acids}/CO_2 + n\ Cl^- \quad (1.14)$$

Beltran et al. (1997) compared the experimental results of wastewater oxidation by three reaction systems: ozone, ozone + H_2O_2, and ozone + UV light. They found that the combination of ozone and UV light was the best oxidation technique among the three methods. Gong et al. (2007) also concluded that the reaction system of UV + O_3 was the more effective for contaminant degradation from the study of oxidation of biotreated municipal wastewater. They observed that the order of reactivity of contaminants depended on polarity: hydrophobic compounds > hydrophilic compounds. Cassidy et al. (2002) successfully used free hydroxyl radical produced by ozone to oxidize two PCBs (2,2′-dichlorobiphenyl and 2,3,4,2′,3′,4′-hexachlorobiphenyl) adsorbed on two type sediments-pure kaolinite (without native organic matter) and river sediments (2% native organic matter). They found that PCBs adsorbed on river sediments required a longer time to achieve the same degradation effect as those adsorbed on pure kaolinite.

1.2.2 Permanganate Anion

Permanganate anion (MnO_4^-) is a highly effective oxidizing agent, and it has been used widely as an oxidizer and disinfectant. Potassium permanganate and sodium permanganate are the common salt forms of permanganate. Although there are several

oxidation states of manganese (Mn), the stable form of manganese in water is manganese dioxide (MnO_2). Thus, permanganate anion has the ability to oxidize many organic pollutants. Permanganate has been used in in-situ water remediation and has been studied extensively (Vella and Veronda, 1992; Truax, 1993; Huang et al., 1999; Siegrist et al., 1999). Yan and Schwartz (1999) reported the first order reaction rates of permanganate with TCE and PCE. Permanganate can be used for oxidation of dichloroethylene isomers (1,2-*cis*-DCE and 1,2-*trans*-DCE), vinyl chloride, phenols, naphthalene, and phenanthrene (Watts and Teel, 2005). Hang et al. (2002) conducted a kinetic and mechanism study for the oxidation of PCE by permanganate. They suggested that there were different reaction pathways at different pH environments following the formation of a common initial intermediate-cyclic hypopermanganate ester. At acidic pH conditions, the PCE oxidation proceeds to CO_2 and chloride ions after phosgene formation. At a neutral or alkaline pH environment, oxalic acid is the major intermediate species and further oxidation leads to complete mineralization.

1.3 Research Objectives

Although there are many oxidation techniques for pollutant detoxification, Fenton reaction stands out for water remediation because it is fast, low-cost and easy to operate at room temperature (Basu and Wei, 1998a; Basu and Wei, 1998b; Kwan and Voelker, 2003; Teel et al., 2001). However, $Fe(OH)_3$ precipitation at a neutral pH environment and fast reactants consumption prevent Fenton reaction's application for groundwater remediation. Chelating agents are well recognized for their ability to increase the

solubility of metal ions. Citrate as a mono-chelate and PAA as a poly-chelate are nontoxic and stable organic compounds in the environment. They can complex iron ion to form a stable metal-chelate and prevent $Fe(OH)_3$ (s) precipitation at a neutral pH environment. Our research project combines these chelating agents and Fenton reaction technology to achieve better detoxification results at a neutral pH environment.

The overall objective of this dissertation is to effectively detoxify chlorinated organic compounds by a chelate modified Fenton reaction and investigate the reaction kinetics of the chelate modified Fenton reaction based on the proposed reaction mechanism. The specific objectives are:

(i) To oxidize chlorinated organic compounds by using a chelate (citrate as a mono-chelate or PAA as a poly-chelate) modified Fenton reaction at a neutral pH environment.

(ii) To study and establish the reaction mechanism of the chelate modified Fenton reaction for pollutant detoxification.

(iii) To quantify iron ion species according to iron-chelate chemistry by using numerical simulation.

(iv) To derive a comprehensive kinetic model incorporating the well-known Fenton reactions and iron ion concentration obtained from numerical simulation.

(v) To explore the mechanism of pollutant dechlorination by the superoxide radical generated from the chelate modified Fenton reaction.

(vi) To identify the intermediates and some final products to verify the reaction pathway of pollutant oxidation by the mono-chelate (citrate) and poly-chelate (PAA) modified Fenton reaction.

(vii) To explore solid surface (membrane and silica particles) modification by using a poly-chelating agent (PAA) and use them as the immobilized chelating agents during the pollutant oxidation.

Chapter 2. Literature Review: The Standard and Modified Fenton Reaction

This chapter will review the background information about the Fenton reaction which is an effective oxidation technique, and discuss the application of the standard and modified Fenton reaction for water remediation. The use of a chelating agent by medical researchers is also explored. Finally, the chelate modified Fenton reaction will be discussed, and a reaction mechanism will be proposed.

2.1 Standard Fenton Reaction

Fenton reaction, as one of the advanced techniques, has been widely studied by many researchers. It generates ferric ion (Fe^{3+}), hydroxyl ion (OH^-) and free hydroxyl radical (OH●**),** which is a very powerful oxidizing agent, from ferrous ion (Fe^{2+}) and hydrogen peroxide (H_2O_2) at an acidic pH environment, as shown in reaction 2.1 (Laat and Gallard, 1999; Kiwi et al., 2000):

$$Fe^{2+} + H_2O_2 \rightarrow Fe^{3+} + OH\bullet + OH^- \qquad (2.1)$$

OH● is a highly reactive radical species and has non-specific oxidizing power to many organic and inorganic compounds at room temperature (Kiwi et al., 2000; Perez et al., 2002a; Zepp et al., 1992). It has a very short lifetime and can be consumed very fast in many reactions. Some major reactions in the Fenton reaction system are discussed below.

OH● provides a rapid reaction with various organic pollutants through hydrogen abstraction or addition (Walling, 1975; Luo et al., 1997; Mckinzi and Dichristina, 1999).

Once Fe^{3+} is formed, it can react with H_2O_2 to regenerate Fe^{2+} at an acidic condition (Sun and Pignatello, 1993a), as shown in reaction 2.2:

$$Fe^{3+} + H_2O_2 \rightarrow Fe^{2+} + HO_2\bullet + H^+ \quad (2.2)$$

This significant characteristic of the standard Fenton reaction provides continuous OH● formation at a low pH environment whenever H_2O_2 is available (Tarr, 2003). However, Fe^{3+} will precipitate as $Fe(OH)_3$ (s) at a neutral pH environment (Huston and Pignatello, 1999). Hence, an acidic pH environment is required by the standard Fenton reaction (Perez et al., 2002b).

OH● generated from reaction 2.1 can react with Fe^{2+} and H_2O_2 also, as shown in reaction 2.3 and 2.4.

$$OH\bullet + Fe^{2+} \rightarrow Fe^{3+} + OH^- \quad (2.3)$$

$$OH\bullet + H_2O_2 \rightarrow H_2O + HO_2\bullet \quad (2.4)$$

The reaction rate constants for reaction 2.3 and 2.4 are $3.2 \times 10^8\ M^{-1}s^{-1}$ and $3.3 \times 10^7\ M^{-1}s^{-1}$, respectively (Pignatello, 2006; De Laat and Gallard, 1999; Lin and Gurol, 1998). They are the main sinks of OH●, if there is no other organic chemical or species present in the reaction system. Perhydroxyl radical (HO_2•) generated in reaction 2.4 will ionize to form a superoxide radical anion ($O_2\bullet^-$) according to the following reaction 2.5 (Watts and Teel, 2005 and 2006; Smith et al., 2006):

$$HO_2\bullet \leftrightarrow H^+ + O_2\bullet^- \quad (2.5)$$

$O_2\bullet^-$ is very important for the Fenton reaction system at a higher pH environment since it has the ability to degrade contaminants through reduction. It will be discussed in more detail in Chapter 6.

The standard Fenton reaction system without other energy sources is called thermal Fenton reaction (Pignatello, et al., 2006). Many scientists explored the potential of combination of the Fenton reaction with UV irradiation (photo Fenton reaction) to increase the overall reaction rate and efficiency for pollutant degradation (Benitez et al., 1999; Andreozzi et al., 2000; Sun and Pignatello, 1993c). With UV light, the following reactions can take place:

$$H_2O_2 + h\nu \rightarrow 2\ OH\bullet \quad (2.6)$$

$$Fe(OH)^{2+} + h\nu \rightarrow Fe^{2+} + OH\bullet \quad (2.7)$$

Reaction 2.6 and 2.7 provide continuous Fe^{2+} formation and high OH● generation for the reaction system with UV irradiation. However, the photo Fenton reaction is not a common method used for groundwater remediation, and this dissertation will focus on the standard and modified Fenton reactions only.

Although OH● is a powerful oxidizing agent and has the ability to detoxify many organic pollutants, the acidic pH requirement and fast reaction rate of the standard Fenton reaction are the obstacles for groundwater remediation application. Thus, many scientists and researchers have explored different modification possibilities to apply the advantages of Fenton reaction at a neutral pH environment.

2.2 Modified Fenton Reaction for Pollutant Degradation in Aqueous Phase

Pignatello (1992) conducted experiments of 2,4-dichlorophenoxyacetic acid and 2,4,5-trichlorophenoxyacetic acid destruction by dark and photo-Fenton reaction using Fe^{3+} + H_2O_2, and found that herbicide destruction rates were accelerated significantly with irradiation above 300 nm. Sun and Pignatello (1993b) identified 2,4-dichlorophenol as the major intermediate for the 2,4-dichlorophenoxyacetic acid dechlorination in a Fe^{3+} + H_2O_2 system with or without UV irradiation. Kwan and Voelker (2002) proposed the chain reaction mechanism for the Fenton reaction generated from dissolved iron and ferrihydrite. Sun and Pignatello (1992) evaluated many chelating agents to solubilize Fe^{3+} at pH 6 and mineralize 2,4-dichlorophenoxyacetic acid in the Fe^{3+} + H_2O_2 system. Their study indicated that several ligands (such as dipicolinic acid, oxalic acid, and gallic acid) could complex with Fe^{3+} to form soluble chelates which had the ability to oxidize pesticide waste, and also proved that Fe^{3+}-citrate had a low capability to decompose H_2O_2 without UV light. Later, they (Sun and Pignatello, 1993c) chose picolinic acid, gallic acid and rhodizonic acid as chelating agents to mineralize pollutants in the Fe^{3+}-chelate + H_2O_2 system (at pH 6) with or without UV irradiation. The experimental results showed that reactions with UV irradiation (within 300-400 nm) were faster than the reactions without UV light. The UV enhancement for pollutants mineralization may be explained by the acceleration of Fe^{2+} formation from Fe^{3+}-chelate under UV irradiation. They also found that reactions with oxalic acid or citric acid as a chelating agent have better results for 2,4-dichlorophenoxyacetic acid mineralization with UV irradiation.

2.3 Mechanism of the Standard and Modified Fenton Reaction Systems for Pollutant Oxidation

Although several radical species (free hydroxyl radical, perhydroxyl radical, and superoxide radical) are generated in the Fenton reaction system as discussed in the previous section, the main principle of pollutant detoxification by the standard and modified Fenton reactions is mainly dependent on OH● (Kiwi et al., 2000; Perez et al., 2002a; Zepp et al., 1992). As mentioned in the previous section, OH● generated from ferrous salt and H_2O_2 is a non-specific oxidizing agent, and it has been widely used for water pollutant detoxification. The mechanism of pollutant oxidation by OH● has been studied extensively in an effort to understand and facilitate the application of the standard and modified Fenton reaction in pollutant degradation.

According to Pignatello et al. (2006), OH● will react with an organic pollutant through hydrogen abstraction (for C–H, N–H, or O–H) or addition, and can be summarized as the following:

$$OH\bullet + R\text{-}H \rightarrow R\bullet + H_2O \qquad (2.8)$$

$$OH\bullet + C{=}C \rightarrow HO\text{–}C\text{–}C\bullet \qquad (2.9)$$

OH● + 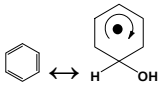 (2.10)

where reaction 2.10 is a reversible reaction and reactions 2.8 and 2.9 are irreversible reactions.

The carbon-centered radicals formed in reactions 2.8-2.10 undergo further reaction to form intermediates (Walling, 1975; Luo et al., 1997). These intermediates can be completely oxidized by OH● to form carboxylic acids or even CO_2. Boye et al. (2003a, 2003b) also conducted a study for dechlorination of 2,4,5-trichlorophenoxyacetic acid by the photoelecto-Fenton reactions in the pH range of 2 to 6. They found that 2,4,5-trichlorophenol, 4,6-dichlororesorcinol and 2,5-dihydroxy-p-benzoquinone were intermediates during the oxidation reaction. Eventually, carboxylic acids and carbon dioxide were identified as the final products for degradation of 2,4,5-trichlorophenoxyacetic acid. The proposed reaction pathway by Boye et al. (2003a) is shown in Figure 2.1. Pignatello and Chapa (1994) studied several PCBs (Aroclor 1242) oxidation by Fe^{3+} + H_2O_2 + UV light. They observed 88% of PCB degradation and found that those highly chlorinated PCBs had very low reactivity with free hydroxyl radicals. They proposed a reaction pathway for PCBs oxidation by OH●, as shown in Figure 2.2.

On the other hand, Smith et al. (2004) found that $O_2\bullet^-$ was a reactive reductant and had the ability for dechlorination of CCl_4 in the Fenton reaction in a high H_2O_2/Fe ratio (200-2000). Phosgene was identified as one of the intermediates in their experiments, and carbonate and CO_2 were confirmed as the final products. The enhanced reactivity of $O_2\bullet^-$ for degradation of CCl_4 was also observed if the concentration of hydroperoxide anion (HO_2^-) was higher than 0.1 M. Smith et al. (2006) explored the degradation of CCl_4 and chloroform ($CHCl_3$) in dense non-aqueous phase liquids (DNAPLs) by $O_2\bullet^-$

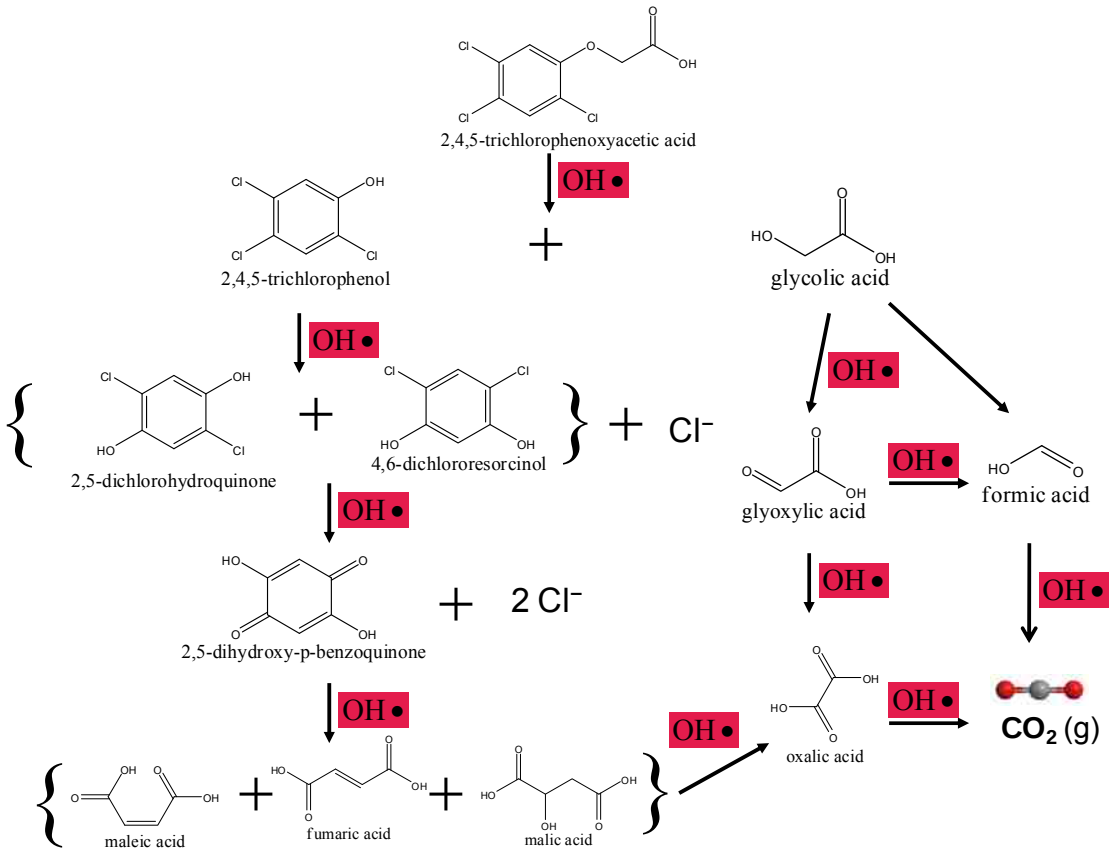

Figure 2.1 Reaction Pathway for Trichlorophenoxyacetic Acid Oxidation by Free Hydroxyl Radical (adapted from Boye et al., 2003)

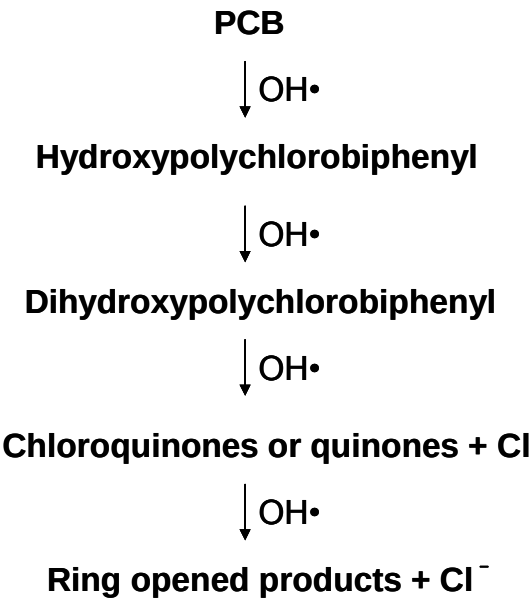

Figure 2.2 The Proposed Reaction Pathway for PCBs Oxidation by Free Hydroxyl Radical (adapted from Pignatello and Chapa, 1994)

generated by a Fenton reaction system. They found that both OH● and $O_2●^-$ were responsible for the destruction of $CHCl_3$ in DNAPLs, while $O_2●^-$ was the only reactive species for destruction of CCl_4 in DNAPLs.

In summary, Fenton reaction, especially the modified Fenton reaction, has extremely complex reaction chemistry. The major steps of the reaction mechanism for contaminants degradation by the Fenton and modified Fenton reaction have not been studied in depth. There are still some controversial and unclear parts for the overall reaction mechanism of the Fenton and modified Fenton reactions (Jacobsen et al., 1997 and 1998; Sheu et al., .1990; Leising et al., 1991; Fish et al., 1993).

2.4 Medical Research Involving Chelating Agent

Although the hydroxyl radical has been studied extensively in environmental remediation, considerable fundamental studies of hydroxyl radical based reactions have also been reported by medical researchers for understanding the role of oxidative damages (Crichton et al., 2002; Winterbourn, 1995). Galey et al. (1996) did research N, N'-bis-(3,4,5-trimethoxybenzyl) ethylenediamine N, N'-diacetic acid (OR10141) as iron chelating agent against oxidation. Their experimental results showed that OR10141 could protect protein against hydroxyl radical oxidation by suppressing the Fenton type reactions. They also compared the effect of OR10141 and EDTA in an iron ascorbate system on damage inhibition of two proteins (bovine serum albumin, glucose-6-phosphate dehydrogenase), and found OR10141 gave better protection than EDTA. Lope

et al. (1999) concluded that tannic acid was more effective as an antioxidant than other chelating agents (such as 1,10-phenanthroline, and EDTA), and even better than classic hydroxyl radical scavengers (such as DMSO, ethanol, and thiourea). The antioxidation ability of tannic acid resulted from sequestering iron rather than being a free radical scavenger. The inhibition of 2-deoxyribose oxidation by tannic acid was controlled by the ratio of tannic acid to Fe^{2+}. Only 20% of 2-deoxyribose (5 mM) was oxidized by OH● at pH 7 when the ratio of tannic acid to Fe^{2+} increased to 100:6 molar ratio. In contrast, all of 2-deoxyribose was oxidized in the experiment without tannic acid. Generally, these studies proved that chelating agents have the ability to control OH● formation rate, and remediation at neutral pH is practical.

2.5 Chelating Modified Fenton Reaction

Multidentate ligand type chelating agents can bind metal ions to form heterocyclic rings (Dwyer and Mellor, 1964; Chaberek and Martell, 1959). Due to this characteristic structure, metal-chelate compounds are more stable than metal complexes by the corresponding monodentate ligand. A metal chelate reduces the activity of a metal and significantly alters its solubility (Chaberek and Martell, 1959). When a chelating agent is present in a solution, it will complex Fe^{2+} or Fe^{3+} to form a more stable compound: Fe^{2+}–chelate or Fe^{3+}–chelate. Thus, the concentration of Fe^{2+} in the solution decreases substantially. Furthermore, as the activities of Fe^{2+}–chelate and Fe^{3+}–chelate are partially or even completely blocked, the reaction rate of reaction 2.1 decreases significantly due to the low concentration of Fe^{2+}. Consequently, the overall reaction rate of the chelate

modified Fenton reaction slows down because reaction 2.1 is the reaction rate limiting step of the whole reaction system. In summary, the OH● formation rate is controlled by the concentration of Fe^{2+} that is determined by the equilibrium reaction of Fe^{2+} with a chelating agent. Therefore, iron/H_2O_2 concentration, pH, and type/concentration of the chelating agent are the main parameters used for reaction control. Based on the information above, the proposed chelate modified Fenton reaction pathway is shown in Figure 2.3.

For environmental applications, the chelating agent should be non-toxic and non-reactive with OH●. Citrate, acting as a mono-chelate, fits these requirements and can be used as a chelating agent for the chelate modified Fenton reaction. Citric acid has three carboxylic groups and one hydroxyl group and has very high equilibrium constants with Fe^{2+} and Fe^{3+}. The chemical structure of citric acid is shown in Figure 2.4. According to Inczedy (1976), citric acid has the following equilibrium reactions:

$$H^+ + L \Leftrightarrow HL,\ K_{HL} = 10^{16}\ M^{-1} \quad (2.11)$$

$$H^+ + HL \Leftrightarrow H_2L,\ K_{H2L} = 10^{6.1}\ M^{-1} \quad (2.12)$$

$$2H^+ + HL \Leftrightarrow H_3L,\ K_{H3L} = 10^{10.5}\ M^{-2} \quad (2.13)$$

$$3H^+ + HL \Leftrightarrow H_4L,\ K_{H4L} = 10^{13.5}\ M^{-3} \quad (2.14)$$

where L represents citric acid and the charges for L and L–containing species are not indicated.

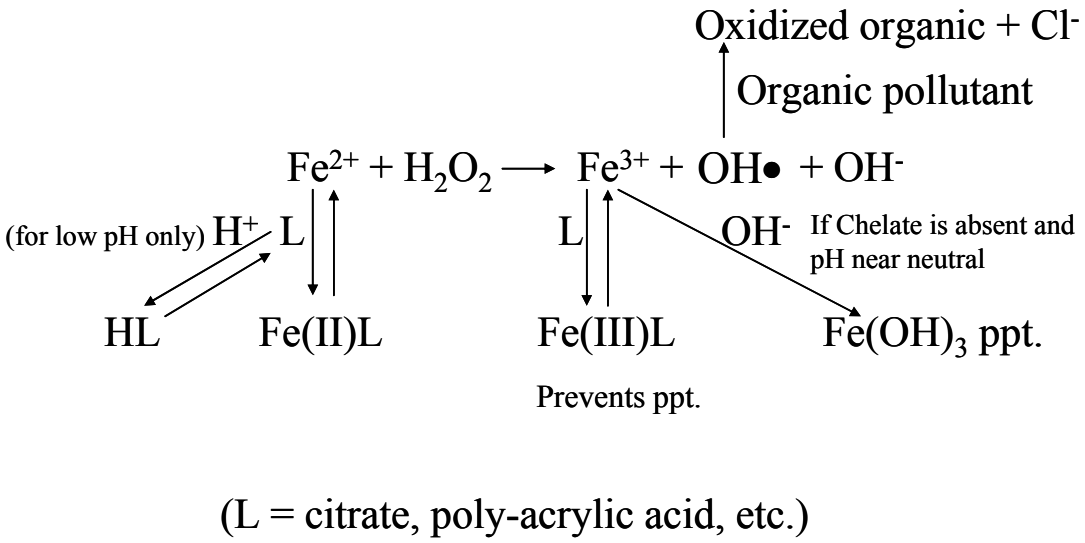

Figure 2.3 Chelate Modified Fenton Reaction Pathway (near neutral pH)

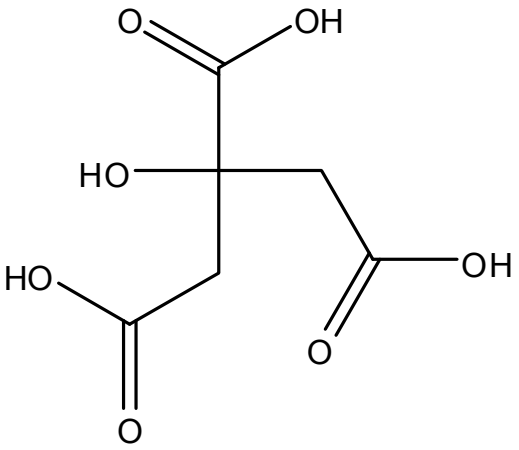

Citric Acid

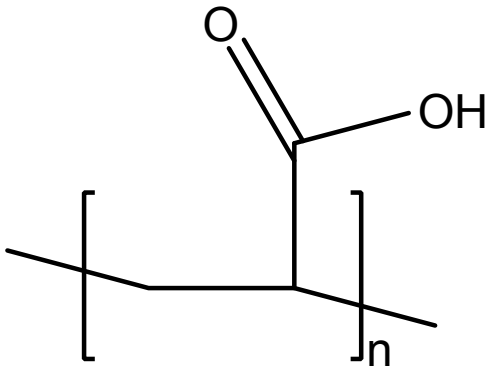

Polyacrylic Acid (PAA)

Figure 2.4 Chemical Structures of Citric Acid and Polyacrylic Acid

With the material balance and equilibrium reactions 2.11–2.14, the following equation can be obtained:

$$[L]_t = [L] + K_{HL} \times [H^+] \times [L] + K_{H2L} \times K_{HL} \times [H^+]^2 \times [L] + K_{H3L} \times K_{HL} \times [H^+]^3 \times [L] + K_{H4L} \times K_{HL} \times [H^+]^4 \times [L] \quad (2.15)$$

Eq 2.15 suggests that the species distribution of citric acid depends on both pH and the total concentration of citric acid-$[L]_t$. It is obvious that the concentrations of all individual species of citric acid will increase as the total concentration of citric acid increases. On the other hand, the different species of citric acid at different pH environments can be obtained from calculation, as shown in Figure 2.5. The calculation was under the condition of $[L]_t$ = 0.2 mM, which was the same condition in most of our experiments. At an acidic pH, the hydroxyl group is very difficult to ionize, and the concentration of L (a completely deprotonated form of citric acid) is over 10 orders of magnitude lower than other species. However, as pH increases, the concentration of L increases significantly, and it cannot be neglected at a neutral pH environment.

In contrast to a citric acid, PAA (a polymeric chelating agent) as a polymer has many functional groups available for iron ion chelation, and the chemical structure of PAA is shown in Figure 2.4. In addition to providing multiple binding sites from a single chain, PAA can be immobilized on solid support for repeated use. In this dissertation, the use of PAA as a poly-chelating agent in the Fenton reaction was explored. The potential of attachment to solid supports (silica particles and PVDF membrane) was also investigated to demonstrate the versatile uses of the poly-chelate (PAA) modified Fenton reaction for water pollutant remediation.

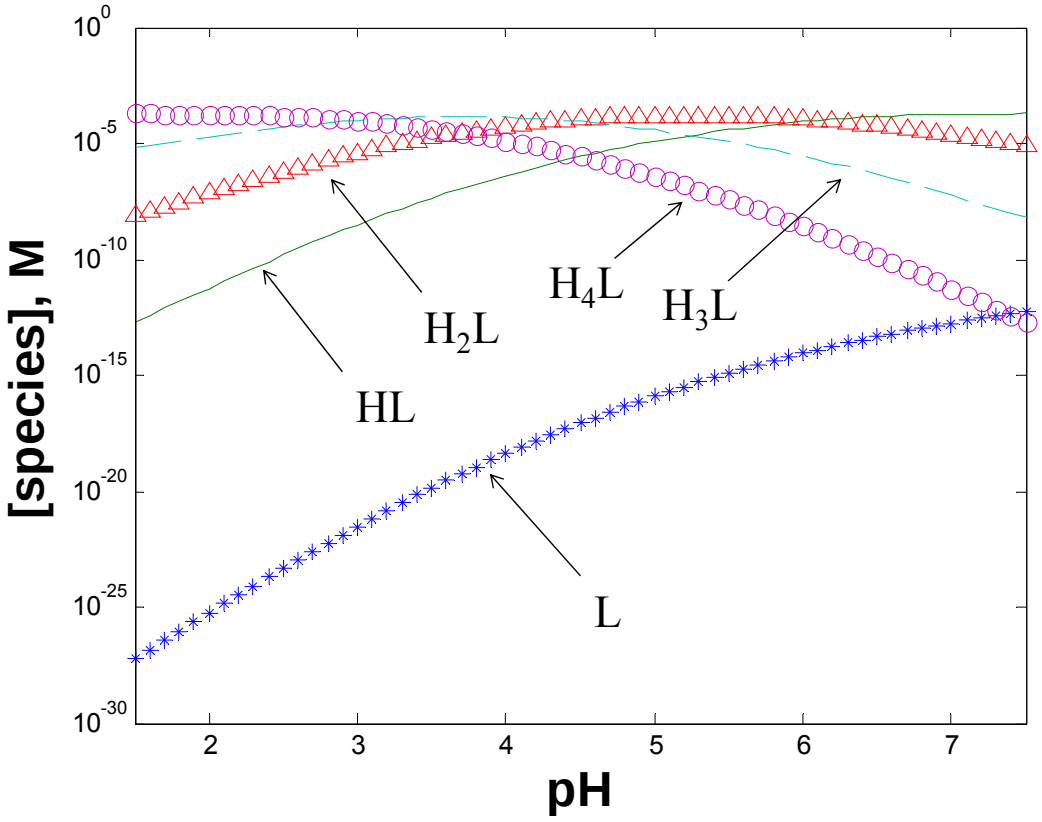

Figure 2.5 Species Distribution of Citric Acid at Different pH ($[L]_t$ = 0.2 mM)

Chapter 3. Experimental and Analytical Procedure

3.1 Materials

All chemicals in this dissertation were reagent grade. The model compounds for the detoxification study by the modified Fenton reaction were: 2,4,6-trichlorophenol (99%, Fisher Scientific), biphenyl (solid, Ultra Scientific), 2,2′-dichlorobiphenyl (solid, Ultra Scientific), carbon tetrachloride (99.5%, Sigma-Aldrich), and Trichloroethylene (99%, Sigma-Aldrich). The chemical structures of these compounds are shown in Figure 3.1 and Figure 3.2. 2-Hydroxybiphenyl (solid, Ultra Scientific) was used for intermediate analysis due to its high water solubility. Sodium citrate (solid) as a mono-chelating agent was obtained from Fisher Scientific, and poly-acrylic acid (MW: 50000 g/mol) as a poly-chelating agent was purchased from Polysciences, Inc. Acrylic acid (99%), benzoyl peroxide (97%, solid), 1,2-dibromoethane (EDB, 99%), 3-(2-pyridyl)-5,6-diphenyl-1,2,4,-triazine-4′,4″-disulfonic acid sodium salt (ferrozine, solid), 2,9-dimethyl-1,10-phenanthroline (DMP, solid), 1,1,1-trimethylolpropane triacrylate (TMPTA), and carbon tetrachloride were purchased from Sigma-Aldrich. Methacryloxypropyltrimethoxysilane (MPTS) was obtained from Gelest (Morrisville, PA). Ferrous sulfate (solid), ferric sulfate (solid) and hydrogen peroxide (30%, wt) were used to generate OH● and were acquired from Fisher Scientific. The organic solvents used for extraction and analysis were methylene chloride (Optima grade, Fisher Scientific), pentanes (Optima grade, Fisher

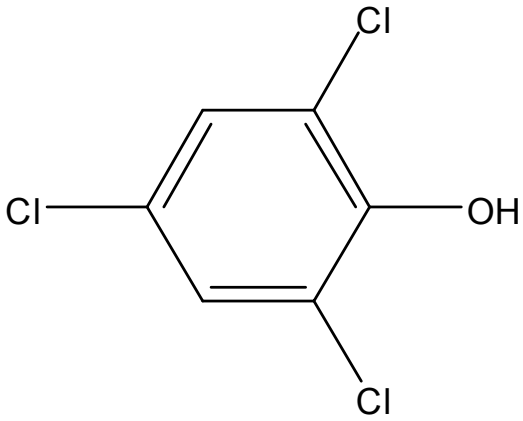

2, 4, 6-Trichlorophenol

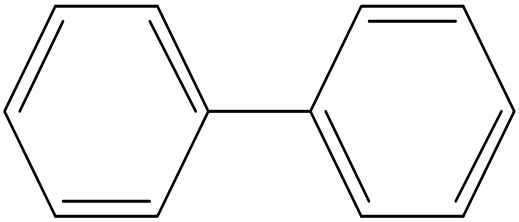

Biphenyl

Figure 3.1 Chemical Structures of 2,4,6-Trichlorophenol and Biphenyl

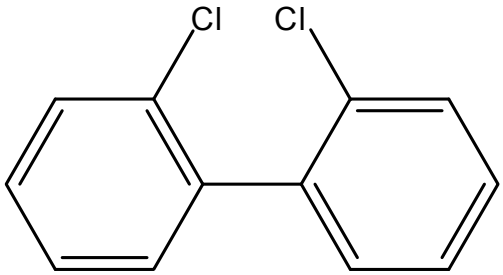

2,2′-Dichlorobiphenyl

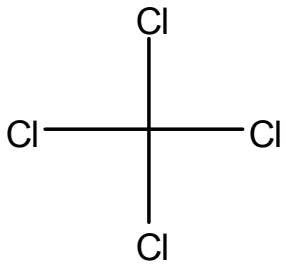

Carbon Tetrachloride

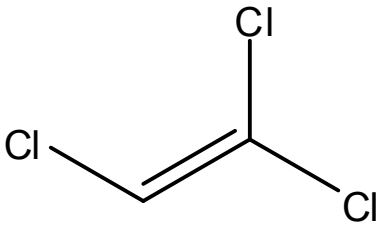

Trichloroethylene

Figure 3.2 Chemical Structures of 2,2′-Dichlorobiphenyl, Carbon Tetrachloride and Trichloroethylene

Scientific), ethyl acetate (Optima grade, Fisher Scientific). Naphthalene-d8 (5000 mg/L in methylene chloride) was used as the internal standard for the quantification of GC/MS analytical results. Deionized ultrafiltered (DIUF) water was purchased from Fisher Scientific. PVDF microfiltration membrane (Millipore) and silica particles (Huber Engineered Materials) were used as the solid supports for PAA immobilization experiments.

3.2 Experimental Reaction Systems

In this dissertation study, there were two types of reaction systems: standard Fenton reaction system and chelate modified Fenton reaction system. The two reaction systems were set up to identify the role of chelating agents during the reaction by comparing experimental results of the two systems. The experiments for the kinetic models were conducted in triplicate and gave the standard deviations reported in the Results section.

3.2.1 The Standard Fenton Reaction

All experiments with the standard Fenton reaction were carried out at room temperature (23-26 ^{o}C). TCP solution was prepared by dissolving TCP (solid) into DIUF water and stirred overnight. Biphenyl (solid) was dissolved in DIUF water through sonication at 35 ^{o}C and cooled down to room temperature. The pH of feed stock solution (200 mL) was adjusted to below 2.5 to avoid Fe^{2+} oxidation. Ferrous sulfate was added into the feed solution and H_2O_2 was added after 10 min to initiate reaction. The reaction was initiated

after H_2O_2 was injected into the system. Experimental samples were taken at different reaction times for analysis.

3.2.2 The Chelate Modified Fenton Reaction

All experiments of the chelate based modified Fenton reaction were contacted at room temperature (23-26 ^oC). Feed stock solutions were the same stock solutions used in the standard Fenton reaction. In addition, 2,2′-dichlorobiphenyl (2,2′-PCB) was also studied at a higher concentration containing undissolved particles. The experimental procedure of chelate modified Fenton reaction is the following: The chelating agent (citrate or PAA) was added into the solution first. Ferrous sulfate was added 10 min later. Then, H_2O_2 was added into the flask to initiate the reaction after pH was adjusted to neutral. The pH of solution was sensitive to the large amount of H_2O_2 addition, so that several times injections of H_2O_2 were necessary to avoid high pH variation. The pH of solution was carefully controlled within 0.2~0.3 by using small amounts of NaOH and H_2SO_4. The experimental procedure diagraph is shown in Figure 3.3. Experiments for the volatile compounds (CCl_4 and TCE) were carried out inside 20 mL vials without headspace due to the volatility of CCl_4 and TCE. Control sample experiments were always conducted to verify the loss of vaporized CCl_4 and TCE. For experiments of Fe^{2+} oxidation by air with PAA, the reaction solution was open to air and stirred continuously. Samples were taken at different times to analyze the concentration of Fe^{2+}.

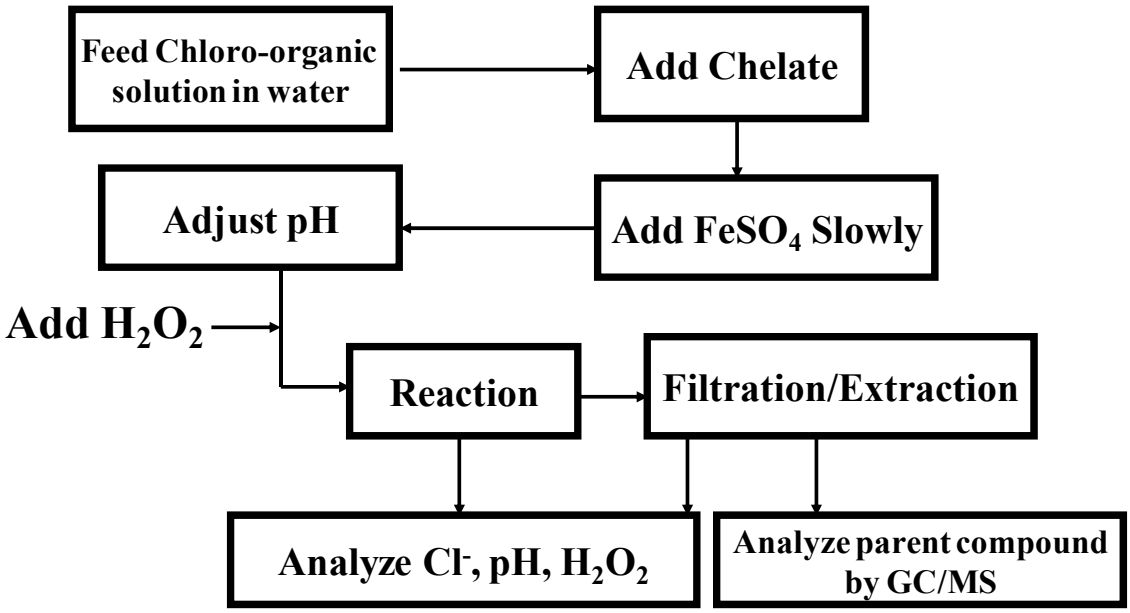

Figure 3.3 Typical Experimental Procedure for the Chelate Modified Fenton Reaction

3.3 Analytical Procedure

Extensive analyses of aqueous samples taken from experiments were carried to determine and quantify the concentration of parent compounds, intermediates, and final products. These analytical techniques are very important to establish and verify the mechanism and kinetic modeling for the chelate modified Fenton reaction. There were five major instrumental methods involving in this study:

1) Gas Chromatography-Mass Spectrometry (GC/MS)

   Determination of the concentration of TCP, biphenyl, and 2,2′-PCB in aqueous samples taken from different reaction times. It was also used to identify intermediates and some final products from oxidation reaction of TCP and biphenyl.

2) Gas Chromatography-Flame Ionization Detector (GC/FID)

   Identification of derivatized carboxylic acids (malonic acid and oxalic acid) as the final products for TCP oxidation by the chelate modified Fenton reaction.

3) Ion Chromatography (IC)

   Quantification of the concentration of inorganic anion (Cl^- in our study).

4) Ultraviolet-Visible Spectrophotometry (UV/vis)

   Determination of the concentration of chemical compounds due to its wavelength absorption.

5) Ion-Selective Electrode

   Quantification of the concentration of inorganic ion in the solution (Cl^- for our study).

3.3.1 GC/MS

(i) GC/MS analysis for TCP: [TCP] was determined by a Saturn 2200 GC/MS/MS equipped with a VARIAN CP-3800 Gas Chromatograph autosampler and a DB5-ms column (Agilent Technologies). Sodium sulfite was added into the collected sample to quench the reaction. After 30 min shaking for reaction quenching, the pH of the sample was adjusted to 2.5 before extraction with methylene chloride with a volume ratio-1:3 (sample **:** methylene chloride) and shaken overnight. Later, 1 mL of the organic phase was injected into an autosampler vial, and 10 μL of 5000 mg/L naphthalene was added into the vial to make a 50 mg/L internal standard. The calibration plot was made up of 7 points between 5 mg/L and 100 mg/L with R^2 = 0.992. One of TCP calibration solutions was always measured at the beginning to verify the calibration plot. With known feed solutions of TCP from 5 to 100 mg/L, the average analytical error was 8.8%. The detection limit for TCP was 2 mg/L.

(ii) GC/MS analysis for biphenyl and 2,2′-PCB: The concentrations of 2,2′-PCB and biphenyl were determined by a Saturn 2200 GC/MS/MS equipped with a VARIAN CP-3800 Gas Chromatograph autosampler and a DB5-ms column (Agilent Technologies). The calibration plot was made up of 10 points between 0.17 mg/L and 33.33 mg/L with R^2 = 0.999. One of the calibration solutions was always measured at the beginning along with samples to verify the calibration plot. With known feed solutions of sample from 0.5 to 10 mg/L, the average analytical error was 8.8%.

(iii) GC/MS analysis for intermediates and products: Samples taken from different reaction times were immediately quenched by adding sodium sulfite. Then, samples were adjusted to pH 2 to make sure all organic acids were in their unionized form.

Ethyl acetate was added in the samples (volume ratio = 1:1) for extraction for 2 h. The organic layer was separated and the aqueous phase was extracted by the same amount of ethyl acetate two more times. All organic liquids were combined and was purged with N_2 (ultra high purity grade) until it reached 1 mL. The sample was carefully transferred to a GC sample vial and continued to purge it with N_2 (ultra high purity grade) until dry. Then, 1 mL BSTFA solution (BSTFA **:** pyridine = 1**:**1) was added in the sample vial. The vial was capped and heated at 60 ^{o}C for 20 min. The sample was cooled to room temperature, and it was subjected to GC/MS (same GC/MS as analysis of TCP and biphenyl) analysis. Any identified intermediate or product was compared with the standard under the same derivatization procedure.

3.3.2 GC/FID

A Varian CP-3800 GC/FID equipped with an autosampler CP-8400 and a Nukol 25327 column (Supelco) was used for derivatized malonic acid and oxalic acid analysis. Samples taken at different reaction times were immediately quenched by adding sodium sulfite. Then, the samples were extracted with diethyl ether (volume ratio = 1:1) for 2 h after pH adjustment to 2. The organic layer was separated, and the aqueous phase was extracted by the same amount of diethyl ether two more times. All organic liquids were combined and was derivatized with methanol (HCl) at 50 °C for 10 min. The derivatized sample was purged with N_2 (ultra high purity grade) until dryness. The sample was ready for analysis after adding pentanes to dissolve the derivatized carboxylic acids.

3.3.3 Ion Chromatography System (ICS 2500) for Cl^- Analysis:

ICS 2500 includes an AS 50 autosampler, a LC 25 chromatograph oven, an EG 50 Eluent Generator (mobile phase-KOH, 39 mM), and an IC 25 ion chromatograph (conductivity detector). It has a guard column IonPac-AG 18 and an anion-exchange column-IonPac AS18. The calibration plot for Cl^- was made up of 13 points (range from 0.075 mg/L to 100 mg/L with R^2 = 0.999). One calibration solution was always measured at the beginning to verify the calibration plot. The detection limit for Cl^- was 0.075 mg/L, and the average analytical error was 3.5%.

3.3.4 UV/vis Spectrophotometry

(i) UV/vis Spectrophotometry for H_2O_2 concentration measurement: The modified DMP method was used for H_2O_2 analysis (Kosaka et al., 1998; Ei-Morsi et al., 2002). A 1 mL of DMP solution (10 mM), 1 mL of $CuSO_4$ solution (10 mM), and 1 mL of buffer were added into the empty vial. A total of 3 mL of sample solution and DIUF water (volume ratio was dependent on the dilution needed) was added later. After 1-2 min of shaking, the absorption at wavelength of 454 was measured immediately. The calibration plot was set up by 6 points between 5 μM to 100 μM with R^2 = 0.998. The detection limit for H_2O_2 was 1 μM, and the average analytical error was 6.7%.

(ii) UV/vis Spectrophotometry for Fe^{2+} concentration measurement: The concentration of Fe^{2+} in solution was analyzed by the ferrozine method (Stookey, 1970; Voelker and Sulzberger, 1996). A sample of 1 mL was injected into an empty vial. Then 246 μL of

ferrozine solution (10 mM) and 120 µL of buffer solution (pH 7) were added into the vial. After 2 min mixing time, the absorption at wavelength of 562 was measured immediately. The calibration plot was made up of 7 points between 5 mM to 100 mM with $R^2 = 0.996$. The detection limit for Fe^{2+} in a solution is 1 mM, and the average analytical error was 5.6%.

3.3.5 Ion-Selective Electrode:

Ion-selective electrode measures the potential readings due to concentration of Cl^- in solution. The Cl^- calibration plot for the electrode was carried out at the same pH as that of the sample. After taking potential readings from the sample, 200 µL of standard NaCl solution (1000 mg/L) was added into the sample and the potential was read again. The average analytical error for this electrode was 7.9%. Table 3.1 shows the Cl^- electrode calibration under the chelate-based Fenton reaction conditions.

Table 3.1 Effect of Fe^{2+} + Citrate + H_2O_2 System for Chloride Electrode Calibration

100 mg/L standard chloride solution + Fe^{2+} + L + H_2O_2

[Fe]=10mM, [L]:[Fe]=1:1, $[H_2O_2]_0$=50mM, L=citrate

Reaction Time, min	24	60	120	300	1200	Average of Error%
Reading, mg/L	94.4	106.1	109.4	108.2	107.8	
Diff%	-5.6	6.1	9.4	8.2	7.8	7.4
Reading, mg/L *	111.5	129.0	129.0	132.7	128.0	
Diff%	-7.1	7.5	7.5	10.6	6.7	7.9

* after adding 20 mg/L chloride

Chapter 4. Experimental Results and Discussion: TCP and Biphenyl Oxidation by OH●

This chapter will concentrate on the oxidation of pollutants by the chelate (mono-chelate and poly-chelate) modified Fenton reaction system. It starts with the comparison of TCP oxidation by the standard and chelate modified Fenton reactions followed by the discussion of the important parameters of the chelate modified Fenton reaction: pH, H_2O_2 decomposition rate, and ratio of iron ion to chelate. PAA was proven to be an effective poly-chelating agent for contaminants degradation in our experiments. Furthemore, the intermediate and product analysis for TCP and biphenyl were carried out to verify the oxidation pathway of the chelate modified Fenton reaction. Finally, a successful dechlorination of 2,2′–PCB demonstrates that the chelate modified Fenton reaction has the ability to oxidize pollutants in a heterogeneous environment. A chemical reduction process (such as with zerovalent metals: Fe, Zn) can successfully dechlorinate PCBs (Lowry and Johnson, 2004; Xu and Bhattacharyya, 2005). However, one of its final products, biphenyl, is still toxic for the environment, and it can only be detoxified by an oxidation reaction. To prove that PCB can be detoxified thoroughly, biphenyl was chosen as a model compound in our studies. On the other hand, TCP was selected as another model compound because it is a common organic pollutant in various contaminated waters and represents a stable single aromatic structure.

4.1 Comparison between the Standard and Chelate Modified Fenton Reactions

OH● is a very reactive species and has a very short lifetime. Thus, the overall reaction rate for pollutant oxidation is mainly dependent on the OH● generation reaction since all sink reactions of OH● are very fast. Due to the presence of the chelating agent, the concentration of free ferrous ion-[Fe^{2+}] (including all hydroxylated species: [Fe^{2+}] + [$Fe(OH)^{+}$] + [$Fe(OH)_2$]) decreases dramatically. Consequently, at the same total concentration of ferrous ion-[Fe(II)], the system with a chelating agent will have a much lower [Fe^{2+}]. Thus, the overall reaction rate of the reaction system with a chelating agent is much lower than that of the standard Fenton reaction system. This can be proven by TCP dechlorination reaction under two reaction systems. Figure 4.1 indicates that the Cl^- formation rate of the chelate modified Fenton reaction is much slower than that of the standard Fenton reaction. Meanwhile, the concentrations of Cl^- for both methods after 48 h of reaction time are nearly the same: 97% and 93% (reaction without chelate, reaction with chelate respectively). From the experimental results, the chelate modified Fenton reaction has the same dechlorination capacity as the standard Fenton reaction at the same reactant loadings ($[Fe(II)]_0$, $[H_2O_2]$ and $[TCP]_0$). However, the overall reaction rate of the chelate modified Fenton reaction is much slower. This will be beneficial for groundwater remediation since it can prevent any local temperature surge and its consequences, due to the exothermic reaction of the Fenton reaction. A lower reaction rate also promotes OH● utilization since a higher concentration of OH● may promote other unwanted side reactions.

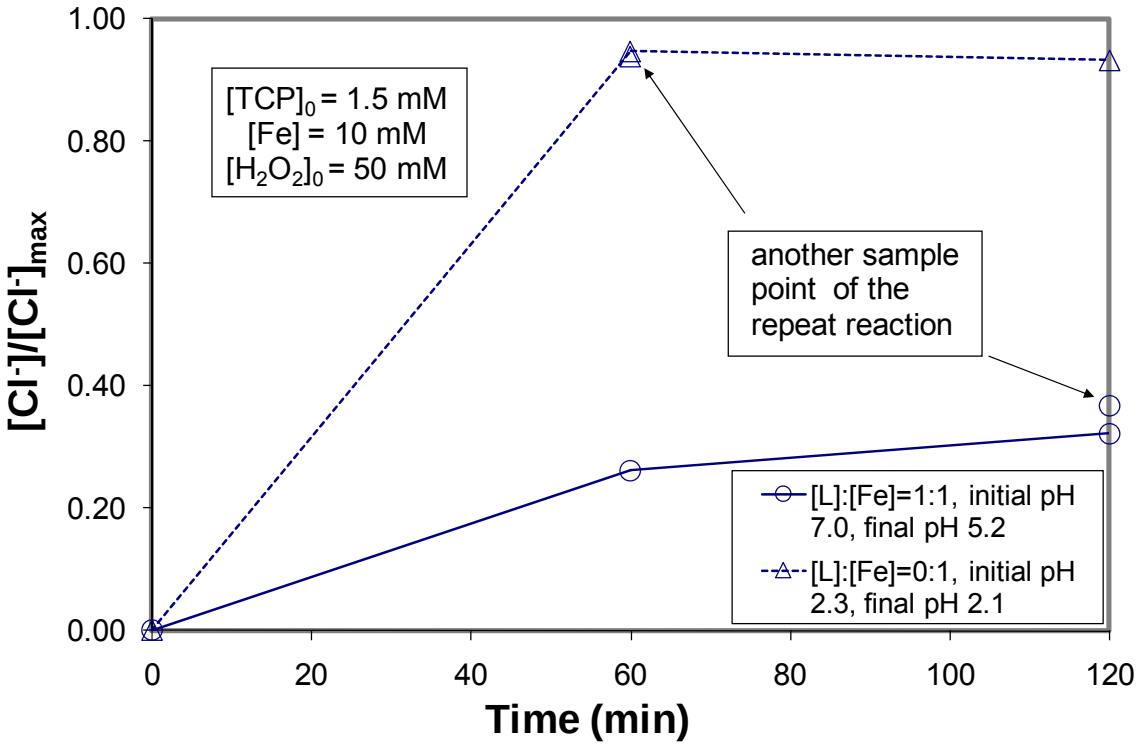

Figure 4.1 Chloride Formation Rate for Standard and Chelate-Based Fenton Reaction during TCP Dechlorination

On the other hand, a polymeric chelating agent can also be used in the modified Fenton reaction for pollutant oxidation. Figure 4.2 indicates that a poly-chelate (PAA) modified Fenton reaction gives a result similar to a monomeric chelate (citrate). However, the overall reaction of TCP dechlorination by the PAA modified Fenton reaction is slower than that of the citrate modified Fenton reaction because there is only 85% of Cl^- formation after 96 h of reaction time. It is also necessary to prove that the polymeric chelating agent (such as poly-acrylic acid) has the ability to complex iron ions in the solution phase. The result from atomic absorption (AA) analysis shows that the free iron (Fe^{2+} + Fe^{3+}) is less than 0.8% of the total concentration of iron ions after separation of the complexed and uncomplexed species. This suggests that almost all ferric ions are complexed by poly-acrylic acid. At the same time, because of its high molecular weight, the polymeric chelate can be easily separated out from the reaction solution by membrane ultrafiltration. Thus, ultrafiltration can be used to completely remove chelated iron ions from the solution, which allows for a more accurate analysis of TCP. Since the pK_a value of poly-acrylic acid is 4.75 (Studart et al., 2003), the low chelating agent to iron ratio may not fix all iron ions at a low pH environment. The precipitation during the experiment at pH 5 was observed at a low functional group to iron ion ratio ($[COO^-]/[Fe] = 2$), which indicates some Fe^{3+} was not sequestered by PAA. From these experimental results, pH and functional group to iron ion ratio are important parameters for the PAA modified Fenton reaction.

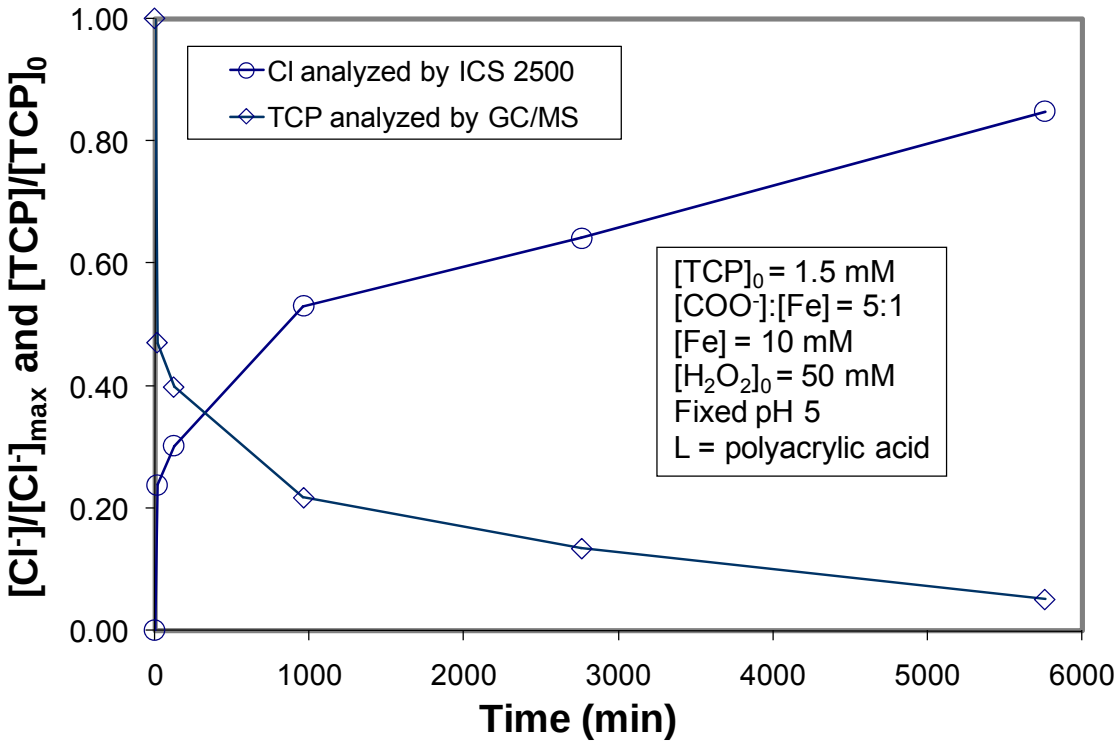

Figure 4.2 TCP Destruction and Chloride Formation for $Fe^{2+} + H_2O_2 + PAA + TCP$ System at pH 5 (PAA as a Chelating Agent)

4.2 Fe^{2+} Oxidation by Air at pH 7

Fe^{2+} oxidation by air at a neutral pH environment is very fast and follows a well-known reaction rate equation:

$$\frac{d[Fe^{2+}]}{dt} = -k_{Fe^{2+},O_2}[Fe^{2+}][p_{O_2}][OH^-]^2 \quad (4.1)$$

The reaction rate constant is $k_{Fe^{2+},O_2} = 8 \times 10^{13}$ M^{-2} atm^{-1} min^{-1} (Willey et al., 2005). However, when a poly-chelating agent (such as PAA) or other type of chelating agent is present in the solution, it combines with Fe^{2+} to form Fe^{2+}–PAA or other chelated species. Thus, the concentration of Fe^{2+} in the solution will decrease substantially, and it may need more time for oxidation of the same amount of Fe^{2+} if PAA is present in the solution.

Figure 4.3 shows the Fe^{2+} oxidation by air at different ratios of PAA to iron. It is clear that the Fe^{2+} oxidation rate decreased dramatically as PAA was added to the solution. The experimental data of Fe^{2+} oxidation by air at pH 7 without chelate were not obtained because Fe^{2+} will precipitate with $Fe(OH)_3$ at pH 7 (Pignatello et al., 2006). The data for Fe^{2+} oxidation without chelate shown in Figure 4.3 were obtained from equation 4.1 using the oxidation rate constant (8×10^{13} $M^{-2}atm^{-1}min^{-1}$), $[P_{O2}] = 0.2$ atm, and assuming that Fe^{3+} would not precipitate as $Fe(OH)_3$ (s). On the other hand, H_2O_2 in the Fenton reaction competes with oxygen for Fe^{2+} oxidation. By assuming that Fe^{3+} would not precipitate as $Fe(OH)_3$ (s), the modeling calculation (discussed in the Kinetic Model section in detail) showed that more than 86% of Fe(II) should be oxidized to Fe(III) in 1 min after the start

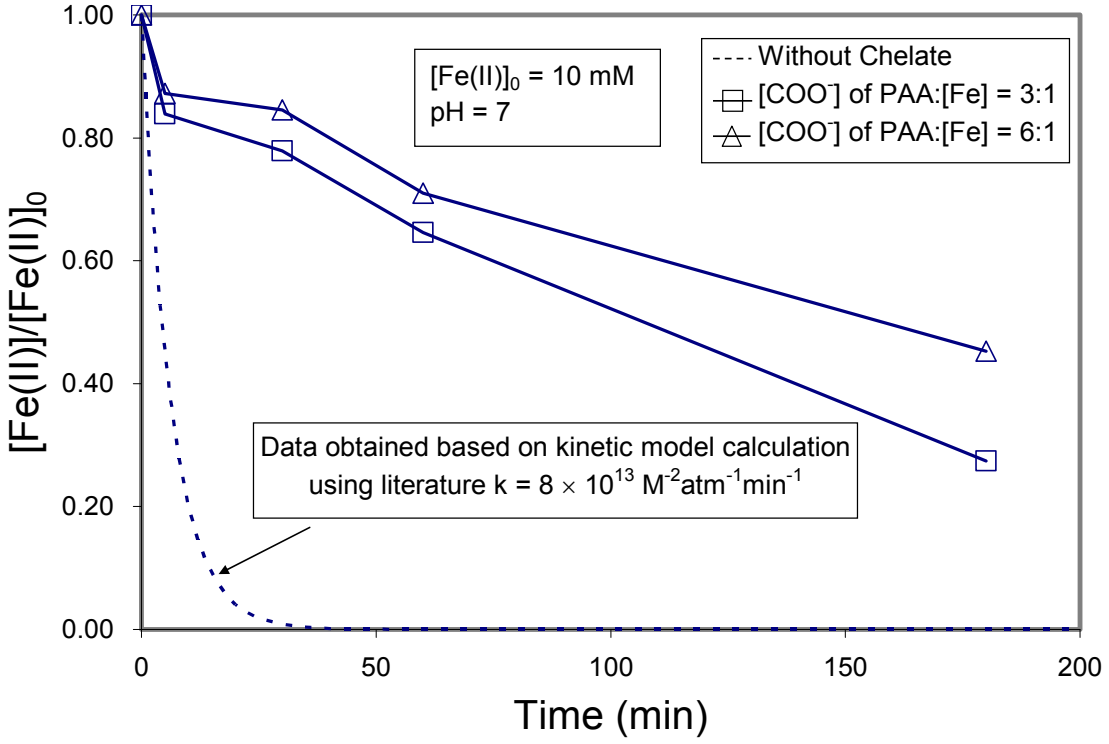

Figure 4.3 Fe^{2+} Oxidation by Air with and without PAA

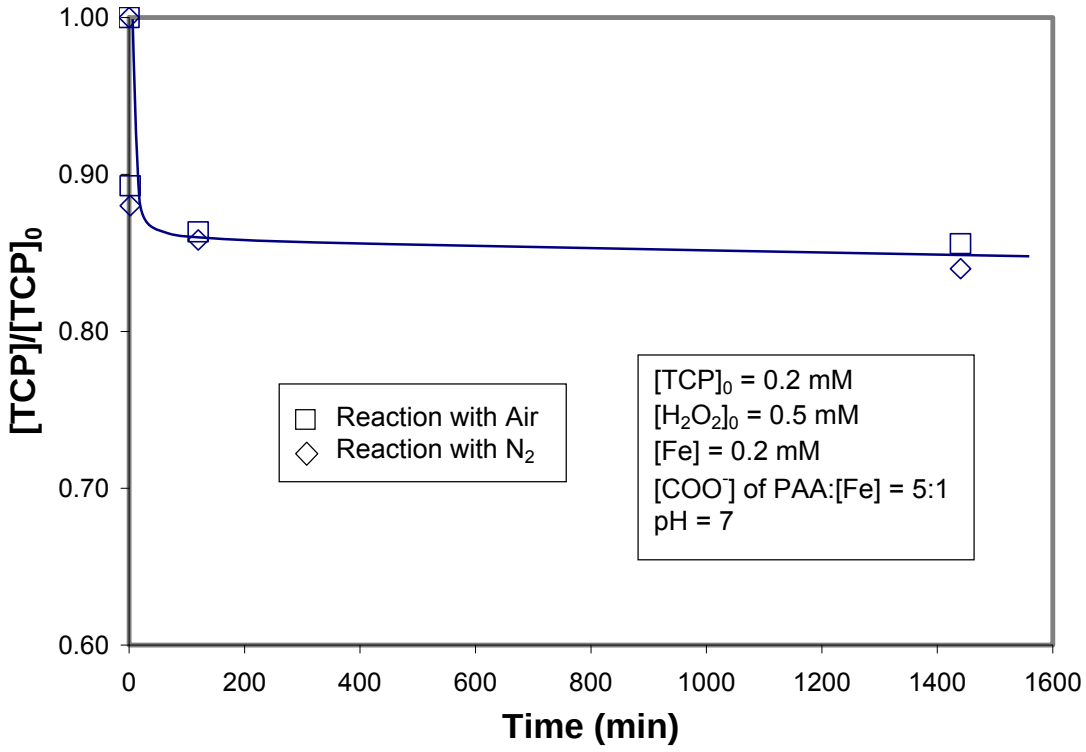

Figure 4.4 Effect of Dissolved Oxygen for TCP Oxidation by Fe^{2+} + PAA + H_2O_2 System

of the reaction with H_2O_2. On the contrary, there is only 14.8% of Fe(II) oxidized to Fe(III) by air after 1 min (Figure 4.3). 2,4,6-Trichlorophenol (TCP) dechlorination reactions with and without air are shown in Figure 4.4. Both experimental sets of data gave similar TCP dechlorination results up to 24 h of reaction time. This suggests that Fe^{2+} oxidation by air is minimized when PAA and H_2O_2 are present in the reaction system.

4.3 pH Control for Chelate Based Modified Fenton Reaction

In the chelate modified Fenton reaction, pH is a very important parameter for reaction control. As the reaction starts, the pH of the solution tends to decline, especially during the first few seconds after H_2O_2 has been added. Thus, the addition of H_2O_2 several times instead of a single injection is necessary to avoid a large pH surge at the initial stage. When the pH of the solution drops below 5, a significant amount of Fe^{2+} is freed from the chelate complex. Experiments showed that the reaction at pH 4 had significantly higher Cl^- formation than the reaction at pH 5. Although we maintained a constant pH of reaction, the variation of pH during the initial stage of the reaction was considerable. Thus, the Cl^- formation rate for the chelate modified Fenton reaction would have been slower than the actual rate in Figure 4.1, if a constant pH of 7 was maintained. The experiments under a constant pH environment proved this hypothesis. The Cl^- formation (at 1 h of reaction time) under a fixed pH 7 is much smaller than those under a fixed pH 6 and 5 (Figure 4.5). Therefore, maintaining low pH would accelerate the reaction rate. In

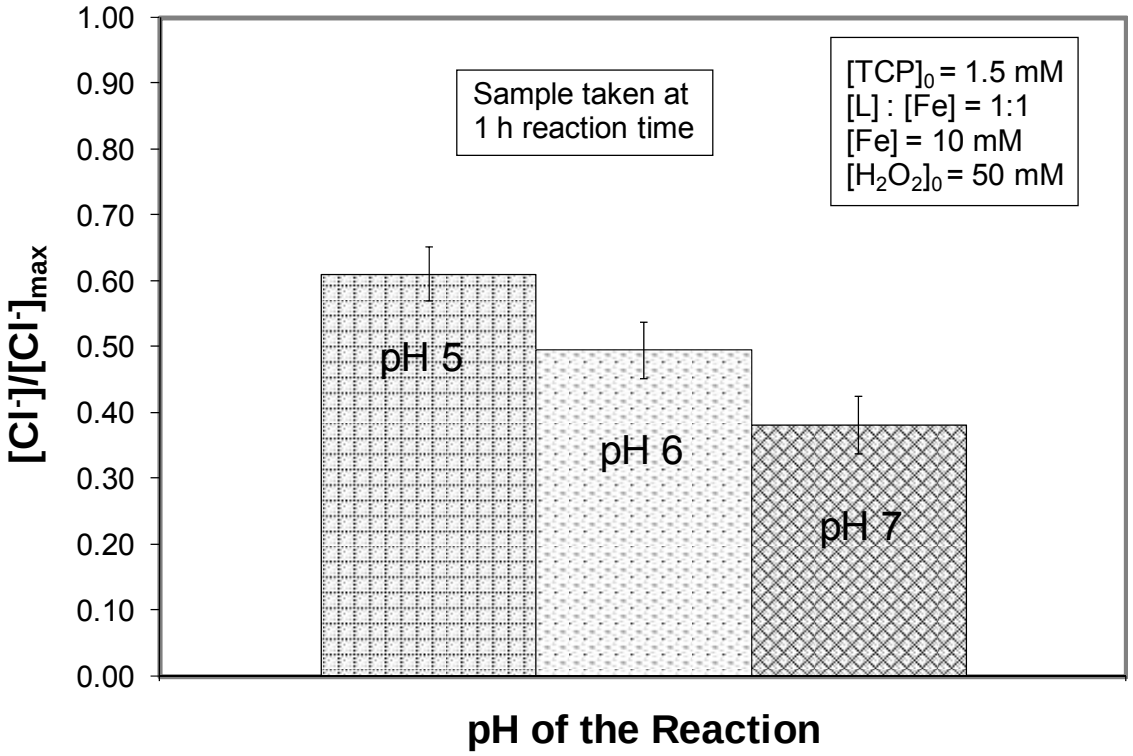

Figure 4.5 Chloride Formation under Different pH Environments at 1 h of Reaction Time

order to prevent a rapid reaction, it is very important to maintain the variation of pH at a minimum level all the time.

4.4 H_2O_2 Decomposition Behavior for the Chelate Modified Fenton Reaction

If H_2O_2 is not present in the Fenton reaction system, there will be no OH● formation and the consequent reactions. Thus, H_2O_2 decomposition is a very important parameter to help us understand the Fenton reaction system. As a chelating agent is present in the solution, the overall reaction rate decreases due to the lower [Fe^{2+}]. Consequently, H_2O_2 decomposition rate should be slower for the reaction system with chelating agent. To understand the role of Fe^{2+}-citrate in the reaction, the experiments for H_2O_2 decomposition under different iron to chelate ratios were carried out. For the reaction without chelate, there were significant precipitation of $Fe(OH)_3$, and [H_2O_2] was taken after sample filtration to avoid interference. In Figure 4.6, H_2O_2 decomposition is strongly dependent on the iron to chelate ratio — the higher the iron to chelate ratio, the slower the decomposition rate. This suggests that the reactivity of Fe^{2+}-citrate in the chelate modified Fenton reaction can be negligible. In order to explore the role of Fe^{3+} in the reaction, the experiments of TCP decomposition initiated by Fe^{3+} were carried out (Figure 4.7) also. From the experimental results, all reactions (under different pH 5, 6, and 7) are very slow. Sun and Pignatello (1992 and 1993c) also concluded that the capability of Fe^{3+} + citrate for contaminants destruction was very low unless UV irradiation was provided.

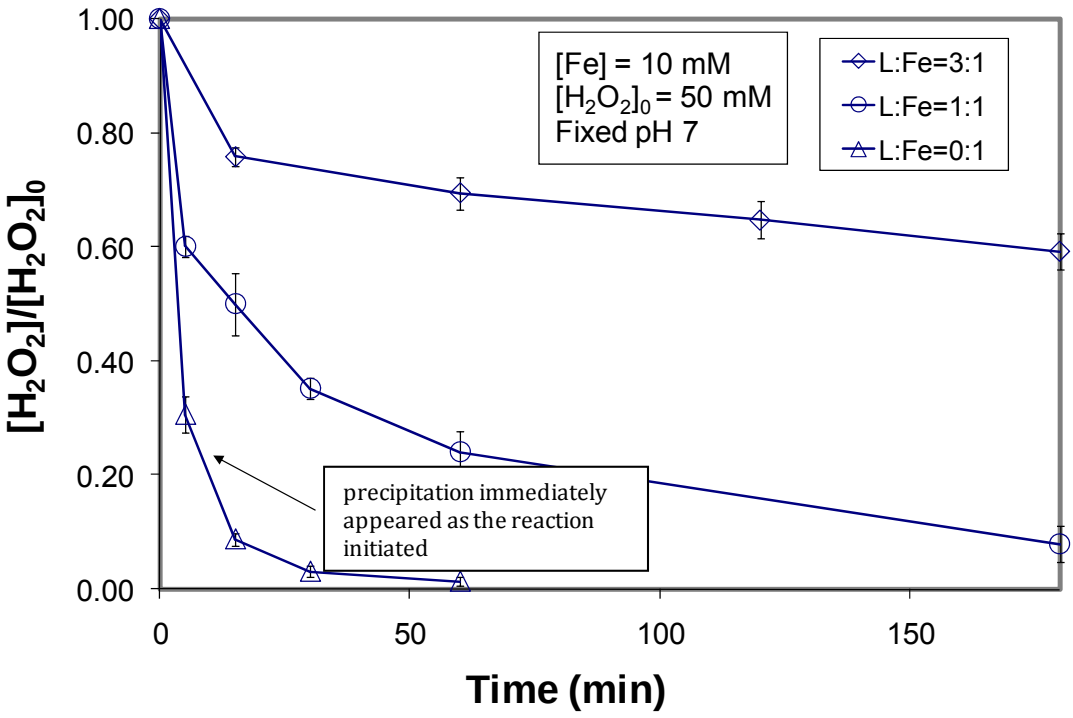

Figure 4.6 H_2O_2 Decomposition under Different Chelating Agent to Iron Ratios

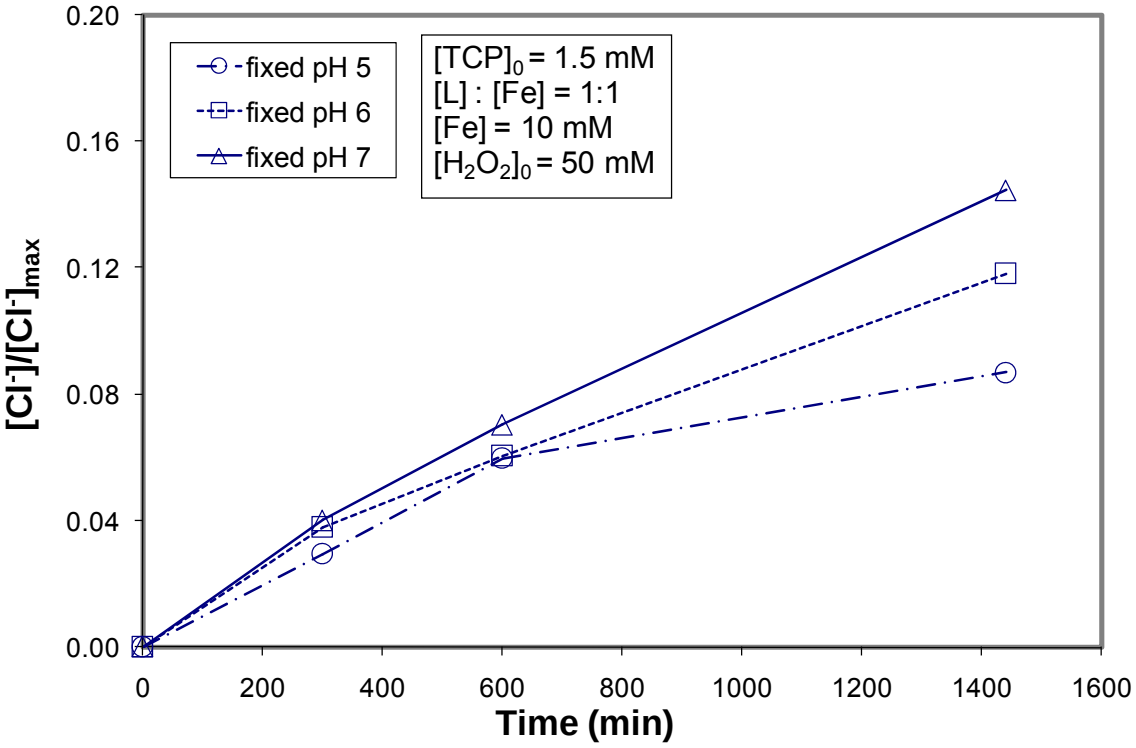

Figure 4.7 Chloride Formation for Fe^{3+} + H_2O_2 + Citrate System during TCP Dechlorination

According to Neyens and Beayens (2003), the behavior of H_2O_2 consumption (with and without organic pollutant) is mainly dependent on the ratio of Fe^{2+} to H_2O_2. OH● is a nonspecific oxidant that can react rapidly with many organic and inorganic compound. The reaction rate constant of free hydroxyl radical with H_2O_2 is 3.3×10^7 M^{-1} s^{-1}. Without any organic pollutant, OH● generated in the reaction will mainly react with H_2O_2 if the ratio of H_2O_2 to Fe^{2+} is high. On the other hand, the pollutant will compete with H_2O_2 for OH● consumption if a pollutant is present in the reaction system. In the chelate modified Fenton reaction, the concentration of free Fe^{2+} (including all hydroxylated species) is very low in comparison to the concentration of H_2O_2 because of the presence of chelating agent in the solution. In the monomeric chelate–citrate–based modified Fenton reaction, the H_2O_2 decomposition in the systems (with and without pollutant, TCP) followed the behavior described above: $[H_2O_2]/[H_2O_2]_0 = 0.03$ after 3 h of reaction time without TCP at pH 7. $[H_2O_2]/[H_2O_2]_0 = 0.45$ after 24 h of reaction time with TCP at pH 7, as shown in Figure 4.8. H_2O_2 decomposition rates for the PAA modified Fenton reactions with and without biphenyl are compared in Figure 4.9. As expected, a higher H_2O_2 consumption was also observed in the reaction without pollutant after 24 h of reaction time. It is interesting to note that H_2O_2 consumption almost falls in the same range at the initial stages of the two reactions. This may be caused by the lower ratio of $[H_2O_2]_0/[Fe^{2+}]_0$ ($[Fe(II)]_0 = [Fe^{2+}]_0 + [FeL]_0$) in the solution for the PAA experiment. With $[Fe(II)]_0 = 0.2$ mM and $[H_2O_2]_0 = 0.5$ mM, $[H_2O_2]_0/[Fe^{2+}]_0 \approx 60$ for the PAA experiment (using an equilibrium constant of citrate–Fe^{2+} binding for estimation), while $[H_2O_2]_0/[Fe^{2+}]_0 = 839$

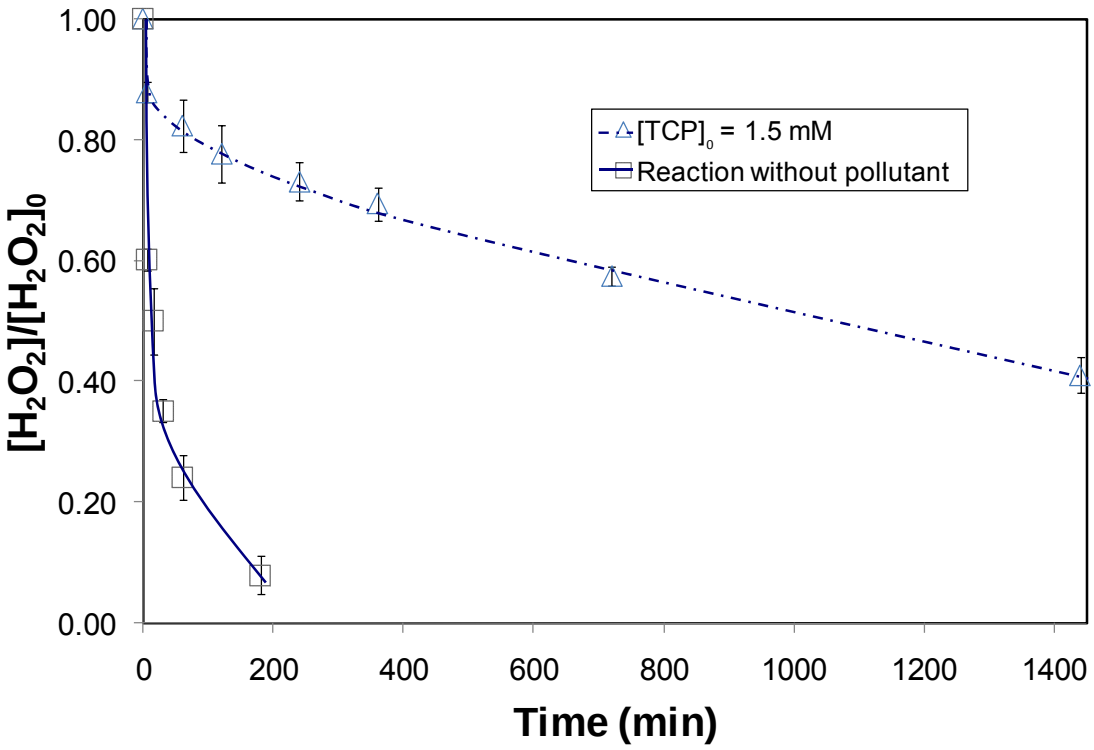

Figure 4.8 H_2O_2 Decomposition Behavior for Citrate + Fe^{2+} + H_2O_2 System with and without Pollutant

.

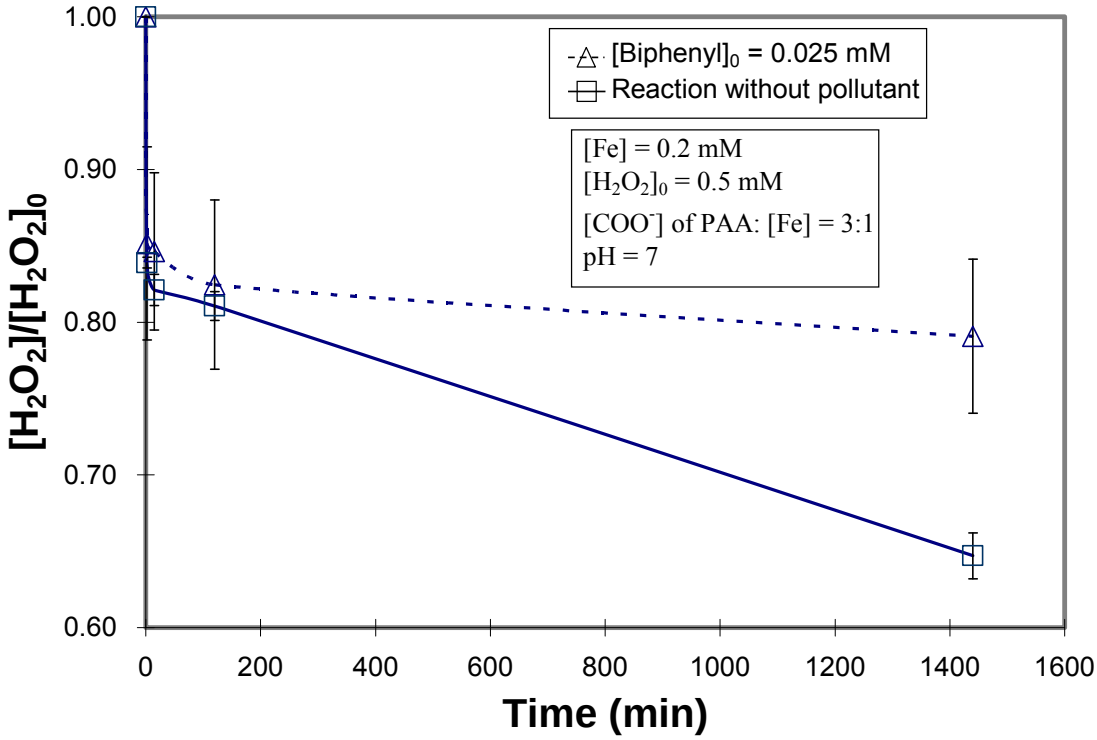

Figure 4.9 H_2O_2 Decomposition Behavior for PAA + Fe^{2+} + H_2O_2 System with and without Pollutant

for the citrate experiment ($[Fe(II)]_0$ = 10 mM and $[H_2O_2]_0$ = 50 mM).

4.5 Chloride Ion Formation during the Oxidation of TCP

In all experiments, the observed Cl^- formation at the end of the reaction was less than 91% of the total chlorine in TCP except for the experiment where additional H_2O_2 was added to get a total concentration of 100 mM. This phenomenon can be explained by the formation of chlorinated intermediates, which are difficult to oxidize. For example, Augusti et al. (1998) observed that chlorohydroquinone and chloroquinone are the intermediates during the hydroxylation process of chlorophenol by using a membrane introduction mass spectrometry. Boye et al. (2003) also proved that 2,5-dichlorohydroquinone and 4,6-dichlororesorcinol were intermediates of the hydroxylation process of 2,4,5-trichlorophenol by analyzing the intermediates during the reaction. Figure 4.10 shows that Cl^- formation from TCP destruction agrees with the reaction pathway proposed by Boye et al. (2003). It is observed that the moles of Cl^- formation per mole of TCP destruction were greater than 1. This can be explained by the simultaneous dechlorination reactions of intermediates.

By assuming that all intermediates and products are not in chlorinated form during the TCP dechlorination process, the expected Cl^- formation will be higher. The calculation based on the complete dechlorination and actual experimental data for pH 5 are compared

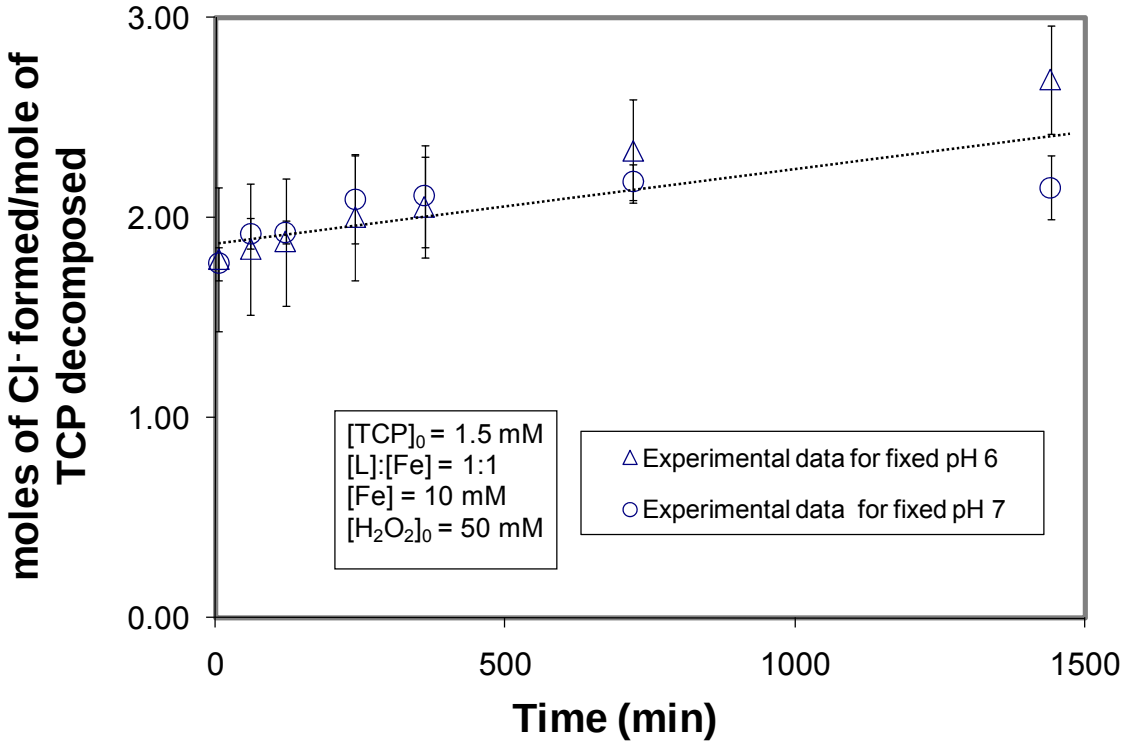

Figure 4.10 Effect of pH and Time on Cl^- Formation Behavior

in Figure 4.11. The difference between these two Cl^- formations becomes lower as pH goes up. After a 4-h reaction time in a separate pH 5 experiment, additional 50 mM H_2O_2 was injected into the system. The percentage of Cl^- formed increased from 91% to 97% after 1 h reaction with the additional H_2O_2. This proves that some intermediates are still in chlorinated form.

TCP will be considered dechlorinated once one chloride ion is removed from it. Figure 4.12 shows the Cl^- formation to the TCP destruction by monomeric chelate and polymeric chelate at pH 5. As expected, Cl^- formation in both systems is low at the initial stage due to the chlorinated intermediates formation. However, the complete dechlorination can be achieved by the use of excess H_2O_2 and near 100% TCP conversion levels.

4.6 Identification of Intermediates and Products for Oxidation Reaction

OH● is a very active radical species, and it will attack the chlorinated organic compounds through hydrogen abstraction or addition to form an organic radical. This organic radical then will decompose to other intermediates and final products. Augusti et al. (1998) proposed two reaction pathways for chlorobenzene oxidation through the intermediate analysis, as shown in Figure 4.13. Based on the experimental data, there was only 40% of Cl^- formation even though more than 90% of the parent compound (chlorobenzene) was

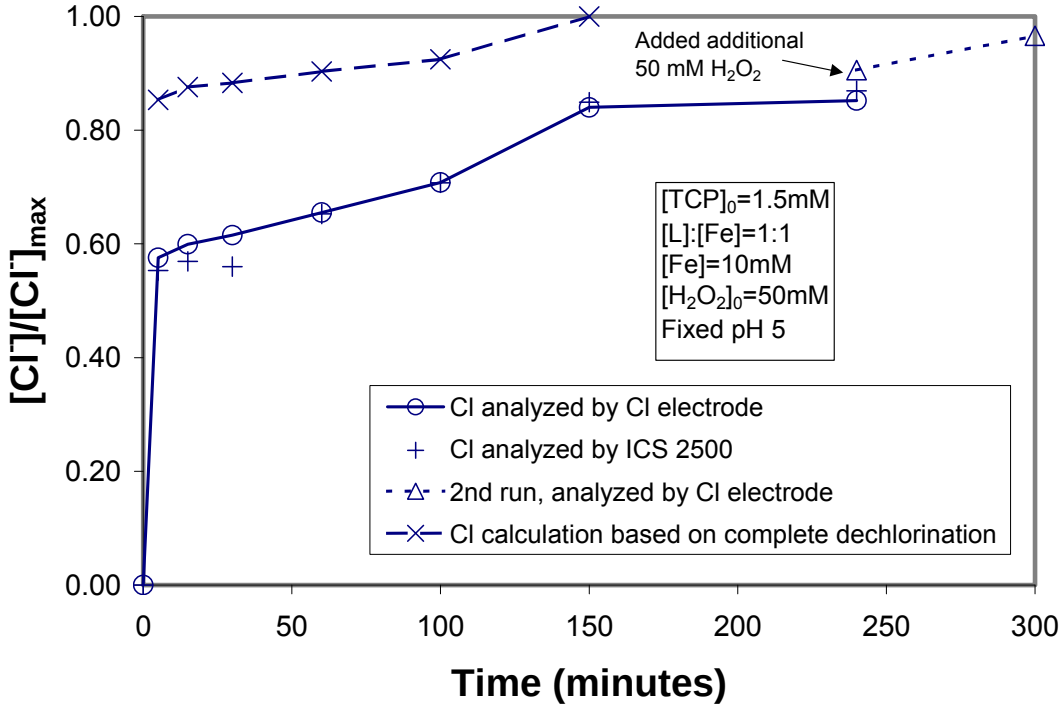

Figure 4.11 Comparison between Calculated and Actual Cl^- Formation for Fe^{2+} + H_2O_2 + Citrate + TCP System at pH 5

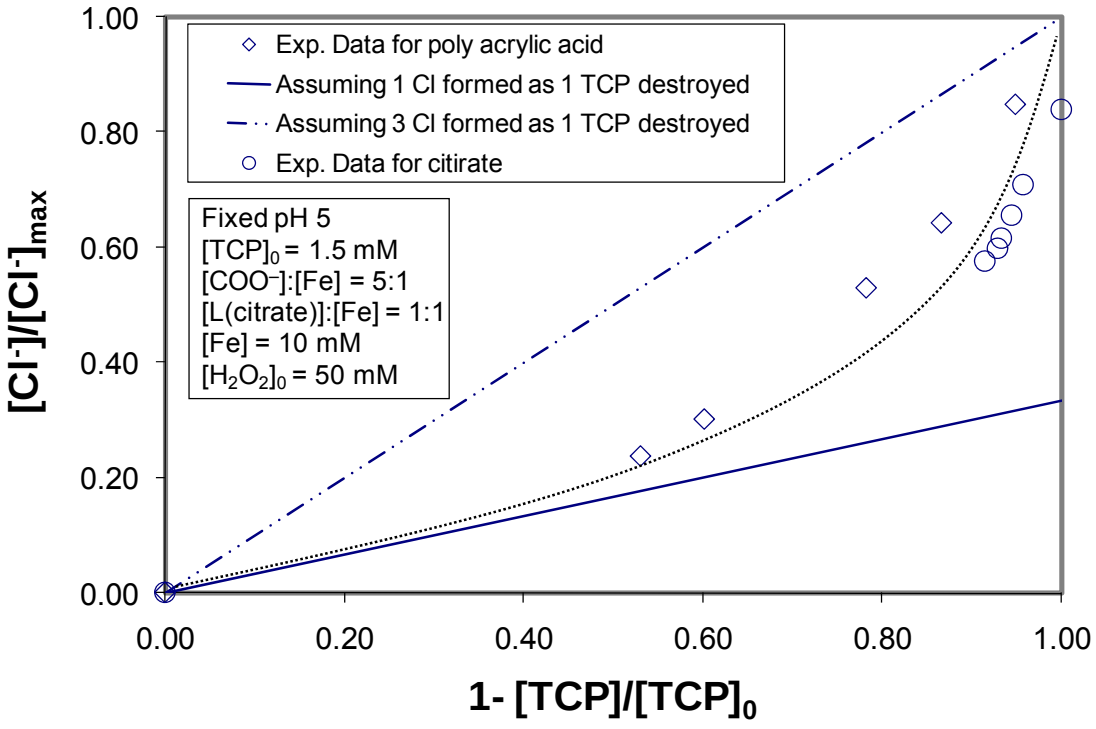

Figure 4.12 Relationship between TCP Destruction and Chloride Ion Formation for Citrate and PAA as Chelates

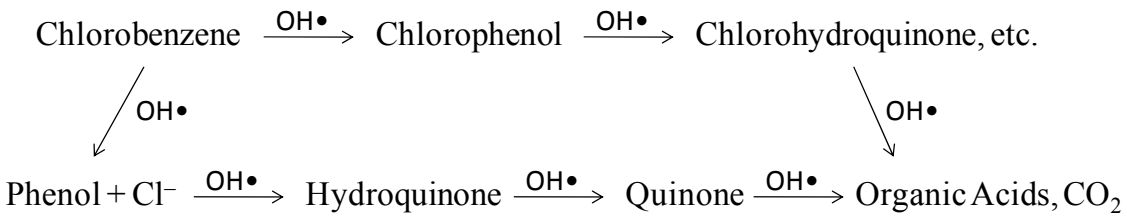

Figure 4.13 The Proposed Reaction Pathway for Chlorobenzene Oxidation by OH●

(adapted from Augusti et al., 1998)

degraded in about 1 h of reaction time. This suggests that hydroxylation reaction is the first step for a chlorinated aromatic compound oxidation by OH●. After further OH● oxidation, the aromatic ring will be ruptured and some organic acids or even carbon dioxide may be the final products. Sedlak and Andren (1991) did a degradation study for 2-chlorobiphenyl and found that seven hydroxychlorobiphenyls (5-hydroxy-2-chlorobiphenyl and six isomers) were intermediates of the oxidation reaction. after comparing the reaction rate constants of OH● with different PCBs, they also concluded that the ortho positions of PCBs were more difficult for hydroxylation reaction. From these studies, it is obvious that hydroxylated products and carboxylic acids will be major intermediates and final products for the oxidation of aromatic compounds by OH●. Since the superoxide radical anion ($O_2^{\bullet -}$) has the reduction ability during the chelate modified Fenton reaction (will be discussed in chapter 6), the intermediate and product analysis will be necessary to identify the dominating reaction pathway.

4.6.1 Product Analysis for TCP Oxidation by Using a Citrate Modified Fenton Reaction System

The product analysis for TCP oxidation by the chelate (citrate and PAA) modified Fenton reaction was carried out at different reaction times. The GC/FID chromatograph of TCP oxidation by a citrate modified Fenton reaction is shown in Figure 4.14. All the experiments for intermediate analysis were carried out at the following conditions: [TCP] = 1.5 mM, [Fe] = 10 mM, [citrate] **:** [Fe] = 1**:**1, $[H_2O_2]_0$ = 50 mM, and pH = 7. The sampling time-t is shown in the top left corner of each chromatograph. In order to

quantify the concentration of carboxylic acids, an internal standard- naphthalene d8 was used at each sample. The following observations can be concluded from Figure 4.14:

1) The several peaks appearing in less than 3 min at each chromatograph represented the solvent peaks-pentanes, as the note '1' inside the each chromatograph.
2) The peak at 21.428 min was identified as TCP since the peak areas also corresponded to the different TCP concentrations. It is obvious that the concentration of TCP decreases as reaction time increases. At the same time, some other peaks appear at different retention times of the chromatograph.
3) Peak "2" on the chromatograph was identified as a product of TCP oxidation. The retention time of peak "2" on the chromatograph of GC/FID is 9.764 min, and the peak area increases slightly after 72 h of reaction time with the further TCP oxidation.
4) Another peak '3' appears after 72 h of reaction time when TCP is below the minimum level. This peak-'3' was identified as another product of TCP oxidation because it had the same retention time as the standard on chromatograph of GC/FID. However, the reaction sample and standard could not be identified by GC/MS.
5) Some unknown peaks '4' appearing after 72 h of reaction time could not be identified by GC/MS. These unknown species may be by-products of TCP oxidation and need to be verified in further study.

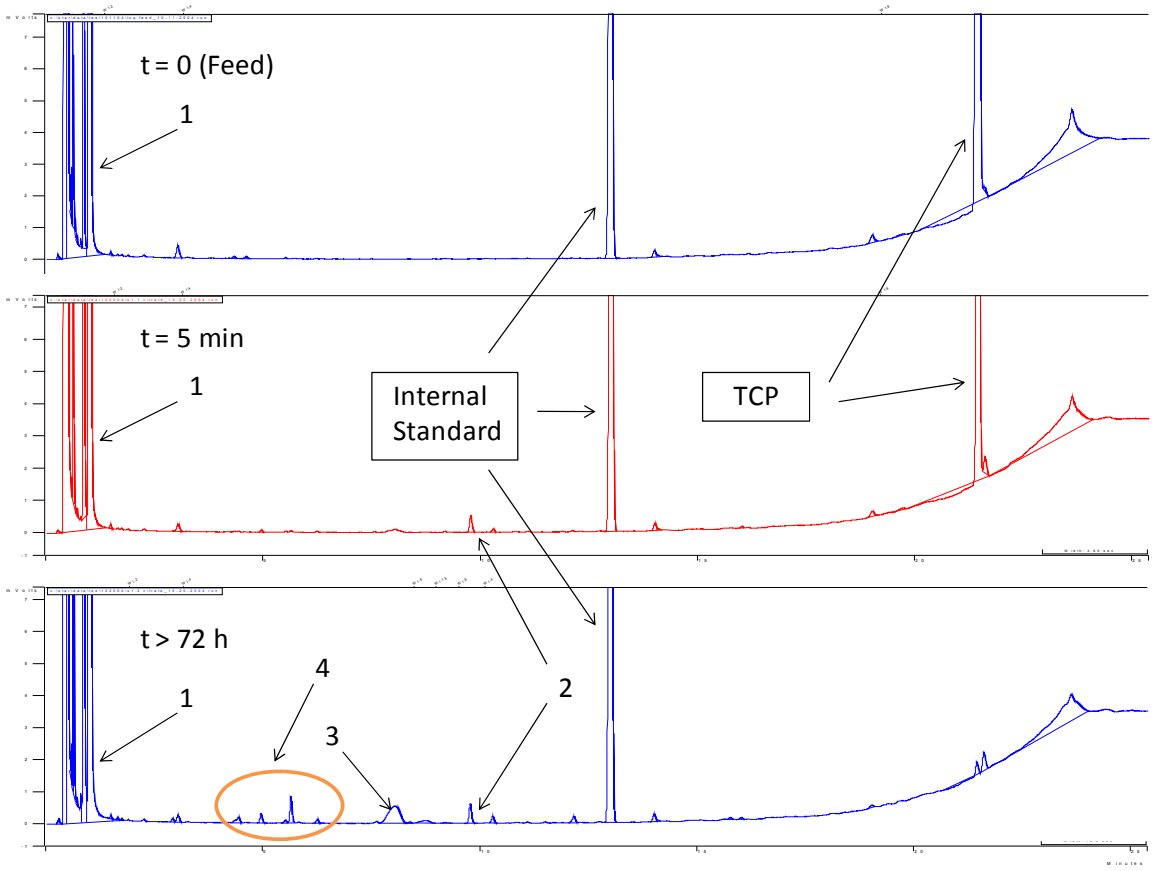

Figure 4.14 The Chromatographs of TCP Oxidation by the Citrate Modified Fenton Reaction (Analyzed by GC/FID)

4.6.1.1 Identification of Carboxylic Acids

Carboxylic acids are the common products from the oxidation of aromatic organic compounds. For example, several carboxylic acids (glycolic acid, glyoxylic acid, formic acid, malic acid, maleic acid, fumaric acid and oxalic acid) were identified by Boye et al. (2003a) during the oxidation of 2,4,5-trichlorophenoxyacetic acid by OH●. Sun and Pignatello (1993b) also identified oxalic acid and formic acid for the oxidation of 2,4-dichlorophenoxyacetic acid by $Fe^{3+}/H_2O_2/UV$. Thus, the identification of the carboxylic acids is an important step to verify the oxidation pathway of aromatic pollutant degradation. The derivatized (methanolic HCl) samples were analyzed by GC/MS, and the spectrum and retention time were used for identification of the unknown peaks which appeared in the chromatograph of Figure 4.14. The peak '2' of Figure 4.14 (GC/FID chromatograph) was identified as a derivatized malonic acid which had a retention time-6.015 min on the GC/MS chromatograph and the possibility to be a derivatized malonic acid is 78.31% according to the library of GC/MS. The spectra of derivatized reaction sample and standard are compared in Figure 4.15. The unknown peak '3' has the same retention time of the derivatized standard of oxalic acid on chromatograph of GC/FID. However, both derivatized reaction sample and the standard of oxalic acid could not be identified by the library of GC/MS. The possible reason is the library of GC/MS is limited to cover every spectra of each compound. However, the derivatized standard of oxalic acid was clearly shown on the chromatograph of GC/FID analysis and its peak

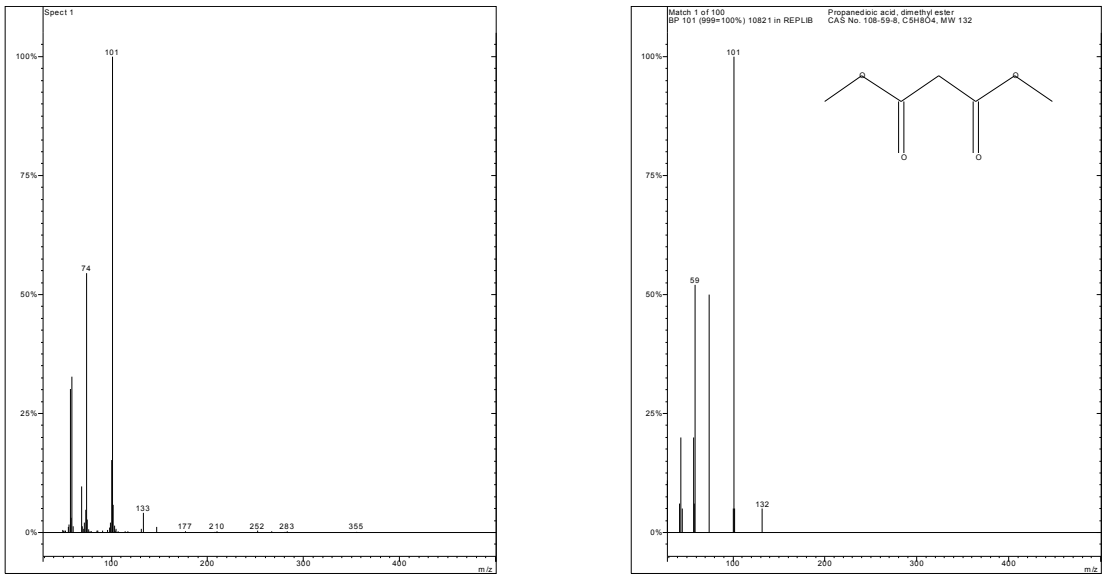

Figure 4.15 GC/MS Spectra of the Derivatized Malonic Acid: (A) Spectrum of the Reaction Sample, (B) Spectrum from the Library of GC/MS

area also corresponded to the different concentrations of derivatized oxalic acid standards (not shown).

4.6.1.2 Products Analysis for TCP Oxidation by Using a PAA Modified Fenton Reaction System

PAA acts as a poly-chelating agent during the TCP oxidation process by the chelate modified Fenton reaction. It should have the same reaction pathway of pollutant oxidation as a citrate modified Fenton reaction. Thus, it is very important to identify the intermediates or products of TCP oxidation by the PAA modified Fenton reaction to verify the reaction pathway. The product analysis for TCP oxidation by the PAA modified Fenton reaction is shown in Figure 4.16. The experimental condition is following: [TCP] = 1.5 mM, [Fe] = 10 mM, [COO^{-}] of PAA **:** [Fe] = 5 **:** 1, $[H_2O_2]_0$ = 50 mM, and pH 7. As mentioned in the previous section, the overall reaction rate of a PAA modified Fenton reaction is relatively slower than one of a citrate modified Fenton reaction under the same concentrations of iron ion and H_2O_2. From Figure 4.16, it is obvious that the concentration of malonic acid is small and the concentration of oxalic acid is below the detection limit, similar as the GC/FID chromatograph of TCP oxidation by the citrate modified Fenton reaction at 5 min of reaction time. On the basis of intermediate and product analysis, it can be concluded that a PAA modified Fenton reaction has the similar pollutants oxidation pathway as a citrate modified Fenton reaction.

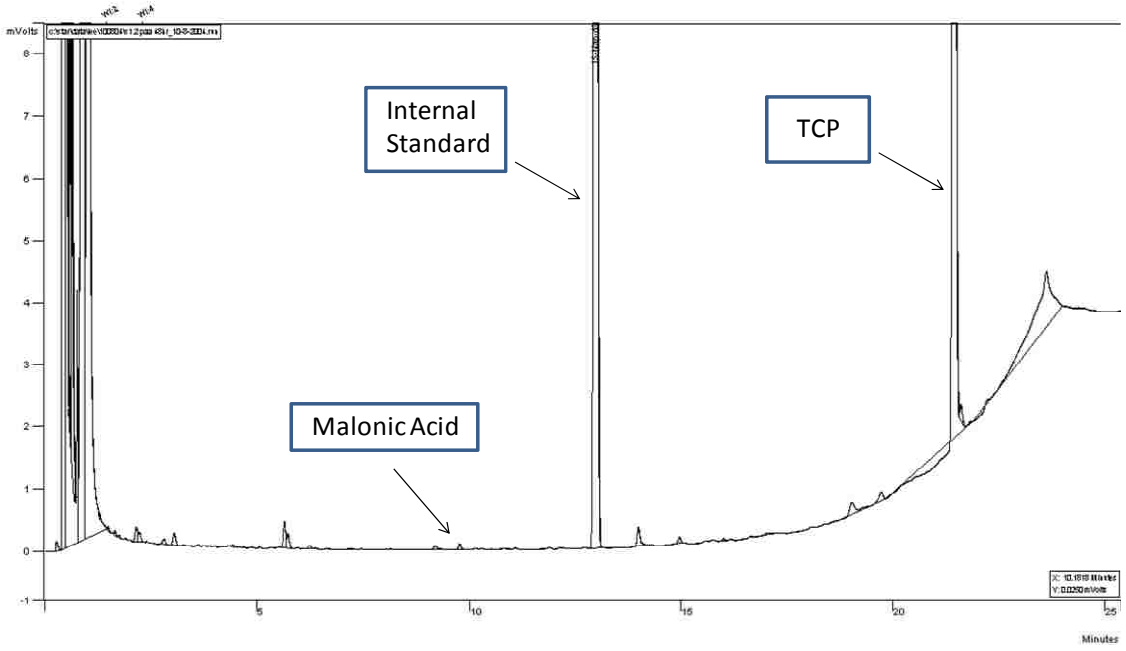

Figure 4.16 Product Analysis for TCP Oxidation by the PAA Modified Fenton Reaction at 48 h of Reaction Time (Analyzed by GC/FID)

4.6.2 Intermediate and Product Analysis for 2-Hydroxybiphenyl Oxidation by the Citrate Modified Fenton Reaction

According to Chen and Schuler (1993), hydroxybiphenyls (2-, 3-, and 4-hydroxybiphenyl) are direct intermediates of biphenyl oxidation process by OH●. They also identified several dihydroxybiphenyls from further hydroxybiphenyl oxidation by OH●. Brubaker and Hites (1998) also concluded that hydroxylation would be the first step for biphenyl oxidation (gas phase reaction) by OH● through the intermediate analysis. On the other hand, Cassidy et al. (2002) conducted experiments for 2,2′-dichlorobiphenyl and 2,3,4,2′,3′,4′-hexachlorobiphenyl oxidation by ozone. They found that two types of hydroxybenzoic acids (2-hydroxybenzoic acid and 2,3,4-trihydroxybenzoic acid), formic acid and oxalic acid were products from PCBs oxidation. Based on the information above, biphenyl oxidation by OH● will follow a hydroxylation reaction first, and further hydroxylation reaction may also take place after hydroxybiphenyl formation. Products of aromatic ring cleavage (such as: benzoic acid, hydroxybenzoic acid, etc) can be found from product analysis. Carboxylic acids or even CO_2 will be formed eventually if the oxidation reaction is maintained continuously.

Due to the low solubility of biphenyl, 2-hydroxybiphenyl was chosen as a parent compound in the intermediates analysis, since it is a well known intermediate of biphenyl oxidation. The result of intermediates and products analysis for 2-hydroxybiphenyl oxidation by the citrate modified Fenton reaction is shown in Figure 4.17. The Reaction

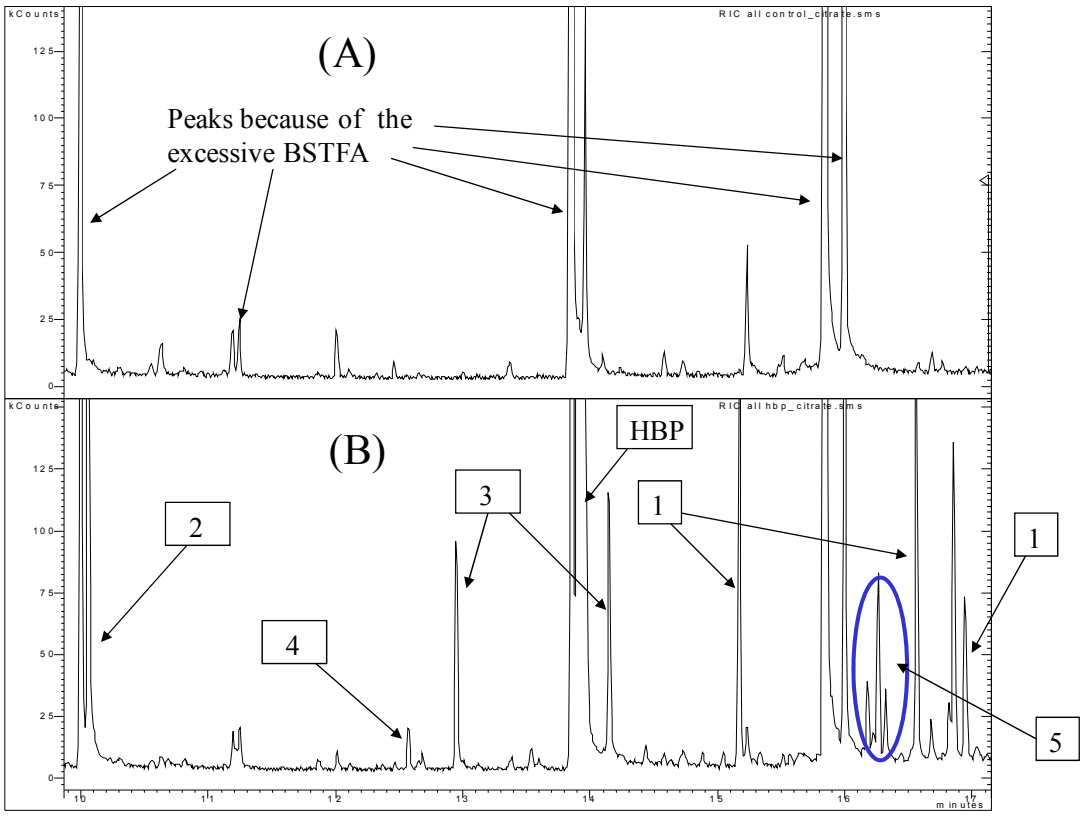

Figure 4.17 Chromatograph of Intermediate and Product Analysis for 2-Hydroxybiphenyl Oxidation by the Citrate Modified Fenton Reaction: (A) Control without 2-Hydroxybiphenyl. (B) Reaction Sample (HBP = 2-hydroxybiphenyl)

conditions are: [2-biphenyl] ~ 100mg/L, [Fe] = 2 mM, [Citrate] **:** [Fe] = 1**:**1, $[H_2O_2]_0$ = 5 mM, and pH 7. The reaction sample was taken at 2 h of reaction time and compared with the control samples to identify intermediates and products. In our analysis, there were two types of the control sample: 1) a sample had the same dosage of reactants as the reaction sample without 2-hydroxybiphenyl. 2) a sample had the same dosage of reactants as the reaction sample except of H_2O_2. The second control sample (not shown in Figure 4.17) was designed to verify feed-2 hydroxybiphenyl because its spectrum was not included in the GC/MS library. In order to be able to analyze carboxylic acids by GC/MS, N,o-bis (trimethylsilyl) trifluoroacetamide (BSTFA) was used as a derivatization reagent during the sample analysis.

Several observations can be made from the chromatogram of 2-hydroxybiphenyl oxidation by the citrate modified Fenton reaction as following:

1) Several peaks with different retention times appear on the all chromatographs. These may be caused by the high dosage of BSTFA used for the derivatization process and they are labeled in the chromatograph of the control sample to distinguish with other peaks.
2) Feed of 2-hydroxybiphenyl was confirmed by comparison of the reaction sample with the two control samples (one with 2-hydroxybiphenyl and the other without it) even though its spectrum could not be identified by the library of GC/MS. The peak area of 2-hydroxybiphenyl also corresponded to the different concentrations of feed samples.

3) Several unknown peaks (have been labeled in a sequence-“1”, “2” “3”, and “4” on the chromatograph) were identified as the intermediates or products by comparison with the spectra and retention times of the derivatized standards. These peaks will be discussed in detail in the following section.
4) Several unknown peaks (peaks referred as number ‘5’ and other peaks with different retention times that are not shown in Figure 4.17) may be some intermediates or by-products that could not be identified by the library of GC/MS. These peaks are needed to be identified in the further study.

4.6.2.1 Identification of Intermediates and Products

By comparing the spectra and retention times with the standards, several unknown peaks with label “1”, “2”, “3”, and ”4” in Figure 4.17 were identified by GC/MS. The chromatographs of the derivatized standard and reaction sample for those unknown peaks-“2”, “3”, and “4” are shown in Figure 4.18. The chromatographs of the derivatized standard and reaction sample for the unknown peaks-“1” are shown in Figure 4.19. There will be several isomers for hydroxylated intermediates or products (such as: dihydroxybiphenyl or hydroxybenzoic acid) according to the different positions of hydroxyl group. The quantification and identification of every isomer are beyond our research goals, and some specific isomers are not even commercially available, so only one of these isomers will be identified in our intermediate and product study.

According to Cassidy et al. (2002), dihydroxybiphenyls will be the products of hydroxybiphenyl oxidation by OH●. In our product analysis for 2-hydroxybiphenyl oxidation by the citrate modified Fenton reaction, three BSTFA-derivatized dihydroxybiphenyls (peaks "1") were observed (different retention times were caused by the different position of the second hydroxyl group), as shown in Figure 4.17. The mass spectra of 2,2′-dihydroxybiphenyl and reaction sample are compared in Figure 4.20. The retention times of three dihydroxybiphenyls are 15.17 min, 16.54 min and 16.94 min. The peak at 15.17 min is 2,2′-dihydroxybiphenyl and the other two peaks are isomers of 2,2′-dihydroxybiphenyl. These three peaks of the reaction sample have 80.71%, 75.11%, and 88.52% match of the spectra from the library of GC/MS, respectively.

On the other hand, many researchers were able to identify benzoic acid or chlorinated benzoic acid as one of the products for biphenyl or PCBs oxidation (Hong, et al., 1998; Cassidy, et al., 2002; Nomiyama, et al., 2007). Since the benzoic acid is the aromatic ring rupture product of PCBs and biphenyl, it is very important to identify this product to confirm the oxidation efficiency of the chelate modified Fenton reaction. The unknown peak '2' of Figure 4.17 was identified as a BSTFA-derivatized benzoic acid. The retention time of peak '2' was matched with that of a BSTFA-derivatized benzoic acid standard, shown in Figure 4.18. Furthermore, the spectra of the BSTFA-derivatized benzoic acid (peak '2') and the standard are shown in Figure 4.21. The retention time of the BSTFA-derivatized benzoic acid is 10.05 min and has a 46.6% match of spectrum from GC/MS library.

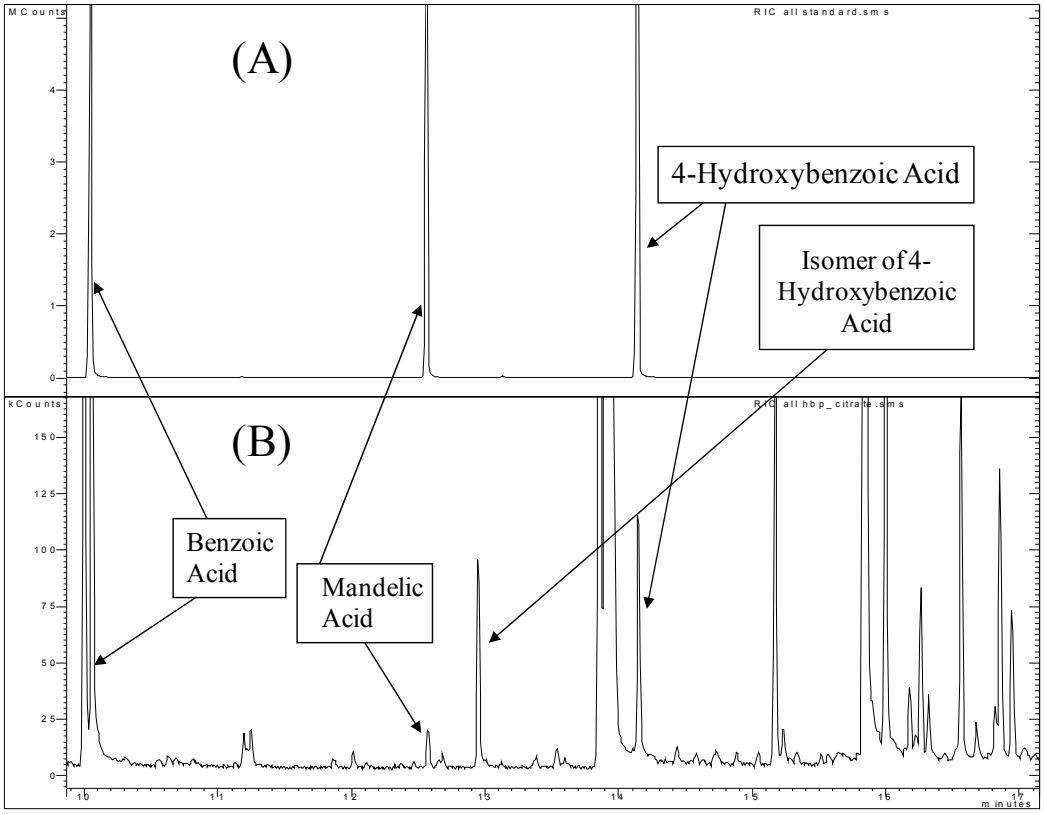

Figure 4.18 Chromatographs of Standard and Reaction Sample for Benzoic Acid, Hydroxybenzoic Acid, and Mandelic Acid: (A) Standard (B) Reaction Sample

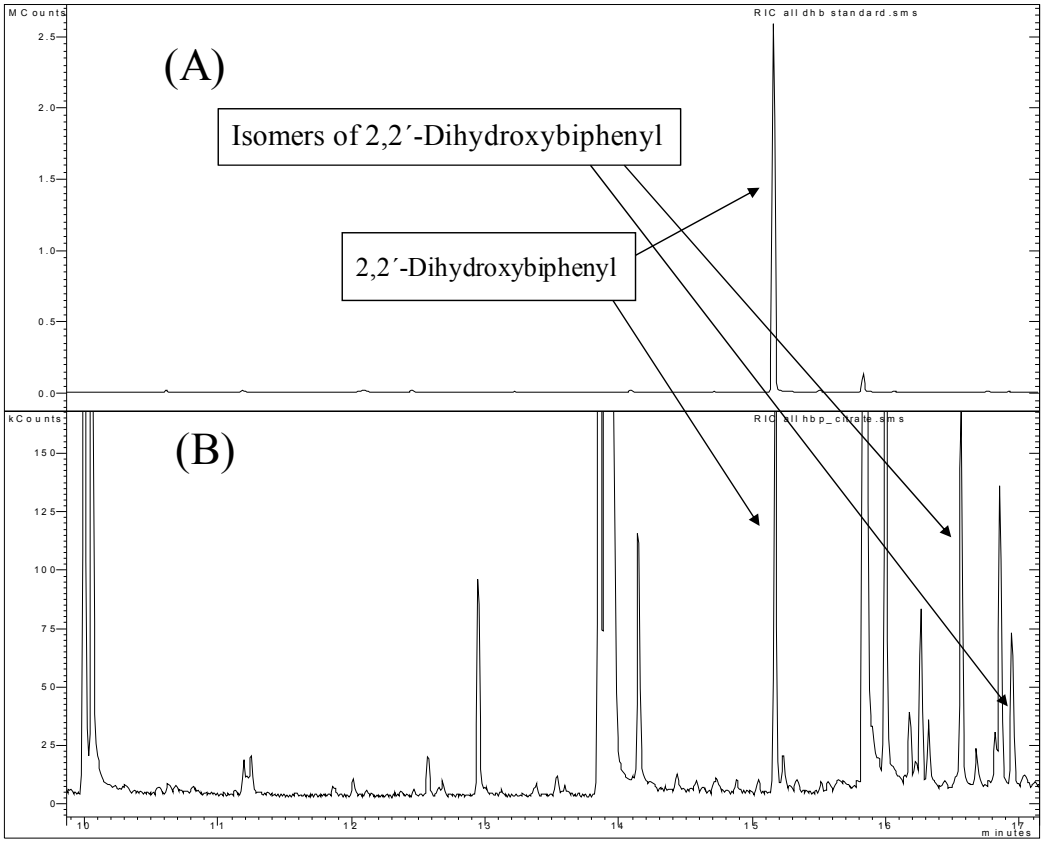

Figure 4.19 Chromatographs of Standard and Sample for 2,2′-Dihydroxybiphenyl: (A) Standard (B) Reaction Sample

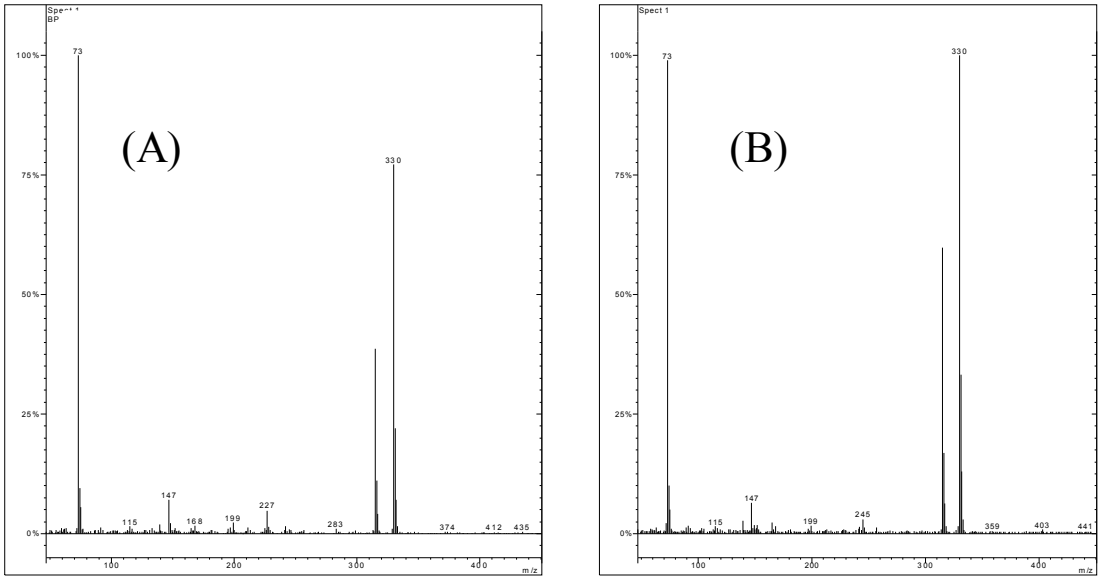

Figure 4.20 Spectra of the BSTFA-Derivatized 2,2′-Dihydroxybiphenyl: (A) Reaction Sample (B) Standard

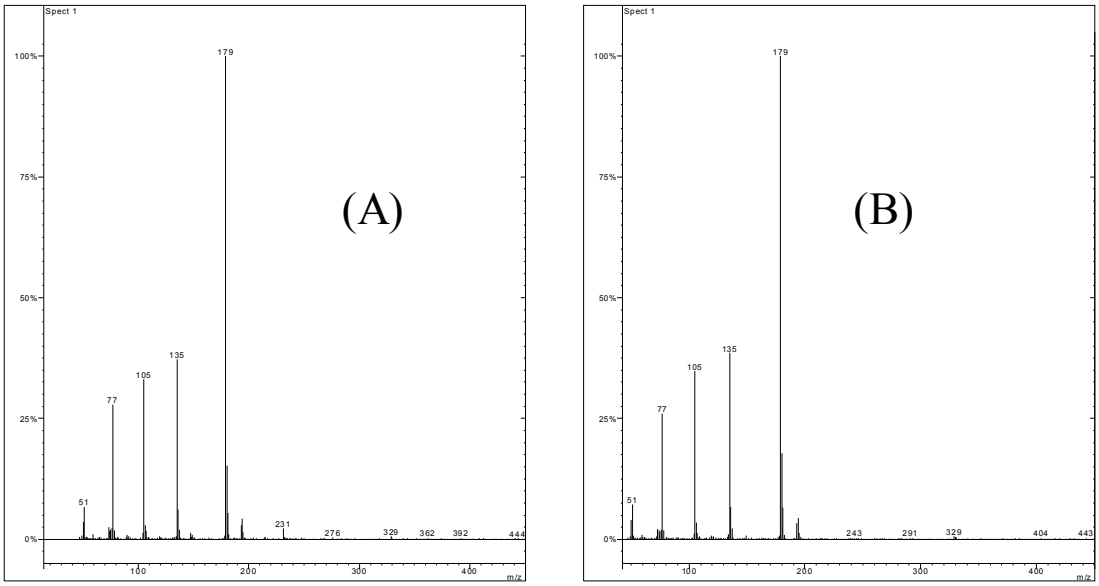

Figure 4.21 Spectra of BSTFA-Derivatized Benzoic Acid: (A) Reaction Sample (B) Standard

There are two unknown peaks labeled as ‘3’ in Figure 4.17. The different retention times may be caused by the isomers of a same compound. These unknown peaks ‘3’ were identified as a BSTFA-derivatized hydroxybenzoic acid. The peak at 14.14 min was identified as 4-hydroxybenzoic acid by comparing the retention time and mass spectra of the standard, as shown in Figure 4.22. Another peak at 12.94 min is an isomer of 4-hydroxybenzoic acid. According the GC/MS library, the possibility of match of these two peaks (12.94 min and 14.14 min) to the BSTFA-derivatized hydroxybenzoic acid are 69.1% and 68.67% respectively.

Another unknown peak ‘4’ shown in Figure 4.17 was identified as a BSTFA-derivatized mandelic acid formed from aromatic ring cleavage due to the hydroxybiphenyl oxidation. The spectra of BSTFA-derivatized mandelic acid standard and the reaction sample are shown in Figure 4.23. The retention time of peak ‘4’ is 12.57 min and has a 87.51% match of the spectrum from GC/MS library. All these intermediates and products that were identified by GC/MS are summarized in Table 4.1. Based on the carbon balance calculation, all identified intermediates and products contain 21.2% carbons of 2-hydroxybiphenyl (feed) loss, while the total carbon of intermediates, products, and remaining 2-hydroxybiphenyl is 85.6% of feed. Small carboxylic acids, such as oxalic acid, malonic acid, etc, should not be excluded from product list for biphenyl oxidation even though they are not found in the analysis. A possible reason for unable to identify these compounds is: the improper extraction method for highly hydrophilic chemicals at very low concentration.

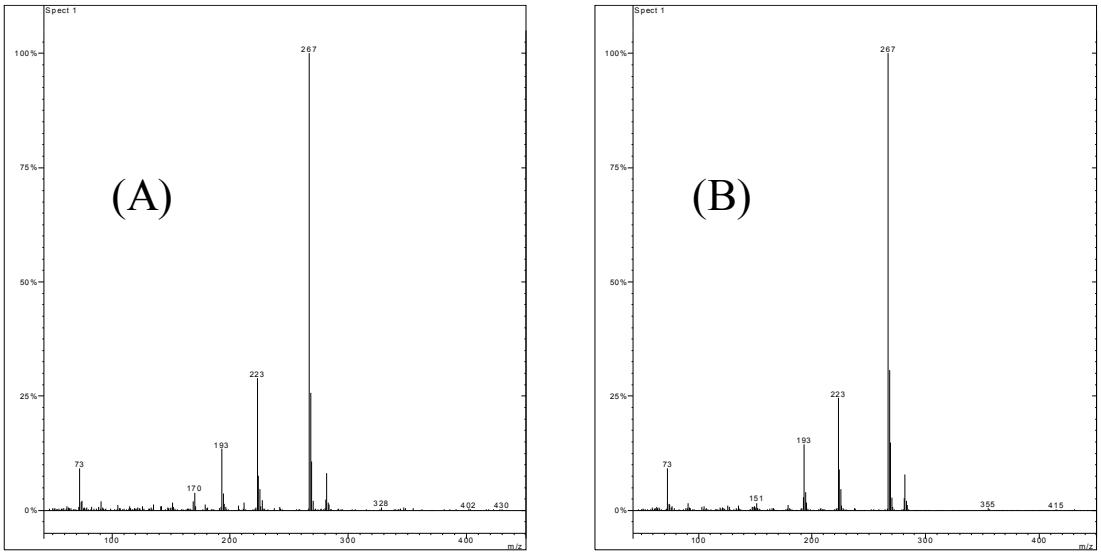

Figure 4.22 Spectra of BSTFA-Derivatized 4-Hydroxybenzoic Acid: (A) Reaction Sample (B) Standard

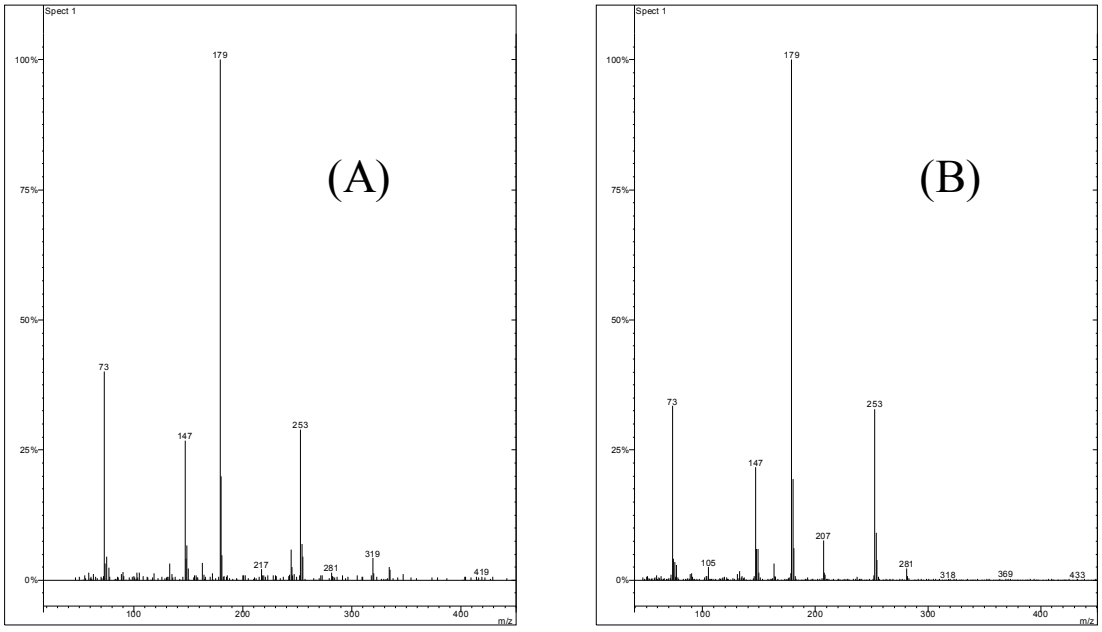

Figure 4.23 Spectra of BSTFA-derivatized Mandelic Acid: (A) Reaction Sample (B) Standard

Table 4.1 Identification of Intermediates and Products from 2-Hydroxybiphenyl Oxidation Corresponding to Unknown Peaks ("1", "2", "3", and "4") in Figure 4.17

Peak	Identified Compound Name	Retention Time (min)
1	Dihydroxybiphenyl isomers	15.17 [a]
		16.54
		16.94
2	Benzoic acid	10.05
3	Hydroxybenzoic acid isomers	12.94
		14.14 [b]
4	Mandelic acid	12.57

a: this peak was identified as 2,2′-dihydroxybiphenyl.

b: this peak was identified as 4-hydroxybenzoic acid.

4.6.2.2 Intermediate and Products Analysis for 2-Hydroxybiphenyl Oxidation by the PAA Modified Fenton Reaction

According to the reaction mechanism proposed in Figure 2.3, PAA acts as a poly-chelate during the chelate modified Fenton reaction. A chelating agent will be stable and non-reactive for OH● during the modified Fenton reaction. Thus, if this hypothesis of reaction mechanism for the chelate modified Fenton reaction is correct, the oxidation products of same pollutant should be unchanged for using different chelating agents. 2-hydroxybiphenyl was chosen as the parent compound for the intermediate and product analysis, which was the same as the citrate modified Fenton reaction experiments. The chromatograph of products analysis for the PAA modified Fenton reaction system is shown in Figure 4.24. The reaction conditions are: [2-hydroxybiphenyl] ~ 100 mg/L, [Fe] = 2 mM, [COO^-] of PAA **:** [Fe] = 3 **:** 1, $[H_2O_2]_0$ = 5 mM, pH 7, and the sample was taken at 2 h of reaction time. Based on the spectra and retention time, BSTFA-derivatized dihydroxybiphenyl (retention time: 15.17 min, 16.57 min and 16.94 min), benzoic acid (retention time: 10.06 min), and hydroxybenzoic acid (12.96 min and 14.16 min) were identified. Once again, peak at 15.17 min is 2,2′-dihydroxybiphenyl, and peak at 14.16 min is 4-hydroxybenzoic acid. All the intermediates and products identified in this study are summarized in Table 4.2. The intermediate and product analysis for the standard Fenton reaction system (pH 2.5) was also carried out, and the results of three systems (citrate, PAA, and standard) are shown in Figure 4.25. In order to compare the intermediates and products, the experiment conditions for the standard Fenton reaction

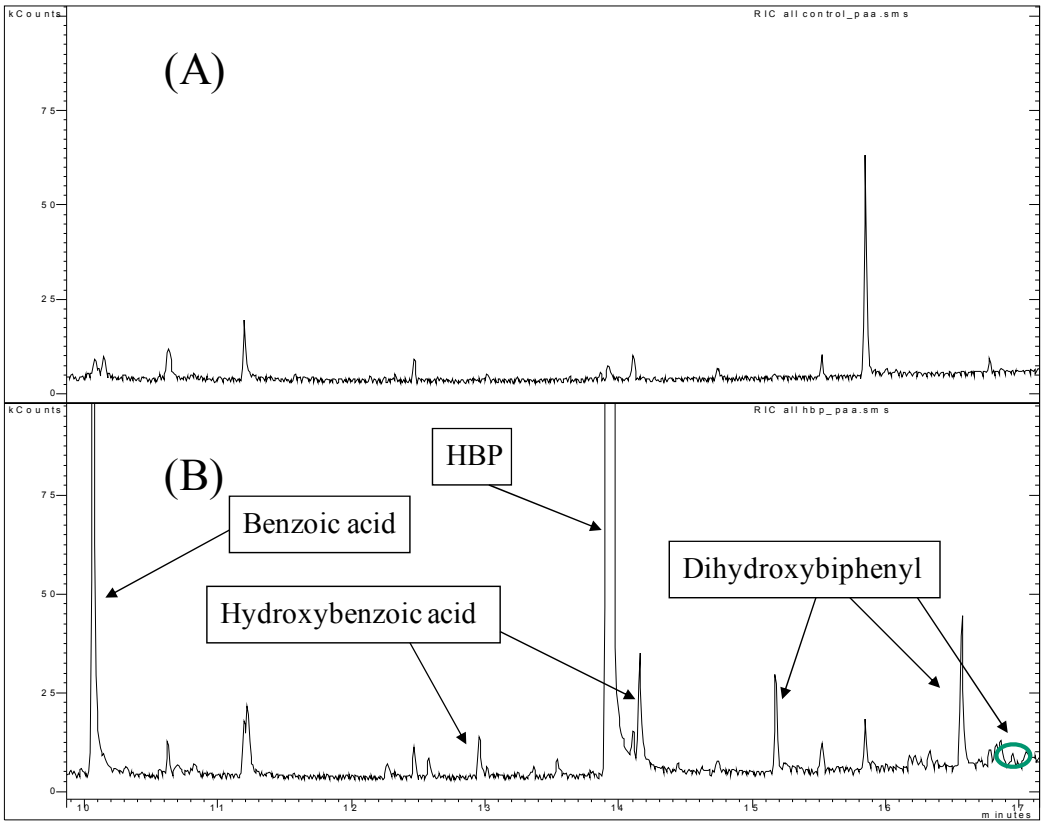

Figure 4.24 Intermediate and Product Analysis for 2-Hydroxybiphenyl Oxidation by a PAA Modified Fenton Reaction System: (A) Control Sample without 2-Hydroxybiphenyl; (B) Reaction Sample (HBP = 2-hydroxybiphenyl)

Table 4.2 Identification of Intermediates and Products from 2-Hydroxybiphenyl Oxidation Corresponding to the Unknown Peaks in Figure 4.24

Identified Compound Name	Retention Time (min)
Dihydroxybiphenyl isomers	15.17 [a]
	16.57
	16.94
Benzoic acid	10.06
Hydroxybenzoic acid isomers	12.96
	14.16 [b]

a: this peak was identified as 2,2′-dihydroxybiphenyl.

b: this peak was identified as 4-hydroxybenzoic acid.

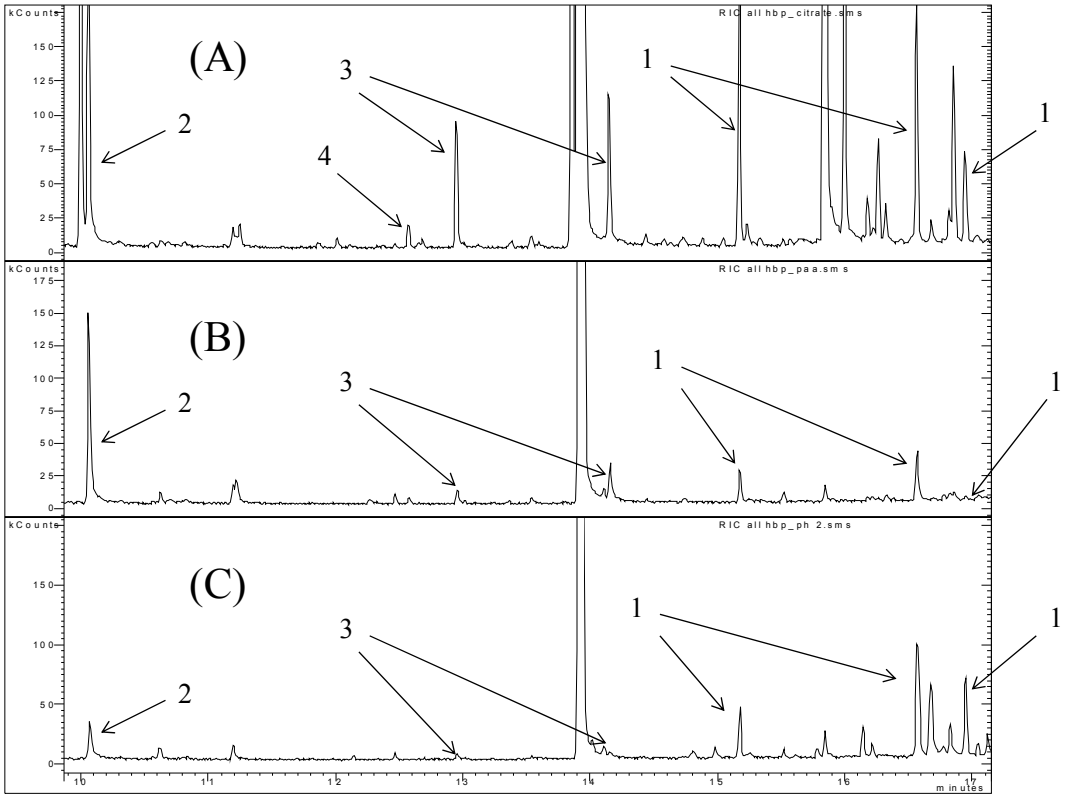

Figure 4.25 Intermediate and Product Analysis for 2-Hydroxybiphenyl Oxidation by Three Reaction Systems: (A) Citrate Modified Fenton Reaction; (B) PAA Modified Fenton reaction (C) Standard Fenton Reaction (1: Dihydroxybiphenyl; 2: Benzoic acid; 3: Hydroxybenzoic acid; 4: Mandelic acid)

are: [2-hydroxybiphenyl] ~ 100 mg/L, [Fe] = 0.2 mM, $[H_2O_2]_0$ = 0.5 mM, pH = 2.5 and sample was taken at 10 min of reaction time. The identification of BSTFA-derivatized dihydroxybiphenyls, benzoic acid, hydroxybenzoic acids as intermediates and products for 2-hydroxybiphenyl oxidation by these three reaction systems validates the proposed reaction mechanism for the chelate modified Fenton reaction in chapter 2 in another way: the use of a chelating agent (either a mono-chelate or a poly-chelate) will not alter the reaction pathway for pollutant oxidation. By summarizing the all information above, the proposed reaction pathway of biphenyl oxidation by the chelate modified Fenton reaction is shown in Figure 4.26.

4.7 Dechlorination of 2,2′-Dichlorobiphenyl Particles by the PAA Modified Fenton Reaction

Polychlorinated biphenyls (PCBs) are highly toxic chemicals for the environment and are present in the groundwater and wastewater due to industry process usage (Chen and Schuler, 1993; Cassidy et al., 2002; Aronstein, et al., 1995; Sedlak, et al., 1994). There are 209 PCB congeners according to the number of chlorines and the position of these chlorines substituents. All these PCB congeners have very limited solubility in water, for example, the solubility of 3,4,3′,4′-tetrachlorobiphenyl (PCB 77) is 1.95×10^{-3} μM (Mackay et al. 2006). Due to the low water solubility of PCB congeners, most of these congeners are present in the groundwater as particles or in DNAPLs form and become a continuous pollutant source for water contamination. It will be very beneficial for in-situ

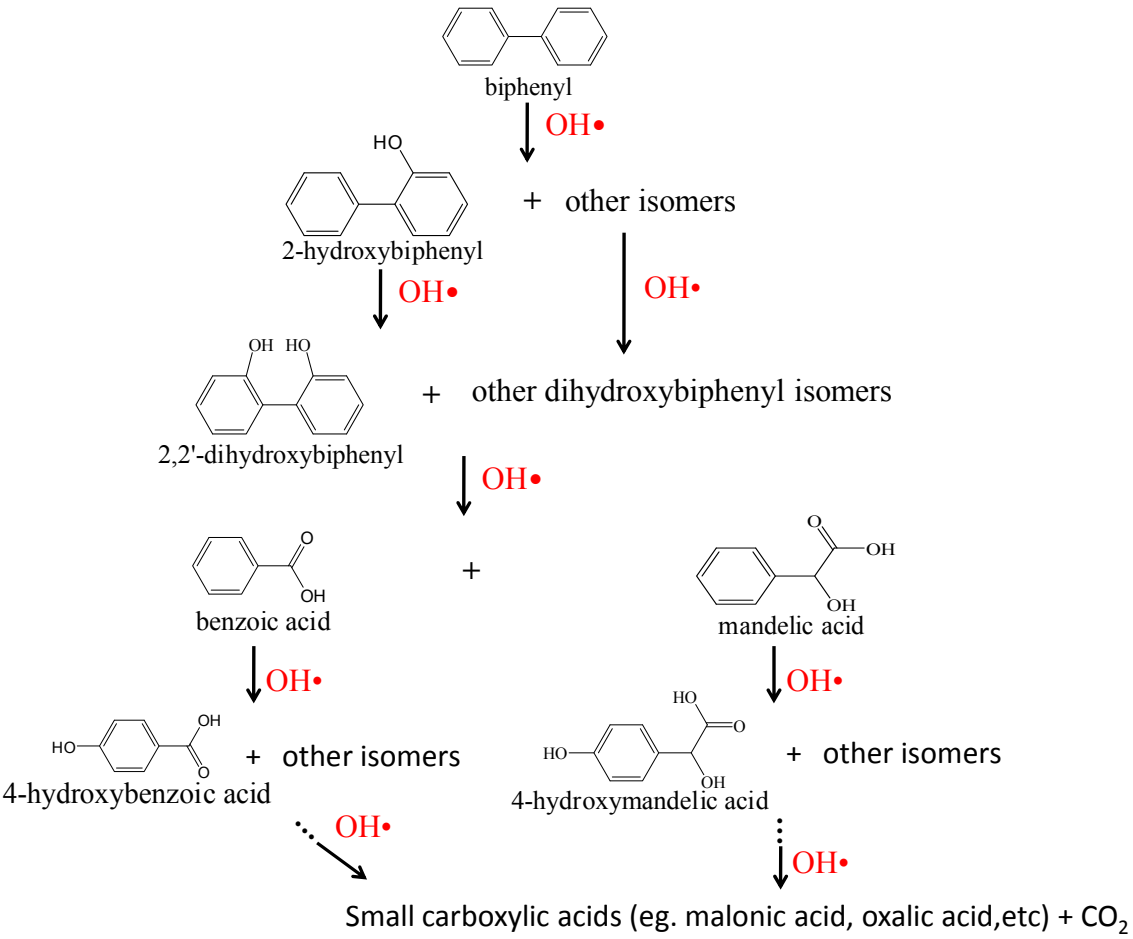

Figure 4.26 Proposed Reaction Pathway for Biphenyl Oxidation by Chelate Modified Fenton Reaction

groundwater remediation, if the remediation technique can be used for detoxifying the pollutant in its particle form.

Since the solubility of 2,2′-PCB is very small (~8.2 μM), chloride formation from a saturated solution will also be small (~16.4 μM). This will be difficult to analyze precisely with the chloride-selective electrode. However, the OH● generated may also react with 2,2′-PCB near the surface of solid 2,2′-PCB, or if the dissolution rate is fast, the dechlorination reaction can be sustained. Thus, if this hypothesis is correct, chloride formation will be much higher if the feed of 2,2′-PCB is 0.51 mM under the condition of continuous reaction. The chloride formation from 2,2′-PCB dechlorination by the PAA modified Fenton reaction is shown in Figure 4.27. It is evident that the chloride formation is continuously increased as long as H_2O_2 is present in the solution. The concentration of chloride after 9 h of reaction time is more than 100 μM, which is much higher than the 16.4 μM chloride from the soluble 2,2′-PCB. This indicates that the oxidation of low soluble PCBs by the chelate modified Fenton reaction can be used for heterogeneous systems containing pollutant particles. It must be noted, 2,2′-PCB is oxidized by free hydroxyl radical- OH●, not reduced by the superoxide radical anion. For a system with carbon tetrachloride, OH• will mainly react with H_2O_2 to generate superoxide radical anion ($O_2•^-$) because of a high reaction rate constant and high concentration of H_2O_2. The reaction between carbon tetrachloride and OH● is very slow due to a very low reaction rate constant (Teel and Watts, 2002). However, PCBs will be the main sink of OH● if any PCBs are present in the system. Consequently, the concentration of $O_2●^-$ is very low

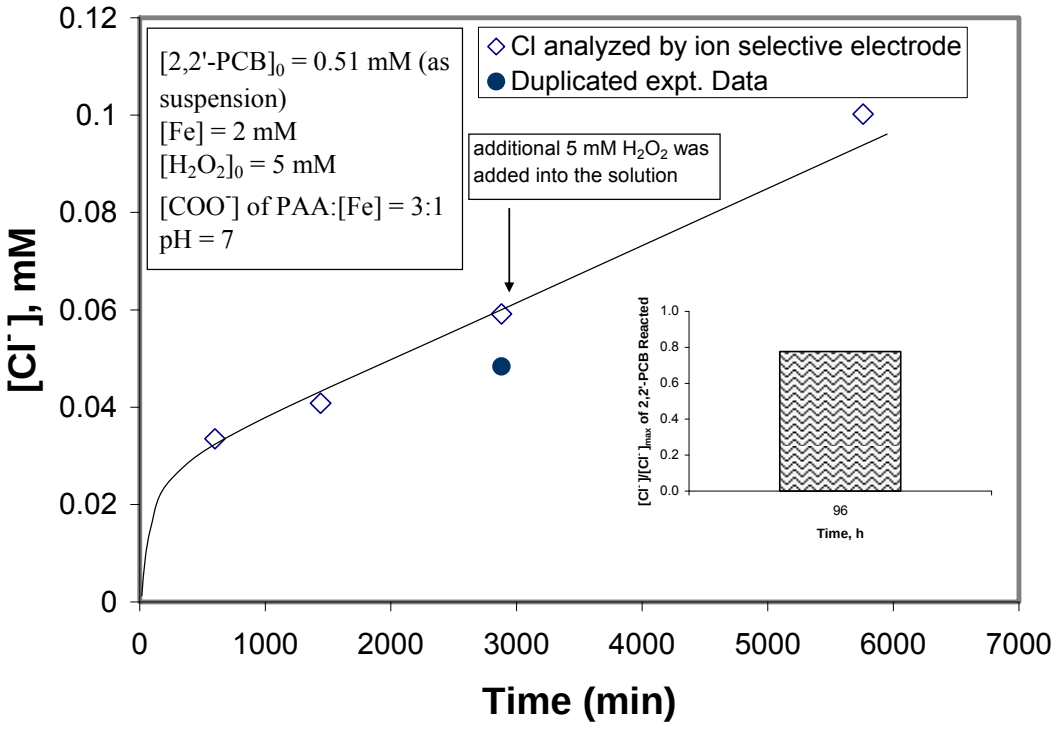

Figure 4.27 Cl^- Formation for 2,2′-PCB Dechlorination by PAA + Fe^{2+} + H_2O_2 System at pH 7

for a system with PCBs. Hence, the oxidation pathway caused by OH• dominates the PCBs dechlorination reaction. Tang and Huang (1996) believed that a ring hydroxylation usually took place at sites which were not occupied by a chlorine atom when OH● attacked the aromatic compound. Chloride entered the solution after the aromatic ring rupture. Augusti et al. (1998) found a similar behavior for chlorobenzene oxidation by Fenton's reagent, even though a very small amount of intermediates were formed through hydroxylation at the halogenated sites of the aromatic ring. Sedlak and Andren (1991) made the same conclusion through comparison of reaction rates of OH● and PCBs. The normalized chloride concentration was calculated by dividing the concentration of chloride in the sample by the maximum value of chloride formed from 2,2′-PCB reacted. From our experimental data, the normalized chloride value is 77.6% after 96 h of reaction time, which indicates aromatic ring cleavage of the 2,2′-PCB during the oxidation process.

Chapter 5. Kinetic Model for Chelate Modified Fenton Reaction

This chapter mainly consists of the kinetic study of TCP and biphenyl detoxification by the chelate modified Fenton reaction. A detail of chemistry about the chelating agent and iron ion was discussed and the species distribution results from the numerical calculation were compared with the data from literature. A comprehensive model based on the well-known Fenton chemistry and the equilibrium reactions of iron ion-chelating agent was set up and compared to the experimental data. Finally, the observation reaction rate constants of pollutant oxidation reactions by the chelate modified Fenton reaction are obtained from experimental data.

5.1 Chemistry of the Chelating Agent

As mentioned in chapter 2, the chemical structures of the mono-chelating agent (citric acid) and the poly-chelating agent (PAA) are different. For example, there are approximately 694 carboxyl groups available in a PAA molecule (the molecular weight of PAA used in our experiments is 50000 g/mol) for Fe^{2+}/Fe^{3+} chelation, while there are only three carboxyl groups available in a citric acid. The structure difference of polymer and mono-chelate (such as citrate) makes the equilibrium constants of metal–ligand different. Polymer PAA has a different molecular weight according to its chain length, and its application as a poly-chelate has not been reported for Fenton–type reactions. The equilibrium constants of PAA and Fe^{2+}/Fe^{3+} cannot be found from the literature. On the other hand, the equilibrium constants of mono-chelating agents (such as citrate) and

Fe^{2+}/Fe^{3+} are well-known. The *K* of citric acid and Fe^{2+}/Fe^{3+} are used in the kinetic model calculations.

The equilibrium reactions of iron ion (Fe^{2+} and Fe^{3+}) and chelating agent (citrate) are (Inczedy, 1976):

$$Fe^{2+} + L \Leftrightarrow Fe(II)L,\ K_{Fe(II)L} = 10^{15.5}\ M^{-1} \quad (5.1)$$

$$Fe^{2+} + HL \Leftrightarrow Fe(II)HL,\ K_{Fe(II)HL} = 10^{3.1}\ M^{-2} \quad (5.2)$$

$$Fe^{2+} + H^{+} + HL \Leftrightarrow Fe(II)H_2L,\ K_{Fe(II)H2L} = 10^{8.2}\ M^{-3} \quad (5.3)$$

$$Fe^{3+} + L \Leftrightarrow Fe(III)L,\ K_{Fe(III)L} = 10^{25}\ M^{-1} \quad (5.4)$$

$$Fe^{3+} + HL \Leftrightarrow Fe(III)HL,\ K_{Fe(III)HL} = 10^{11.8}\ M^{-2} \quad (5.5)$$

$$Fe^{3+} + H^{+} + HL \Leftrightarrow Fe(III)H_2L,\ K_{Fe(III)H2L} = 10^{12.4}\ M^{-3} \quad (5.6)$$

$$H^{+} + L \Leftrightarrow HL,\ K_{HL} = 10^{16}\ M^{-1} \quad (5.7)$$

$$H^{+} + HL \Leftrightarrow H_2L,\ K_{H2L} = 10^{6.1}\ M^{-1} \quad (5.8)$$

$$2H^{+} + HL \Leftrightarrow H_3L,\ K_{H3L} = 10^{10.5}\ M^{-2} \quad (5.9)$$

$$3H^{+} + HL \Leftrightarrow H_4L,\ K_{H4L} = 10^{13.5}\ M^{-3} \quad (5.10)$$

(For simplicity, charges for L and L–containing species are not indicated above. For citrate, L is L^{4-}).

It is important to note that the equilibrium constants *K* of citric acid and Fe^{2+}/Fe^{3+} is a quite controversial topic even though there are many scientists who had done a lot of studies on this compound. Königsberger et al. (2000) suggested that this controversy might be caused by the hydroxylate group of citric acid. It is obvious that the equilibrium constants, $K_{Fe(II)HL}$, $K_{Fe(II)H2L}$, $K_{Fe(III)HL}$, $K_{Fe(III)H2L}$, K_{H2L}, K_{H3L}, and K_{H4L} above, are within

the range given by Königsberger et al. (2000) Although the hydroxylate group of citric acid is quite difficult to dissociate, it cannot be negligible at a neutral pH environment, as shown in Figure 2.5. Thus, there were four dissociable protons for a citric acid in our model calculation. Other metal-citrate species (such as FeL_2, FeL_2H, FeL_2OH, etc.) are very small for the ratio of Fe to citrate = 1:1, so these species are not included in our model calculation.

The hydrolysis reactions for iron ion (Fe^{2+} and Fe^{3+}) are as follows (Pignatello et al., 2006; Baes and Mesmer, 1976):

$$Fe^{2+} + H_2O \Leftrightarrow Fe(OH)^+ + H^+,\ K_1 = 10^{-9.5}\ M \quad (5.11)$$

$$Fe^{2+} + 2H_2O \Leftrightarrow Fe(OH)_2 + 2H^+,\ K_2 = 10^{-20.5}\ M^2 \quad (5.12)$$

$$Fe^{3+} + H_2O \Leftrightarrow Fe(OH)^{2+} + H^+,\ K_3 = 10^{-3.05}\ M \quad (5.13)$$

$$Fe^{3+} + 2H_2O \Leftrightarrow Fe(OH)_2^+ + 2H^+,\ K_4 = 10^{-6.31}\ M^2 \quad (5.14)$$

$$2Fe^{3+} + 2H_2O \Leftrightarrow Fe_2(OH)_2^{4+} + 2H^+,\ K_5 = 10^{-2.95}\ M \quad (5.15)$$

On the base of material balance, the following equation can be obtained:

$$[Fe(II)] = [Fe^{2+}] + [Fe(OH)^+] + [Fe(OH)_2] + [Fe(II)L] + [Fe(II)HL] + [Fe(II)H_2L] \quad (5.16)$$

$$[Fe(III)] = [Fe^{3+}] + [Fe(OH)^{2+}] + [Fe(OH)_2^+] + [Fe_2(OH)_2^{4+}] + [Fe(III)L] + [Fe(III)HL] + [Fe(III)H_2L] \quad (5.17)$$

$$[Fe] = [Fe(II)] + [Fe(III)] \quad (5.18)$$

$$[L]_{total} = [L] + [HL] + [H_2L] + [H_3L] + [H_4L] + [Fe(II)L] + [Fe(II)HL] + [Fe(II)H_2L] + [Fe(III)L] + [Fe(III)HL] + [Fe(III)H_2L] \quad (5.19)$$

On the base of the material balance (eqs 5.16−5.19), the Fe^{2+} and Fe^{3+} equilibrium reactions 5.1–5.15 listed above, and the condition $[L]_{total}$ **:** [Fe] = 1**:**1, the following equations can be obtained:

$$[Fe(II)] = K_m' \times [Fe^{2+}] + K_{ml}' \times [Fe^{2+}] \times [Fe]/(K_{hl}' + K_{ml}' \times [Fe^{2+}] + K_{nl}' \times [Fe^{3+}]) \quad (5.20)$$

$$[Fe(III)] = K_n' \times [Fe^{3+}] + K_{nl}' \times [Fe^{3+}] \times [Fe]/(K_{hl}' + K_{ml}' \times [Fe^{2+}] + K_{nl}' \times [Fe^{3+}]) + K_5 \times [Fe^{3+}]^2/[H^+]^2 \quad (5.21)$$

$$[Fe] = [Fe(II)] + [Fe(III)] \quad (5.22)$$

Where $K_{ml}' = K_{Fe(II)L} + K_{Fe(II)HL} \times [H^+] + K_{Fe(II)H2L} \times [H^+]^2$, $K_m' = 1 + K_1/[H^+] + K_2/[H^+]^2$, $K_n' = 1 + K_3/[H^+] + K_4/[H^+]^2$, and $K_{nl}' = K_{Fe(III)L} + K_{Fe(III)HL} \times [H^+] + K_{Fe(III)H2L} \times [H^+]^2$, $K_{hl}' = K_{HL} \times [H^+] + K_{HL} \times K_{H2L} \times [H^+]^2 + K_{HL} \times K_{H3L} \times [H^+]^3 + K_{HL} \times K_{H4L} \times [H^+]^4$.

By solving eqs 5.20, 5.21, and 5.22 simultaneously for different [Fe(II)], the profiles of concentration of free Fe^{2+} ($[Fe^{2+}] + [Fe(OH)^+] + [Fe(OH)_2]$) and free Fe^{3+} ($[Fe^{3+}] + [Fe(OH)^{2+}] + [Fe(OH)_2^+] + [Fe_2(OH)_2^{4+}]$) can be obtained (Figure 5.1). Another set of data for free Fe^{2+} and free Fe^{3+} will be obtained also by using $\beta_{011} = 10^{6.10}$ for K_{H2L}, $\beta_{012} = 10^{10.636}$ for K_{H3L}, $\beta_{013} = 10^{13.742}$ for K_{H4L}, $\beta_{110} = 10^{4.80}$ for $K_{Fe(II)HL}$, $\beta_{111} = 10^{8.62}$ for $K_{Fe(II)H2L}$, $\beta_{110}' = 10^{11.18}$ for $K_{Fe(III)HL}$, $\beta_{111} = 10^{12.37}$ for $K_{Fe(III)H2L}$ (β_{011}, β_{012}, β_{013}, β_{110}, β_{111}, β_{110}', β_{111}' are taken from Königsberger et al. (2000)) The variations of two sets of calculation data are within 1.5%, as shown in Figure 5.1.

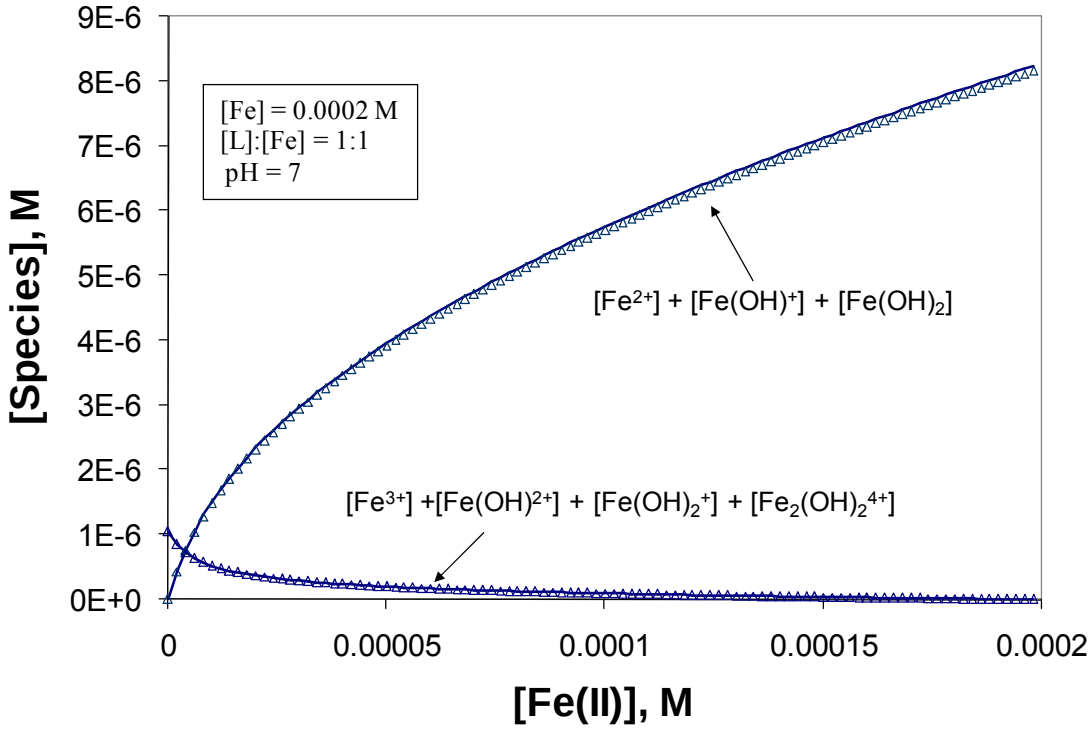

— Model simulation by using equilibrium constants: K_{HL}, K_{H2L}, K_{H3L}, K_{H4L}, $K_{Fe(II)L}$, $K_{Fe(II)HL}$, $K_{Fe(II)H2L}$, $K_{Fe(III)L}$, $K_{Fe(III)HL}$, $K_{Fe(III)H2L}$

△ Model simulation by using equilibrium constants: K_{HL}, β_{011}, β_{012}, β_{013}, $K_{Fe(II)L}$, β_{110}, β_{111}, $K_{Fe(III)L}$, β_{110}', β_{111}'

Figure 5.1 Iron Ion Hydroxylated Species Distribution at pH 7

5.2 Kinetic Model for Chelate Modified Fenton Reaction

For the chelate modified Fenton reaction, there are two assumptions for kinetic modeling: (1) the reaction between chelate (L, Fe^{2+}-L, and Fe^{3+}-L) and OH● or H_2O_2 is very slow and can be considered negligible; and (2) the equilibrium between Fe^{2+} and Fe^{2+}–L is always maintained.

5.2.1 Kinetic Model for Reaction without Pollutant

The common main reactions in the Fenton reaction system without pollutant are well-known, as shown in Table 5.1 (Pignatello et al., 2006; De Laat and Gallard, 1999; Lin and Gurol, 1998). On the base of these reactions, the following equations are obtained (r_1, r_2… r_{16} are reaction rates of reaction 1-16 in Table 5.1):

$$\frac{\mathrm{d}[\mathrm{Fe}^{2+}]}{\mathrm{d}t} = -r_1 + r_2 - r_3 - r_4 + r_5 + r_{12} - r_{13} \tag{5.23}$$

$$\frac{\mathrm{d}[\mathrm{H_2O_2}]}{\mathrm{d}t} = -r_1 - r_2 - r_6 - r_7 + r_8 + r_9 + r_{13} + r_{14} \tag{5.24}$$

$$\frac{\mathrm{d}[\mathrm{OH}\bullet]}{\mathrm{d}t} = r_1 - r_3 - r_6 + r_7 - r_9 - r_{15} - r_{16} \tag{5.25}$$

$$\frac{\mathrm{d}[\mathrm{Fe}^{3+}]}{\mathrm{d}t} = r_1 - r_2 + r_3 + r_4 - r_5 - r_{12} + r_{13} \tag{5.26}$$

$$\frac{\mathrm{d}[\mathrm{HO_2}\bullet]}{\mathrm{d}t} = r_2 - r_4 - r_5 + r_6 - r_7 - r_8 - r_{10} + r_{11} - r_{14} - r_{15} \tag{5.27}$$

Table 5.1 Fenton Reaction Sequences

r_1	$Fe^{2+} + H_2O_2 \rightarrow Fe^{3+} + OH\bullet + OH^-$	$k_1 = 63\ M^{-1} s^{-1}$
r_2	$Fe^{3+} + H_2O_2 \rightarrow Fe^{2+} + H^+ + HO_2\bullet$	$k_2 = 2\times10^{-3}\ M^{-1} s^{-1}$
r_3	$OH\bullet + Fe^{2+} \rightarrow Fe^{3+} + OH^-$	$k_3 = 3.2\times10^{8}\ M^{-1} s^{-1}$
r_4	$HO_2\bullet + Fe^{2+} \rightarrow Fe^{3+} + HO_2^-$	$k_4 = 1.2\times10^{6}\ M^{-1} s^{-1}$
r_5	$HO_2\bullet + Fe(III) \rightarrow Fe(II) + O_2 + H^+$	$k_5 = 2\times10^{3}\ M^{-1} s^{-1}$
r_6	$OH\bullet + H_2O_2 \rightarrow H_2O + HO_2\bullet$	$k_6 = 3.3\times10^{7}\ M^{-1} s^{-1}$
r_7	$HO_2\bullet + H_2O_2 \rightarrow H_2O + OH\bullet + O_2$	$k_7 = 3.1\ M^{-1} s^{-1}$
r_8	$HO_2\bullet + HO_2\bullet \rightarrow H_2O_2 + O_2$	$k_8 = 8.3\times10^{5}\ M^{-1} s^{-1}$
r_9	$OH\bullet + OH\bullet \rightarrow H_2O_2$	$k_9 = 6\times10^{9}\ M^{-1} s^{-1}$
r_{10}	$HO_2\bullet \rightarrow H^+ + O_2\bullet^-$	$k_{10} = 1.58\times10^{5}\ M^{-1} s^{-1}$
r_{11}	$H^+ + O_2\bullet^- \rightarrow HO_2\bullet$	$k_{11} = 1\times10^{10}\ M^{-1} s^{-1}$
r_{12}	$O_2\bullet^- + Fe^{3+} \rightarrow Fe^{2+} + O_2$	$k_{12} = 5\times10^{7}\ M^{-1} s^{-1}$
r_{13}	$O_2\bullet^- + Fe^{2+} \xrightarrow{2H^+} Fe^{3+} + H_2O_2$	$k_{13} = 1\times10^{7}\ M^{-1} s^{-1}$
r_{14}	$HO_2\bullet + O_2\bullet^- + H_2O \rightarrow H_2O_2 + O_2 + OH^-$	$k_{14} = 9.7\times10^{7}\ M^{-1} s^{-1}$
r_{15}	$OH\bullet + HO_2\bullet \rightarrow H_2O + O_2$	$k_{15} = 7.1\times10^{9}\ M^{-1} s^{-1}$
r_{16}	$OH\bullet + O_2\bullet^- \rightarrow OH^- + O_2$	$k_{16} = 1.01\times10^{10}\ M^{-1} s^{-1}$

$$\frac{d[O_2 \bullet^-]}{dt} = r_{10} - r_{11} - r_{12} - r_{13} - r_{14} - r_{16} \quad (5.28)$$

By solving the ordinary differential eqs 5.23–5.28 (using the Numerical Differentiation Formulas method, NDFs) simultaneously with initial conditions ($[Fe^{2+}]_0$, $[H_2O_2]_0$, and pH value), the concentration profiles of Fe^{2+}, H_2O_2, OH● , Fe^{3+}, HO_2● , and O_2●$^-$ at different reaction times can be obtained. Figure 5.2 shows that the H_2O_2 decomposition profile at pH 2.5 calculated from the above kinetic model fits well with the experimental data.

However, the numerical calculation based on the kinetic model of chelate modified Fenton reaction is quite different. The equilibrium reactions 5.1−5.15 are still maintained during Fenton reaction process. Thus, the kinetic model calculation for the chelate modified Fenton reaction can be obtained by the conjunction of eqs 5.20–5.22 and 5.23–5.28. The detail of the calculation diagram of the chelate modified Fenton reaction is shown in Figure 5.3. The H_2O_2 decomposition profile at pH 7 for the chelate reaction (citrate as chelate) calculated from the kinetic model (eqs 5.20–5.28) fits well with the experimental data, as also shown in Figure 5.2. However, the model predicted that $[H_2O_2]/[H_2O_2]_0$ was 0.45 after 24 h of reaction time, while the experimental data showed that $[H_2O_2]/[H_2O_2]_0$ was 0.32 with a standard deviation of 6.7%. The possible reason may be the pH variation during the experiments. Since metal–ligand is very sensitive for pH, a small pH variation may affect the overall reaction kinetics.

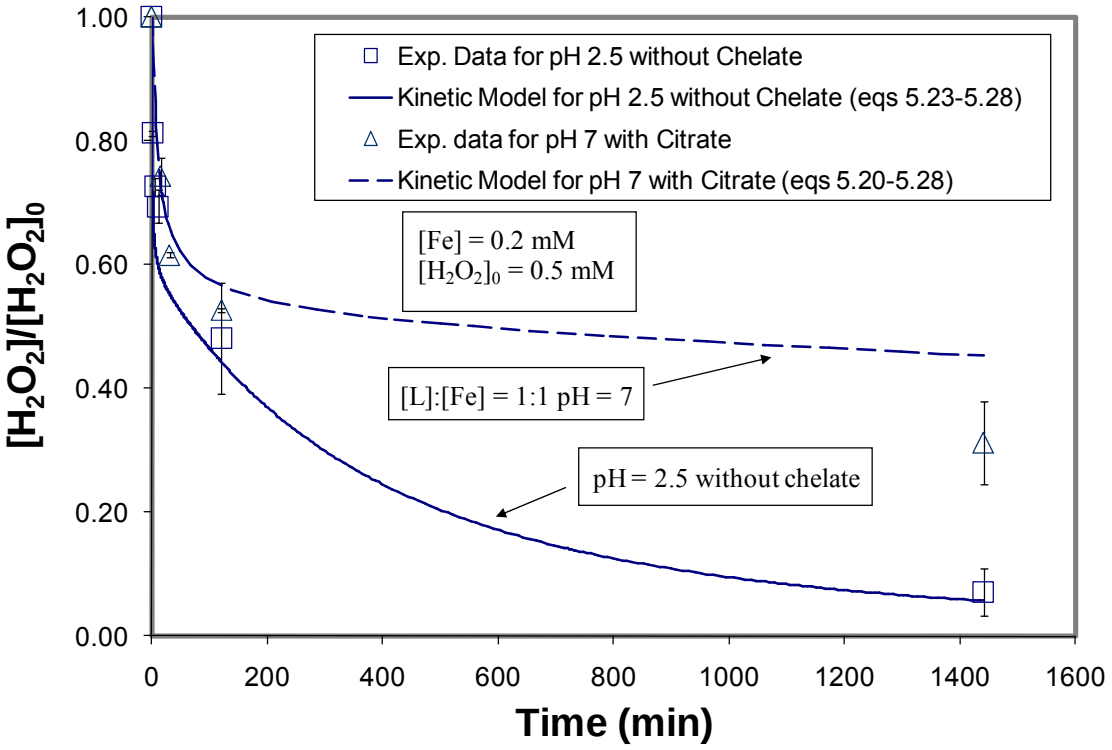

Figure 5.2 H_2O_2 Decomposition Profile and Kinetic Model Calculation for Fe^{2+} + H_2O_2 System

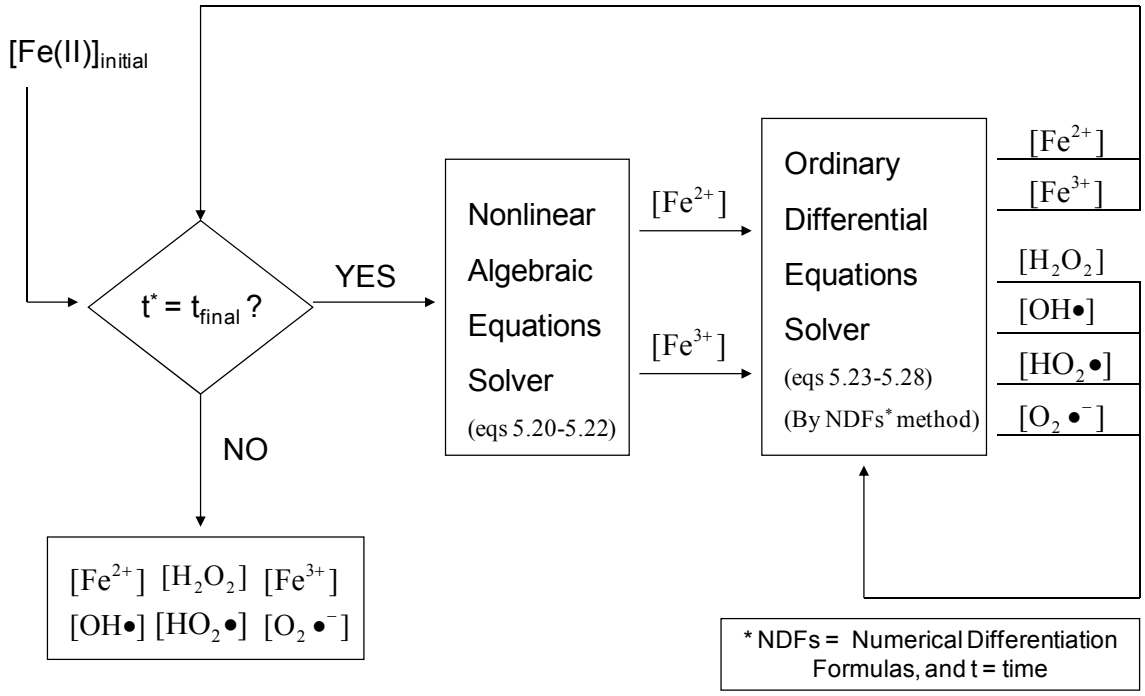

Figure 5.3 Schematic Diagram of Numeric Calculation Procedure for Kinetic Model of Chelate Based Modified Fenton Reaction

5.2.2 Kinetic Model for Reaction with a Pollutant

Organic pollutant oxidation by OH● is reported to be a second-order reaction (Pignatello et al., 2006; Tang and Huang, 1996; Benitez et al, 1999; Chu and Law, 2003), which can be expressed as:

$$\frac{\mathrm{d[A]}}{\mathrm{d}t} = -k_{\mathrm{A,OH}}[\mathrm{A}][\mathrm{OH}\bullet] \tag{5.29}$$

where A represents the organic pollutant.

The reaction rate constant $k_{\mathrm{A,\,OH}}$ is known for many organic pollutants. However, OH● is a very reactive species with a short lifetime. Hence, the concentration of OH● is difficult to measure directly in the experiment. From the free radical reaction theory, OH● generated by Fe^{2+} and H_2O_2 will attack pollutants through hydrogen abstraction or addition (Walling, 1975; Luo et al., 1997; Mckinzi and Dichristina, 1999). The organic radicals formed will decompose to intermediates. Eventually, organic acids or even carbon dioxide will be formed as final products through further oxidation reactions if OH● is still available. On the base of the information above, the reaction system with organic pollutant is more complicated than the one where only ferrous salt and H_2O_2 are present. In theory, the kinetic models for reactants or products can be established through numerical calculation of ordinary differential equations if all the reactions and reaction rate constants are known. However, many intermediate reactions in the pollutant oxidation process by OH● are still not clearly established and some intermediates (such as quinone) can reduce Fe^{3+} to Fe^{2+} to accelerate the oxidation reaction (Pignatello et al., 2006), so that a kinetic model that is directly based on all reactions in the system is not

feasible. Reaction 1 in Table 5.1 is a slow reaction with a reaction rate constant of 63 $M^{-1}s^{-1}$ in comparison to the other reactions listed in Table 5.1. Reaction 1 is also the major source for generation of OH●, and it becomes the rate-limiting step since other OH• consumers have higher reaction rates. As a result, [OH●] is very low and can be assumed as constant in the reaction system (Benitez et al, 1999 and 2001).

On the base of eq 5.29, TCP dechlorination can be expressed as:

$$\frac{[\text{TCP}]}{[\text{TCP}]_0} = \exp(-(k_{\text{TCP}})' \times t) \tag{5.30}$$

It should be noted that $(k_{\text{TCP}})'$ is a function of hydroxyl radical concentration ($(k_{\text{TCP}})' = k_{\text{TCP,OH}\bullet} \times$ [OH●]). The observed rate constants $(k_{\text{TCP}})'$ can be obtained by experimental data correlation (non-linear least-square method) from equation 5.30 at different pH environments. The observed $(k_{\text{TCP}})'$ is $(1.01 \pm 0.39) \times 10^{-2}$ min^{-1}, $(8.11 \pm 0.15) \times 10^{-4}$ min^{-1}, $(4.86 \pm 0.25) \times 10^{-4}$ min^{-1} for pH 5, 6, 7, respectively. The kinetic models fit well with the experimental data, as shown in Figure 5.4.

Similarly, biphenyl oxidation can be expressed as:

$$\frac{[\text{Biphenyl}]}{[\text{Biphenyl}]_0} = \exp(-(k_{\text{biphenyl}})' \times t) \tag{5.31}$$

where $(k_{\text{biphenyl}})' = k_{\text{biphenyl, OH}\bullet} \times$ [OH●].

After fitting experimental data with eq 5.31, $k_{\text{biphenyl}}' = 3.61 \times 10^{-3}$ min^{-1} ($R^2 = 0.996$ and

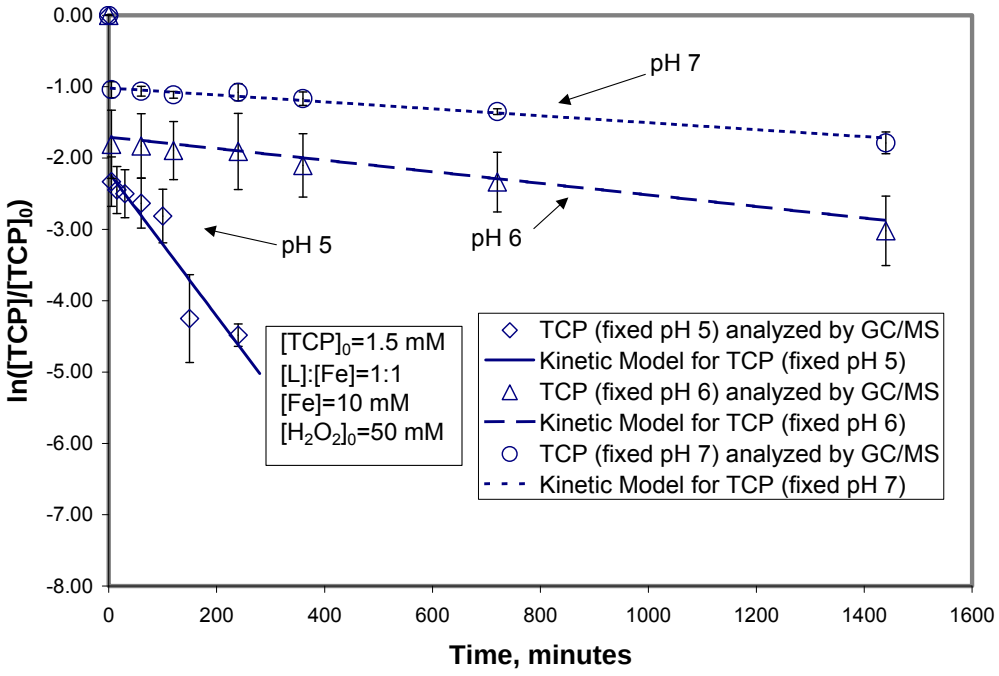

Figure 5.4 Kinetic Model (Equation 5.30) for TCP Dechlorination at pH 5, 6, and 7

the range of $k_{biphenyl}'$ at 95% confidence level is 6.64×10^{-4} to 5.81×10^{-3} min^{-1}) for PAA as a chelating agent. The kinetic model and experimental data are shown in Figure 5.5. The oxidation of biphenyl became very slow after 2 h of reaction time. The [biphenyl]/[biphenyl]$_0$ remained 0.48 after 24 h of reaction time. In order to investigate the reason of the slow reaction rate of biphenyl oxidation after 2 h of reaction time, another experiment was conducted: the concentration of biphenyl at 2 h of reaction time was analyzed and another 0.5 mM H_2O_2 was added to the solution. However, the oxidation reaction rate did not accelerated much after adding another 0.5 mM of H_2O_2, and this indicated that the oxidation reaction rate was limited by the low concentration of Fe^{2+}. The similar behavior for TCP oxidation by a citrate modified Fenton reaction system was observed also, as mentioned in Figure 4.11.

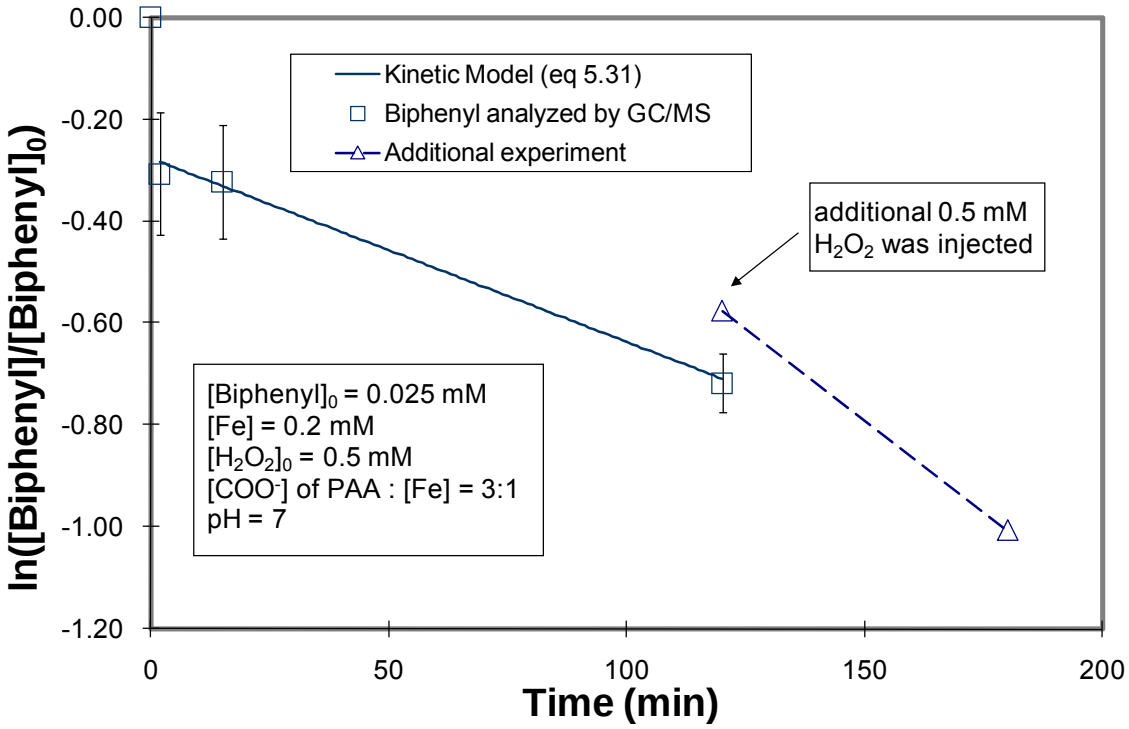

Figure 5.5 Biphenyl Oxidation by Fe^{2+} + H_2O_2 + PAA System at pH 7

Chapter 6. Superoxide Radical Anion Formation during Chelate Modified Fenton Reaction

This chapter will discuss the superoxide radical ($O_2\bullet^-$) generated from the chelate modified Fenton reaction and its application for dechlorination of CCl_4. The kinetic model proposed in chapter 5 will help us to understand the mechanism of $O_2\bullet^-$ during the chelate modified Fenton reaction. The experimental data and kinetic model are also compared with the results of other researchers.

6.1 Introduction

Carbon tetrachloride (CCl_4) is a toxic, carcinogenic chemical compound and is present as a pollutant in the environment because of improper usage and disposal. It has four chlorine atoms symmetrically around central carbon, and the chemical structure of CCl_4 is shown in Figure 3.2. Because of the electrophilicity of chlorine, the carbon of CCl_4 is actually in a pseudo-oxidized status. This characteristic of CCl_4 makes it difficult to be degraded by an oxidation technique. However, reduction technique, on the other hand, is an effective method to detoxify CCl_4. Many researchers have conducted studies for CCl_4 dechlorination at low temperature by using a reduction technique (Maithreepala and Doong, 2004; Lin, et al., 2005; Feng and Lim, 2005).

6.2 Dechlorination of CCl_4 by the Chelate Modified Fenton Reaction

According to Teel and Watts (2002), CCl_4 cannot be oxidized by OH● at an acidic pH environment even though OH• generated by Fe^{2+} and H_2O_2 is a powerful oxidant for most organic pollutants. Superoxide radical anion ($O_2•^-$) has been proven to be a reactive reductant and has the ability to dechlorinate CCl_4 in a Fenton reaction (without a chelating agent) in which the range of H_2O_2-to-Fe^{2+} ratio was 200 to 2000 (Smith et al., 2004, 2006). The perhydroxyl radical ($HO_2•$) is generated from the Fenton reaction system according to the following reactions:

$$Fe^{3+} + H_2O_2 \rightarrow Fe^{2+} + HO_2● + H^+ \quad (6.1)$$

$$OH● + H_2O_2 \rightarrow H_2O + HO_2● \quad (6.2)$$

$HO_2●$ lost its proton to form $O_2●^-$ according to the following equilibrium reactions:

$$H\,O_2● \leftrightarrow H^+ + O_2●^- \quad (6.3)$$

The pK_a value of perhydroxyl radical ($HO_2●$) is 4.8, which means [$O_2●^-$] is very small in comparison to [$HO_2●$] at acidic pH (pH < 3). On the contrary, [$O_2●^-$] increases significantly in the chelate modified Fenton reaction operating at a neutral pH environment. Figure 6.1 shows that the concentration of $O_2●^-$ for the modified Fenton reaction with citrate at pH 7 is 2 orders of magnitude higher than that of the standard Fenton reaction at pH 2.5. This calculation is based on the same initial condition ([Fe] = 0.2 mM, [H_2O_2] = 0.5 mM), but eqs 5.20-5.28 were used for the chelate modified Fenton

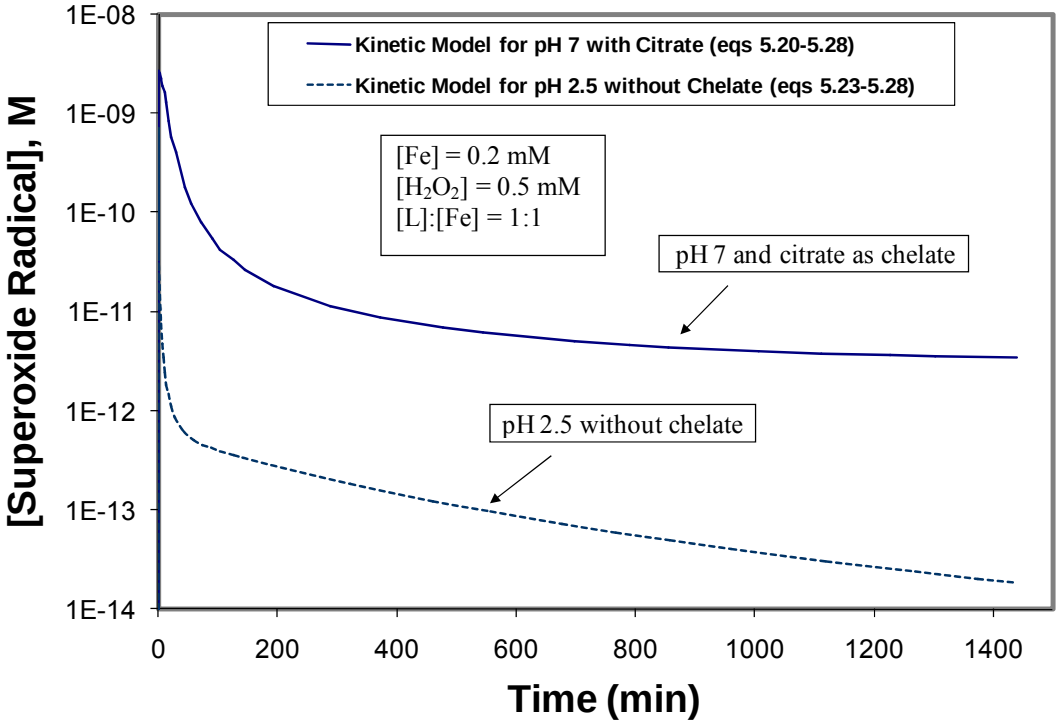

Figure 6.1 The Profiles of $[O_2\bullet^-]$ for the Standard and Modified Fenton Reactions

reaction following the calculation diagram shown in Figure 5.3. The experimental results for dechlorination of CCl_4 at 24 h of reaction time demonstrate that $O_2\bullet^-$ is capable of CCl_4 degradation. In Figure 6.2, the standard Fenton reaction (pH 2.5, without chelate) and citrate-based ([L]/[Fe] = 1:1) and PAA-based ([COO^-] of PAA/[Fe] = 3:1) modified Fenton reactions are compared. The chloride formation in the graph is calculated from the concentration of chloride in the sample divided by the maximum value of chloride that could be formed from the reacted CCl_4. For the citrate modified Fenton reaction, the value is 0.71, and for the PAA modified Fenton reaction, the value is 0.63. On the contrary, the concentration of chloride was below the detection limit in the standard Fenton reaction. This indicates that $O_2\bullet^-$ reactions are very important in the chelate-based Fenton reaction, and $O_2\bullet^-$ may be capable of altering reaction pathways even at a low H_2O_2 to Fe^{2+} ratio of 2.5.

6.3 Kinetic Model for Dechlorination of CCl_4

Smith et al. (2004) observed 0.79 mM of CCl_4 degradation within 2 h of reaction time for the following reaction conditions: $[Fe(III)]_0$ = 0.5 mM, $[H_2O_2]_0 = [H_2O_2]_{final}$ = 1 M ($d[H_2O_2]/dt = 0$), pH = 3 without chelate. Meanwhile, there was only 0.4 mM of CCl_4 dechlorination after 24 h of reaction time in our experimental conditions: $[Fe(II)]_0$ = 0.2 mM, $[H_2O_2]_0$ = 0.5 mM, [L]/[Fe] = 1:1, *L* = citrate, pH = 7. [$O_2\bullet^-$] for both reaction conditions without CCl_4 can be calculated from the kinetic model simulation. The calculations show that [$O_2\bullet^-$] for the experimental condition of Smith et al. (2004) is

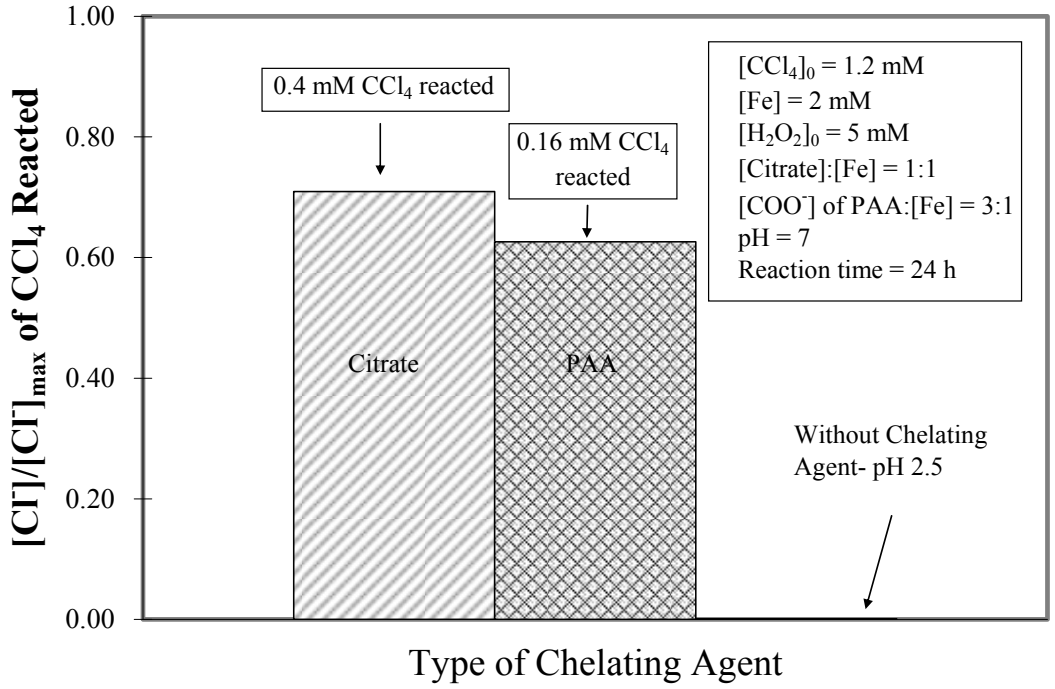

Figure 6.2 Chloride Formation under the Standard and Chelate Based Modified Fenton Reaction at 24 h Reaction Time

maintained at 4.84×10^{-9} M after 3 min of reaction time (pH = 3, no chelating agent). On the other hand, $[O_2\bullet^-]$ for the reaction at pH 7 with citrate is 1–3 orders of magnitude lower (the value can be found in Figure 6.1). This may explain the difference of CCl_4 dechlorination rate for both reaction conditions.

The intermediate reactions of carbon tetrachloride dechlorination by superoxide radical anion are still not clearly established. Thus, a precise concentration of superoxide radical anion derived from the kinetic model simulation is not feasible. Consequently, a pseudo-first-order reaction rate is suitable for the kinetic model calculation. The disappearance of CCl_4 can be expressed as:

$$\frac{d[CCl_4]}{dt} = -k_{obs} \times [CCl_4] \tag{6.1}$$

From the experimental data and eq 28, the k_{obs} is 2.05×10^{-3} min^{-1} (R^2 = 0.995 and the 95% of confidence level is 1.78×10^{-3} to 2.32×10^{-3} min^{-1}) at pH 7. Figure 6.3 shows that this kinetic model fits well with the experimental data.

It will be very beneficial to compare our CCl_4 dechlorination with the work of other scientists. Smith et al. (2004) did several experiments of CCl_4 dechlorination by a modified Fenton reaction with high dosage of Fe^{2+} and H_2O_2 at pH 3. Their experimental data can be modeled by the pseudo first order equation 6.1 also, and the k_{obs} for different reaction conditions can be deduced from their experimental data. It will be more reasonable to compare the observed reaction rate constant of the chelate modified Fenton system with that of Smith et al.'s data by considering the concentration of $O_2\bullet^-$, as shown

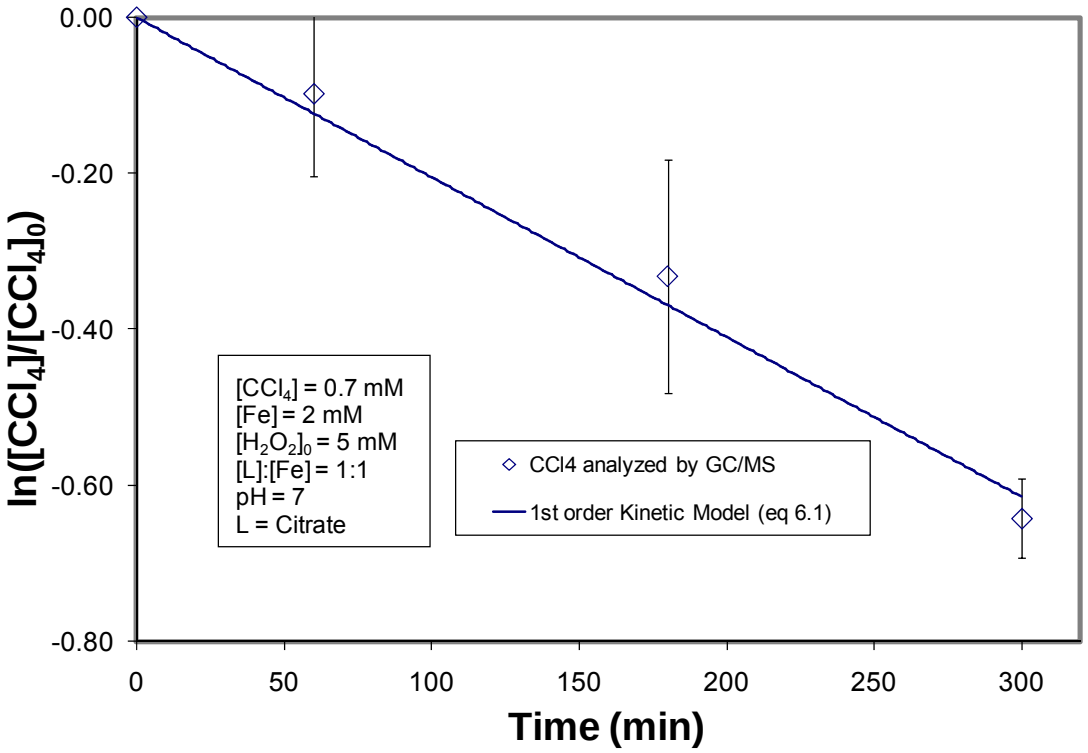

Figure 6.3 Dechlorination of CCl_4 by Fe^{2+} + H_2O_2 + Citrate System at pH 7

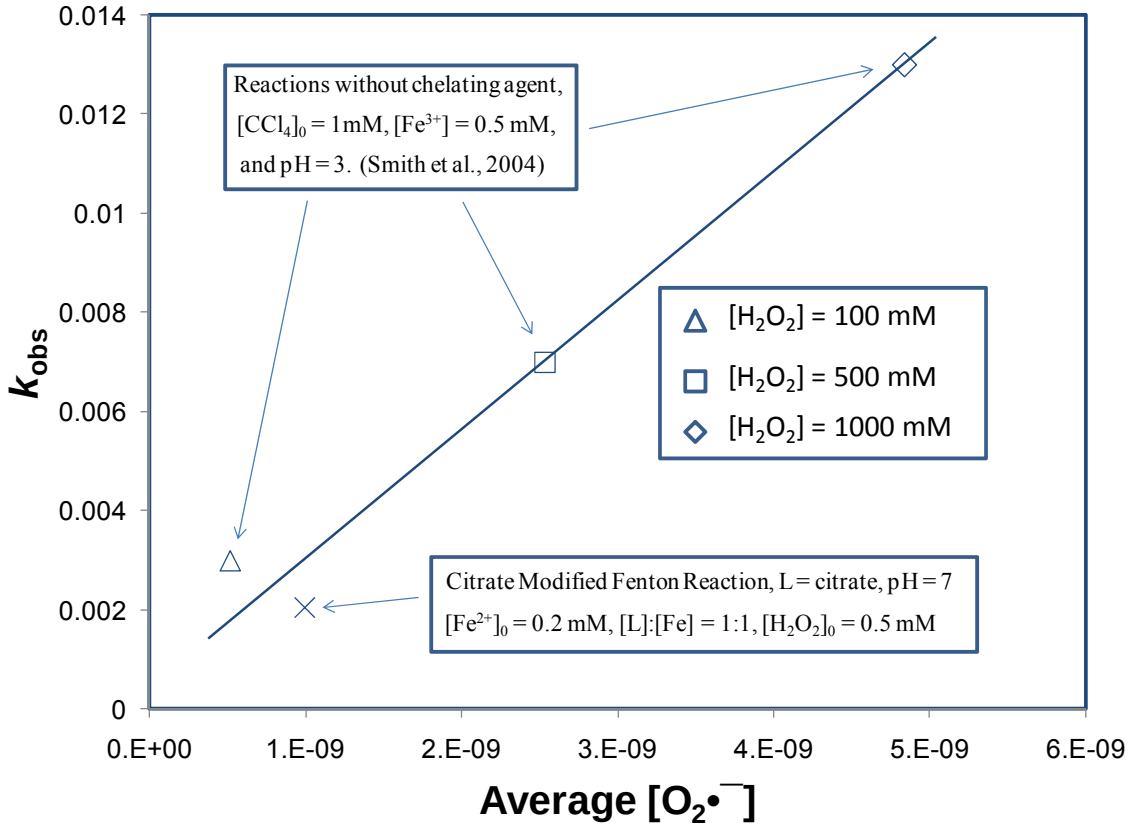

Figure 6.4 Correlation of Average $[O_2•^-]$ and The Observed Reaction Rate Constant k_{obs} for CCl_4 Dechlorination

in Figure 6.4. The average concentrations of $O_2\bullet^-$ were estimated from the kinetic model simulation without pollutant: eqs 5.23-5.28 were used for reaction system without chelating agent (pH 3) and eqs 5.20-5.28 were used for the reaction system with chelating agent (pH 7). It is obvious that the observed reaction rate constant-k_{obs} for CCl_4 dechlorination at different reaction conditions show a linear correlation with the concentration of $O_2\bullet^-$. This also demonstrates that a chelate modified Fenton reaction is effective as the modified Fenton reaction systems with very high dosage of reactants ($[H_2O_2]$ maintained at 0.1 M, 0.5 M, and 1M) at an acidic pH environment.

Chapter 7. The Modified Fenton Reaction Involving Immobilized Iron-Chelate

7.1 Introduction

PAA is a well-known polymer for solid surface modification. Many researchers have carried out studies for solid surface modification by PAA because of different industrial requirements. A lot of researchers did studies for silica modification with PAA under different ways. For example, Zengin et al. (2002) did a study for the surface modification of glass beads with PAA to increase its compatibility with polymer film for faster production. They successfully grafted PAA to the nonporous glass beads through amide bonds after a process of deposition of silane coupling agent (2-aminopropyltriethoxysilane or glycidoxypropyltrimethoxysilane) to the surface of glass beads. Yin et al. (1997) did experiments of deposition of silane coupling agent (methacrylpropylsiloxane) to the surface of nonporous glass beads under an anhydrous condition. PAA was successfully grafted to these nonporous glass beads by polymerization reaction with monomer (acrylic acid).

On the other hand, modification of membrane with different functional groups has many advantages in the applications of bioreaction, separation, and purification, etc. These are the following types porous polymer membranes according to their pore size: microfiltration (MF: 100 ~ 10000 nm), ultrafiltration (UF: 10 ~ 100 nm), nanofiltration (NF: 1 ~ 10 nm), and reverse osmosis (RO: 0.1 ~ 1 nm). Microfiltration membrane was widely used for modification with different functional groups for various requirements.

For instance, Bhattacharyya et al. (1998) developed a new approach for metal capture by using a PLGA (poly-L-glutamic acid) modified cellulose acetate membrane. They were able to achieve 1.5 g Pb/g membrane and 0.8 g metal /g membrane for Cd and Ni. Gabriel and Gillberg (1993) conducted a study for modification of hydrophobic membrane (Celgard® 2500, Hoechst Celanese Corp.) by polymerization of different concentrations of acrylic acid. They found that at least 50 wt% of acrylic acid was needed for an effective membrane modification without a crosslink agent. The concentration of monomer (acrylic acid) went down to 15 wt% if a crosslink agent (TMPTA) was added into the modification process.

From the view of pollutant remediation, PAA can be used to immobilize the soluble iron reactant on a suitable support to suppress the unwanted reaction of Fe^{2+}/Fe^{3+} with water in order to promote the catalytic nature of iron. Silica particles are nontoxic and can be used in groundwater remediation. Moreover, PAA-functionalized PVDF membranes can be used in wastewater treatment, as shown in Figure 7.1. PAA-functionalized silica particles or membranes can be used in the modified Fenton reaction after ion-exchange with Fe^{2+}. The process diagrams for both silica particles and PVDF membrane are summarized in Figure 7.2. This chapter will discuss synthesis of PAA functionalized silica particles/PDVF membrane and their uses for pollutant detoxification reaction.

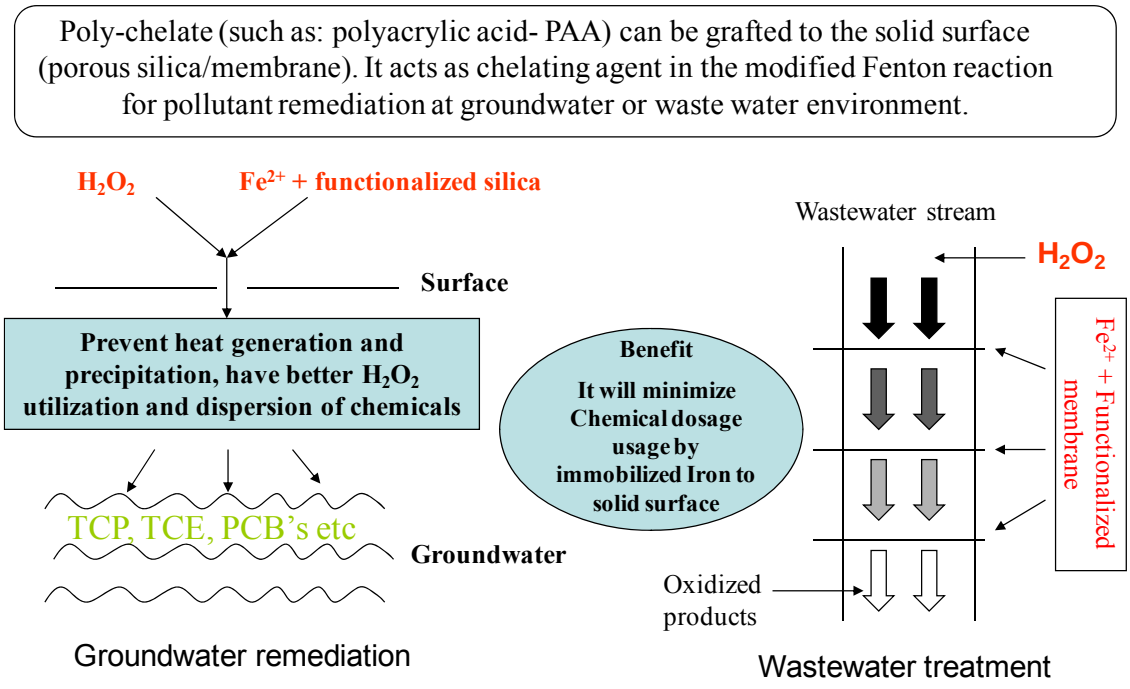

Figure 7.1 Application for Modified Fenton Reaction Involving Immobilized Iron-chelate

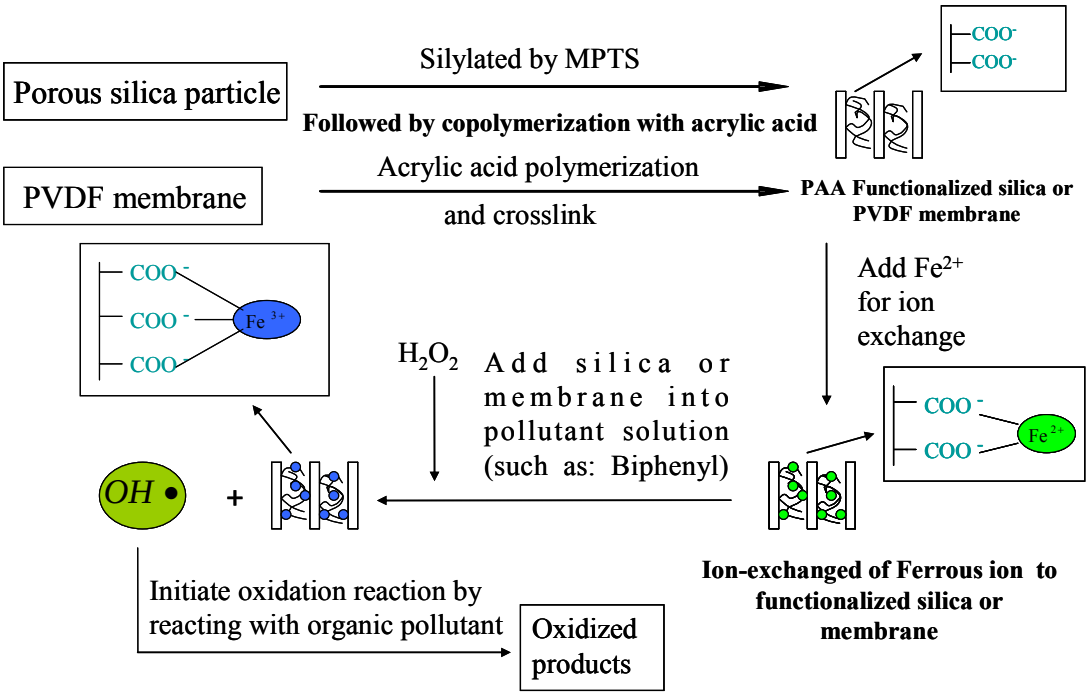

Figure 7.2 Schematic Diagram for Modified Fenton Reaction Involving Immobilized Iron-Chelate

7.2 Synthesis of PAA Functionalized Silica Particles

Silica particles are very small in particle size, but have a very high surface area. For example, silica particles (874-86-2, Huber Engineered Materials) used in this study have 444 m^2/g by BET test and the average particle size is 7 μm. The average pore size of this silica particle is 12 nm. Due to these physical properties of silica particles, an in-situ polymerization and cross-linking technique (this will be discussed in the next section) will lead to an aggregation of silica particles that are not suitable for groundwater remediation. However, a precursor, like a silane coupling agent with a functional group, can be used to attach to the surface of a silica particle. The functional group then will co-polymerize with acrylic acid to achieve PAA functionalized silica particles. The silane coupling agent can be attached to the silica particles by two ways: hydrolytic deposition and anhydrous deposition. An anhydrous deposition for silica particles usually generate a monolayer deposition with extended reaction time (> 12 h). Hydrolytic deposition technique, on the other hand, will have a multilayer deposition on the silica surface with an easy and fast process. In this study, a hydrolytic deposition method was used for the silica modification and the principle of hydrolytic deposition to silica surface is shown in Figure 7.3.

The experimental procedure of PAA functionalized silica particles is the following: After mixing 95 mL of ethanol with 5 mL DIUF water, the pH was adjusted to 5 by acetic acid (98%). A volume of 9 mL of MPTS (silane coupling agent) was spiked into the solution and mixed for 10 min. Pure silica particles (3 g; 7 μm particle size with 12 nm of pore

size, Huber) were added to the solution and were silylated for 30 min. Silica particles were put in the 110 ^{0}C oven for 20 min after being washed with ethanol twice. Toluene (100 μL), 0.29 g of benzoyl peroxide (initiator), 3 mL acrylic acid, and 2.5 g of silylated silica were put into a 250 mL flask, and the mixture was purged with N_2 for 10 min. The polymerization was initiated by putting the flask into a 90 ^{o}C oil bath and continuously stirring for 24 h under N_2. PAA-functionalized silica particles were retrieved after 48 h of extraction with methanol and acetone (v/v = 1:1). The synthesis procedure is summarized in Figure 7.4.

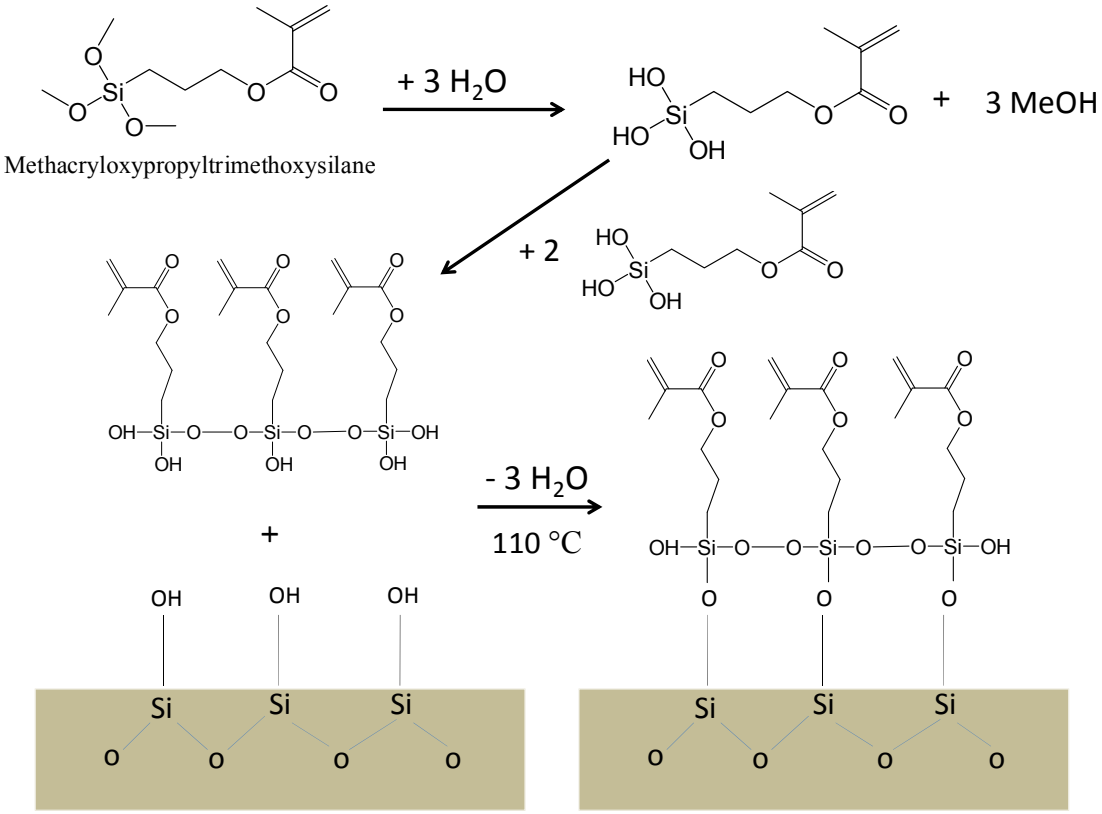

Figure 7.3 The Principle of Hydrolytic Deposition of a Silane Coupling Agent to the Silica Particle Surface (adapted from Silane Coupling Agents brochure, Gelest Inc.)

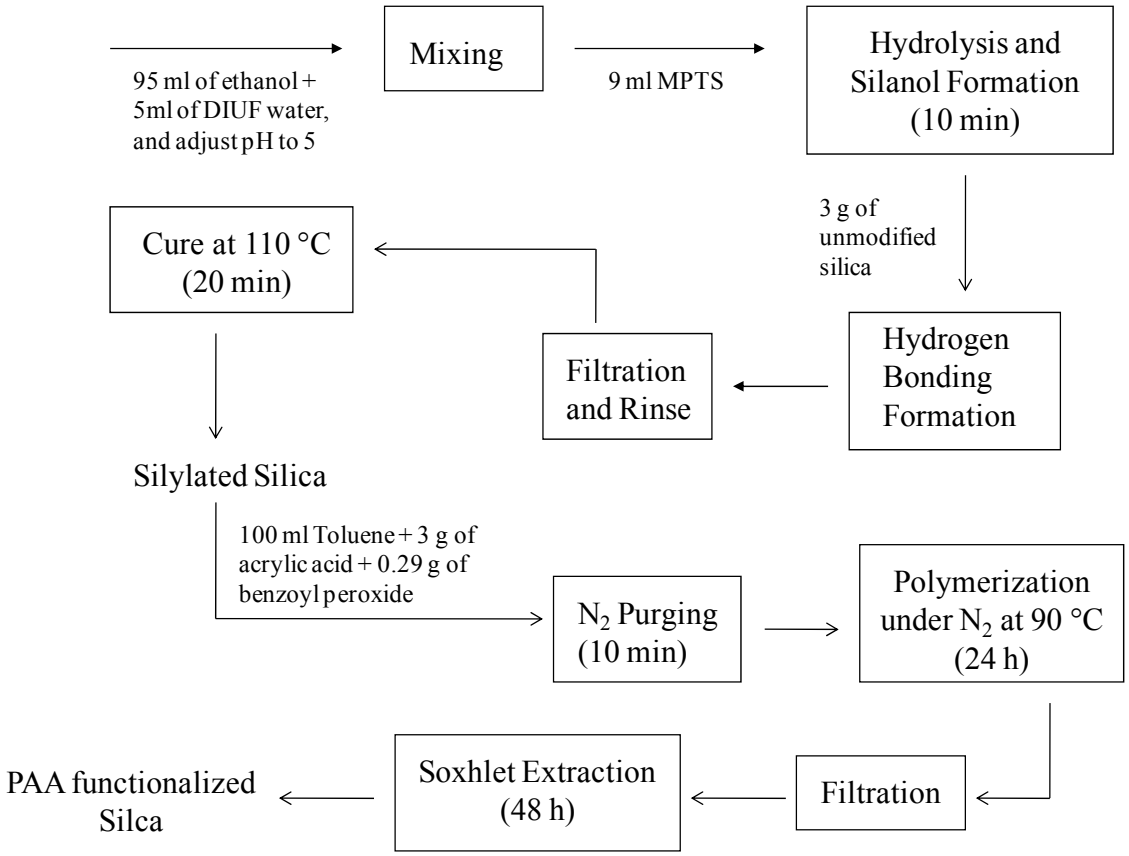

Figure 7.4 Synthesis Procedure of PAA-Functionalized Silica Particles

7.3 Synthesis of PAA Functionalized PVDF Membranes

In contrast to the silica particles, a microfiltration membrane has a large pore size-200 nm on average. Polymerization of acrylic acid in-situ and cross-linking technique will make a meshwork of PAA, which permanently load inside the pore of the membrane (Gabriel and Gillberg, 1993) According to Xu and Bhattacharyya (2007), the principle of the thermal polymerization and crosslink for PAA functionalized membrane is shown in Figure 7.5. PVDF microfiltration membrane was chosen in our study for modification and dechlorination study because it is inert and stable for OH● reaction.

The detail of synthesis procedure is the following: Toluene (70 g), 1.23 g of TMPTA (crosslink agent), 0.502 g of benzoyl peroxide (initiator), and 30 g of acrylic acid were mixed together, and the mixture was purged with ultrahigh-purity N_2 for 1 h. The PVDF MF membrane was immersed into the deoxygenated mixture for 30 s, and the polymerization reaction was carried out at 90 ^{o}C under N_2 purge for 3 h. All PAA-functionalized PVDF membranes (90 mm in diameter) were soaked in $NaNO_3$ solution (1 M) overnight before usage. The synthesis procedure is summarized in Figure 7.6.

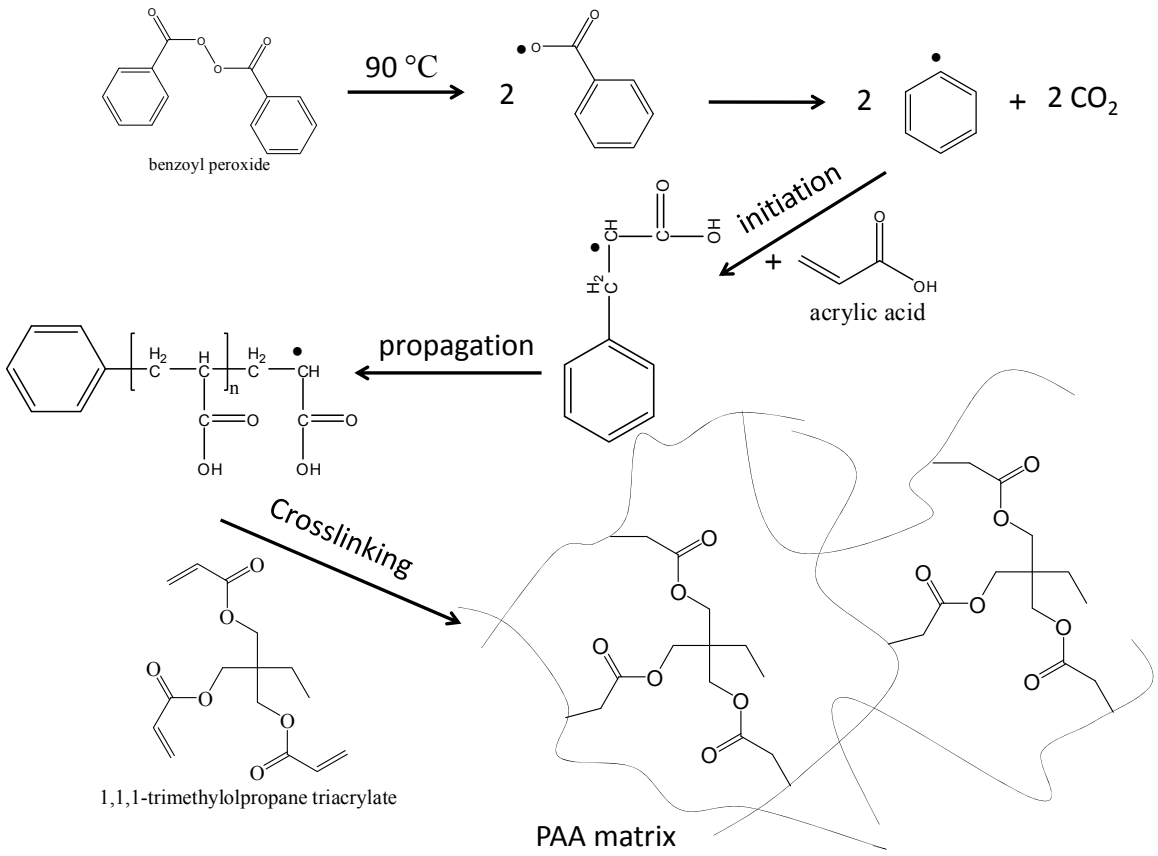

Figure 7.5 The Principle of Thermal Polymerization of Acrylic Acid and Crosslinking for Permanent Modification of PVDF Membrane (adapted from Xu and Bhattacharyya, 2007)

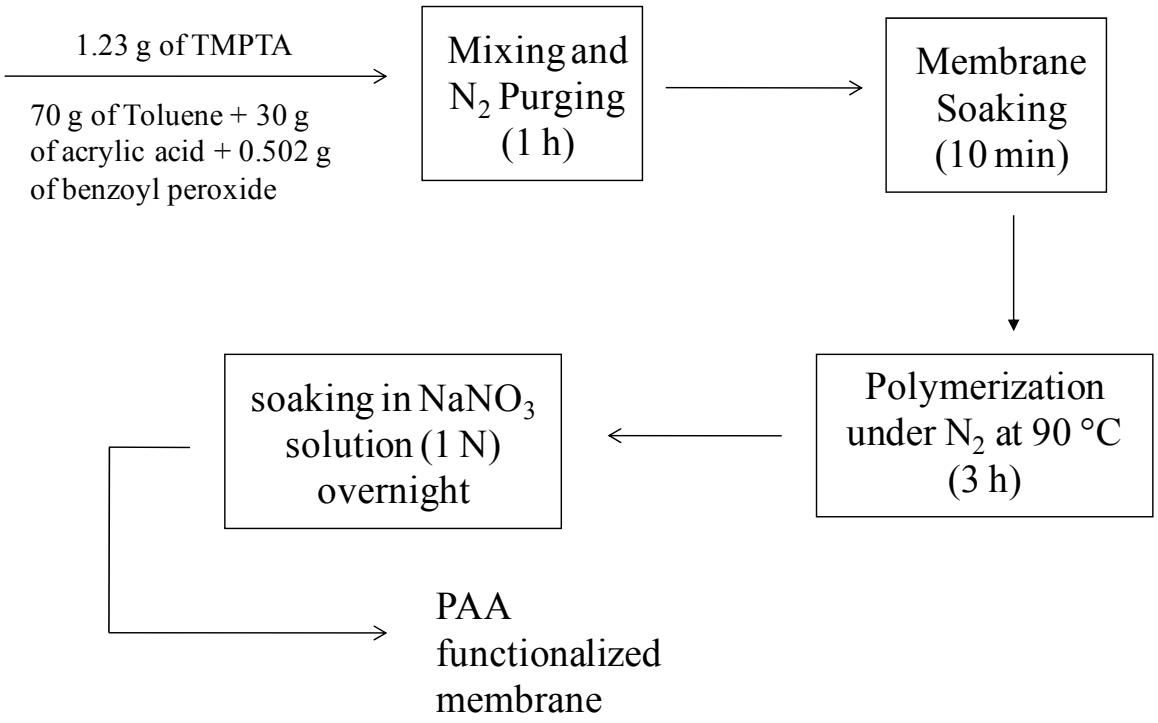

Figure 7.6 Synthesis Procedure of PAA-Functionalized Membrane

7.4 Detoxification of Biphenyl by Modified Fenton Reaction Involving Iron-Chelate

The chemical structures of unmodified silica particles and PAA functionalized silica particles can be analyzed by FTIR. The FTIR spectra of pure silica and modified silica (after silane and PAA functionalization) particles are shown in Figure 7.7. The PAA-modified silica has a new peak at 1730 cm^{-1}, a symmetric stretching of C=O bond, and a weak absorbance at 2980 cm^{-1}, asymmetric stretching of C–H bond, (Ottenbrite et al., 2000; Zengin, et al. 2002; Chen, et al., 2005). As an alternative, thermo-gravimetric analysis (TGA) can provide information about the mass of the sample as a function of temperature. Figure 7.8 shows the thermal stability of pure silica particles and PAA functionalized silica particles. The PAA functionalized silica particles accelerate to lose their weights after 300 °C, while the pure silica particles show minimum weight loss until 650 °C. Both FTIR and TGA analysis indicate that the silica particles had been functionalized successfully. The TGA analysis for the pure PVDF membrane and PAA functionalized membrane are shown in Figure 7.9. The pure PVDF membrane shows a one-step big weight loss after 450 °C which is related to the decomposition of CF_2 chain (Shen et al., 2006; Ying et al., 2004). On the other hand, PAA functionalized membrane start to lose its weight after 160 °C corresponding to the initial condensation of carboxylic functional group of PAA (Moharram and Khafagi, 2006).

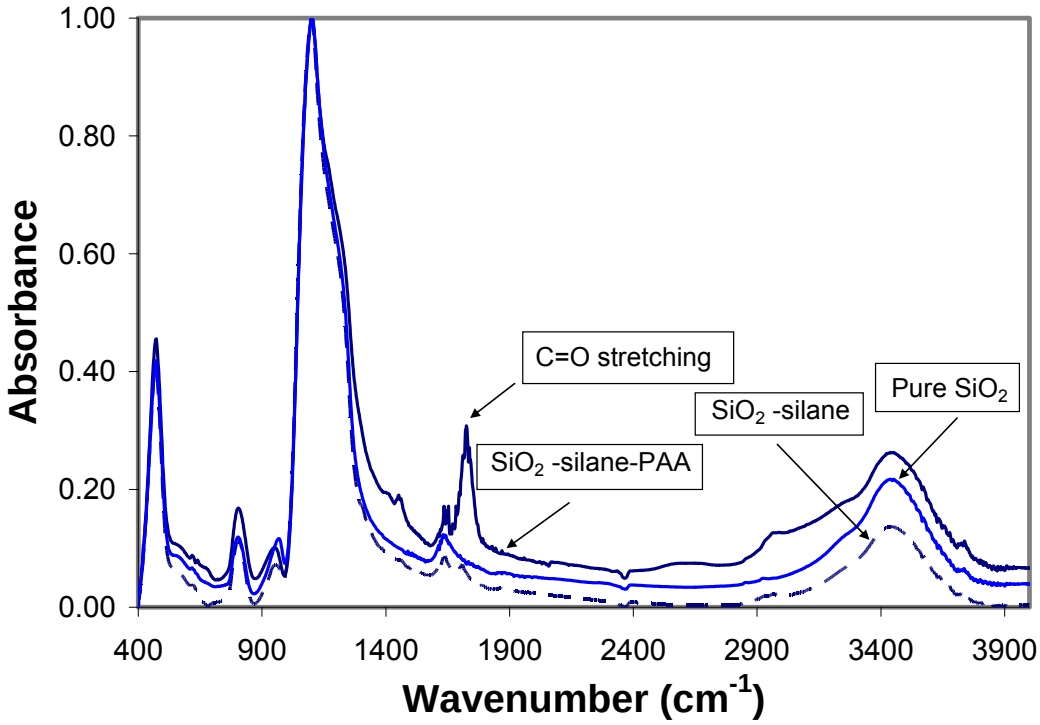

Figure 7.7 FTIR Spectra of Pure Silica and Functionalized Silica

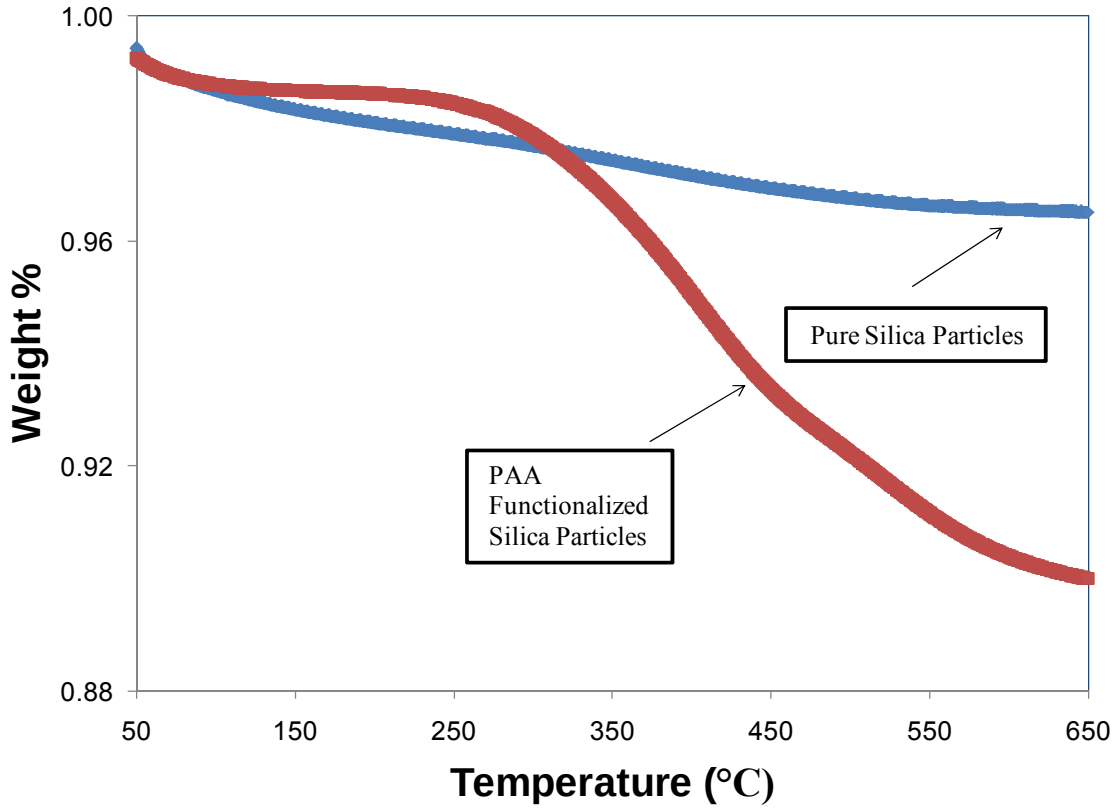

Figure 7.8 TGA Analysis of Pure Silica Particles and PAA Functionalized Silica Particles

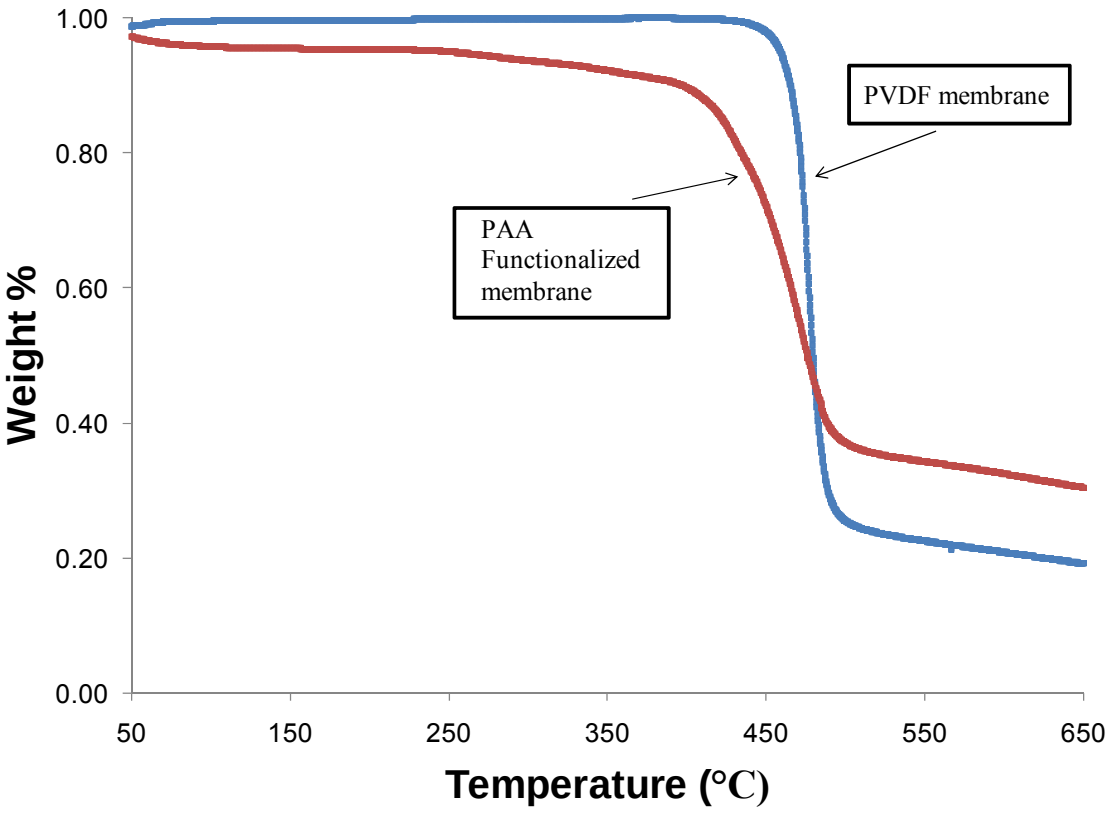

Figure 7.9 TGA Analysis of Unmodified PVDF Membrane and PAA Functionalized Membrane

After ion exchange with Fe^{2+}, the PAA functionalized materials (silica particles/membrane) are ready for use in the pollutant detoxification. Duplicate experimental results for biphenyl oxidation using two different types of immobilized chelate (PAA-functionalized silica particles and PAA-functionalized PVDF membrane) are listed in Table 7.1. The reaction using PAA-functionalized silica particles demonstrate a better detoxification result. This is reasonable because silica particles are small in size (7 μm in diameter) and have higher contact surface area for reaction in the solution. The experimental data for biphenyl oxidation by PAA-functionalized membrane within 2 h of reaction time are shown in Figure 7.10. The reaction rate of biphenyl oxidation is very slow and there is no significant difference for the remaining concentration of biphenyl at 2 h and 24 h of reaction time (data for 24 h are shown in Table 7.1). The low reaction rate of pollutant oxidation by the PAA-functionalized membrane may be caused by a low mass transfer rate of batch reactor model, which we used for all experiments. A convective reactor model will improve the overall reaction rate for a system using a PAA-functionalized membrane.

Table 7.1 Biphenyl Detoxification by Immobilized PAA-Based Modified Fenton Reactions [a]

at 24 h reaction time	PAA-silica	PAA-membrane
$\frac{[\text{Biphenyl}]}{[\text{Biphenyl}]_0}$	0.52 ± 0.03	0.61 ± 0.03
$\frac{[H_2O_2]}{[H_2O_2]_0}$	0.47 ± 0.01	0.03 ± 0.01

a: $[\text{Biphenyl}]_0 = 0.025$ mM, $[H_2O_2]_0 = 5$ mM, and pH = 7
Fe loading for experiments: 3.6-3.7 mM, $[COO^-]$ of PAA**:**[Fe] ≈ 2.8:1
Silica = 3 g, membrane dimension: diameter = 90 mm, thickness = 0.1 mm

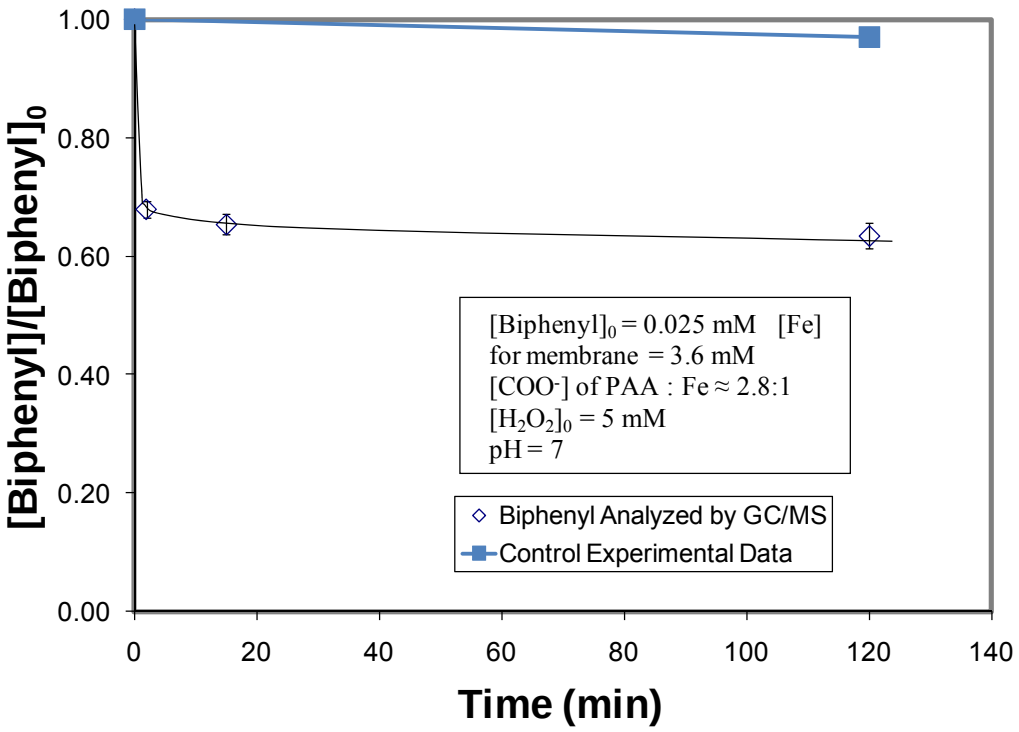

Figure 7.10 Biphenyl Oxidation by Iron-Immobilized System (Membrane) at pH 7

7.5 Dechlorination of TCE by Using PAA-Functionalized Silica Particles

TCE is a chlorinated hydrocarbon that has three chlorine atoms and an unsaturated carbon bond. The chemical structure of TCE is shown in Figure 3.2. TCE is present as a major water contaminant in many NIEHS-SBRP sites because of misusage and improper handling. Glaze et al. (1993) studied PCE and TCE oxidation by a TiO_2-mediated photocatalytic reaction system. They were able to identify dichloroacetic acid and trichloroacetic acid as the major byproducts for PCE, and dichloroacetaldehyde and dichloroacetic acid as the major byproducts for TCE oxidation. They also proposed a reaction mechanism including both reductive and oxidative pathways for the TiO_2-mediated photocatalytic reaction system. Ravikumar and Gurol (1994) explored the oxidation of PCE and TCE by H_2O_2 and sand packed columns in the presence and absence of ferrous sulfate. They found that the natural iron present in sand and H_2O_2 are effective to oxidize PCE and TCE even though the system with ferrous sulfate had better mineralization results for PCE and TCE. Teel et al. (2001) conducted a study for TCE oxidation by the standard and modified Fenton reactions. They used H_2O_2 to react with mineral or soluble iron to generate the free hydroxyl radicals for TCE oxidation at different pH environments. They found that the dechlorination rate for goethite system at pH 7 was the lowest among the four reaction systems they used.

PAA-functionalized silica particles can be used for TCE dechlorination reaction after the iron ion exchange process. Figure 7.11 shows our experimental results about TCE dechlorination by two different reaction systems: homogeneous PAA + Fe^{2+} + H_2O_2 and

Fe^{2+}−PAA−functionalized silica particles + H_2O_2. It is obvious that there is no significant difference between the two reaction systems for TCE dechlorination. The reaction rate is slow after 2 h of reaction time and a similar behavior of biphenyl detoxification by PAA-functionalized membrane was observed in Figure 7.10. The concentrations of chloride ion formation based on the TCE degradation for these two reaction systems are also compared, as shown in Figure 7.12. From the experimental data, the moles of chloride ion formation per mole of TCE degradation for two reaction systems at different reaction times−2 h, 10 h, and 24h are similar as well. This result indicates that PAA-functionalized silica particles have the same reactive efficiency as the homogenous PAA modified Fenton reaction system. Moreover, there are still some chlorinated organic intermediates present in the reaction system and this is the same as the observations of TCP dechlorination by the citrate modified Fenton reaction system, as shown in Figure 4.10. On the other hand, experiments of a lower concentration of TCE (5 times lower) oxidation by using the same dosages of Fe^{2+}-PAA functionalized silica particles/pure PAA and H_2O_2 were also carried out, as shown in Figure 7.11. Obviously, the higher percentages of TCE degradation were observed as expected: 67.0% and 62.4% of TCE were oxidized for systems of pure PAA and PAA functionalized silica particles, respectively. However, the amounts of oxidized TCE by different reaction systems are not consistent, as shown in Figure 7.13. This phenomenon may be explained by the high reactivity of OH● generated in the reaction systems. The lifetime of OH● is very short due to its high reactivity, and it cannot travel far away because there are many other OH● sinks (Fe^{2+}, H_2O_2, etc) around. Unless there is a perfect mixing for the reaction system,

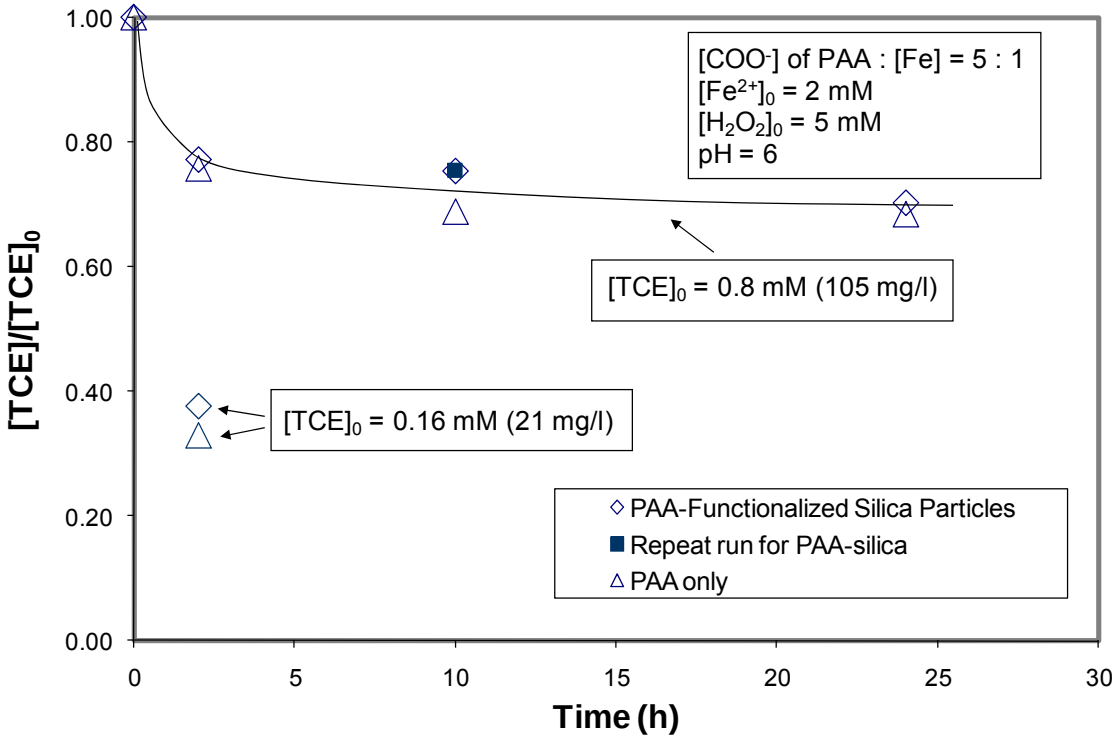

Figure 7.11 TCE Dechlorination by Homogeneous PAA and PAA-Functionalized Silica Reaction Systems

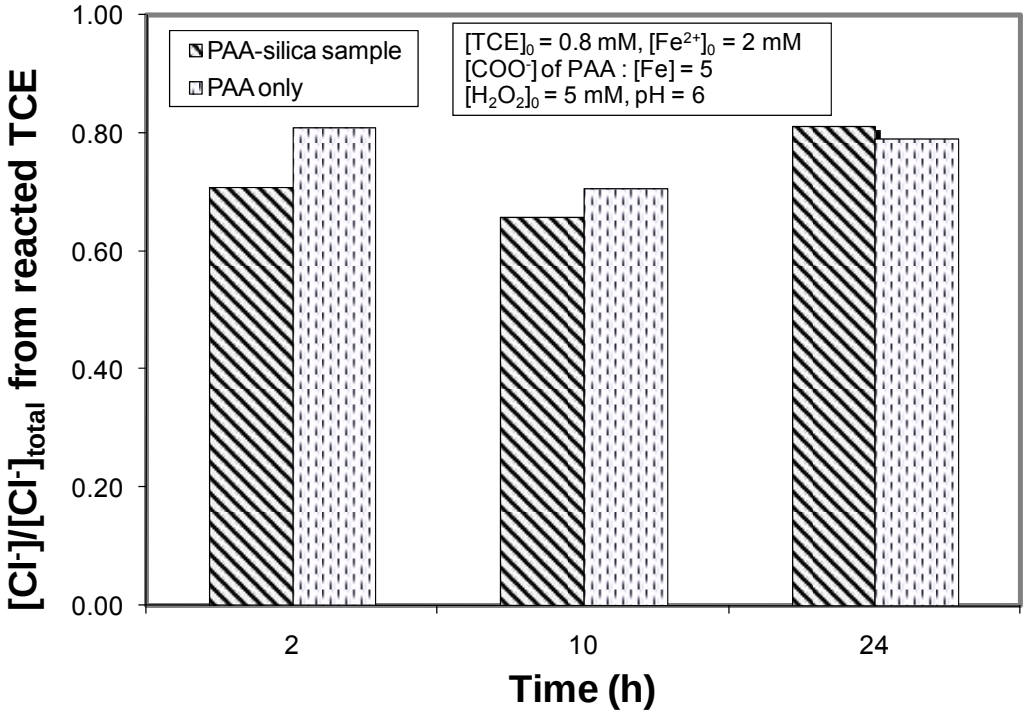

Figure 7.12 Chloride Formation from TCE Dechlorination by Homogeneous PAA and PAA−Functionalized Silica Particles Reaction Systems

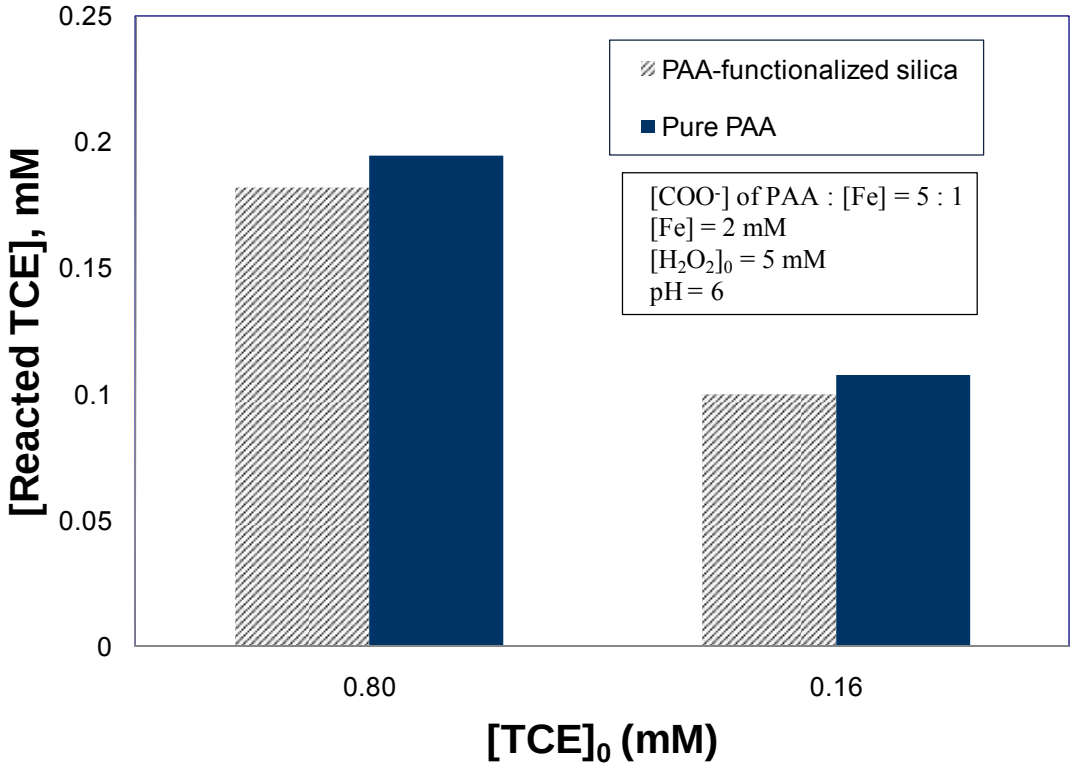

Figure 7.13 TCE Dechlorination by the Chelate Modified Fenton Reaction under Different Initial TCE Concentrations

the mass transfer is an obstacle for a better OH● utilization in an environment of low concentration of pollutant. Thus, the high concentration of OH● in a short time is not favored by pollutants oxidation. This proves that a chelate modified Fenton reaction will more suitable for groundwater remediation because of its slow overall reaction rate.

Chapter 8. Conclusions

This dissertation focuses on the oxidation of chlorinated organic compounds by the chelate modified Fenton reaction system near a neutral pH environment. The hypothesis of the chelate modified Fenton reaction system is that a chelating agent can prevent $Fe(OH)_3$ (s) precipitation and slows down the overall reaction rate of pollutants oxidation by complexation of iron ions. Fenton reaction with a mono-chelating agent (citrate) or a poly-chelating agent (polyacrylic acid, PAA) was shown to be able to detoxify chlorinated organic compounds at a neutral pH environment. Superoxide radical anion was proven to be another benefit of using the chelate modified Fenton reaction at a neutral pH environment. Moreover, the successful synthesis of PAA-functionalized PVDF membrane/silica particles can also be used for pollutant detoxification.

8.1 Fundamental Science and Engineering Advancements:

- The use of a chelating agent with the Fenton reaction is capable of oxidizing chlorinated organic compounds at a neutral pH environment and decreases the overall reaction rate to reduce the waste of reactants for potential groundwater remediation applications.
- Proof of superoxide radical anion generation is demonstrated by using the chelate modified Fenton reaction near neutral pH environment.
- Polymeric chelate (such as: polyacrylic acid) can be used to modify a solid support and immobilize iron ions after ion exchange process for the use of organic pollutants oxidation.

- Numerical simulation based on the kinetic model developed from the well-known Fenton reaction and iron–chelate chemistry fits the experimental data well for both standard and chelate modified Fenton reactions without a pollutant.
- The potential combination of reduction and oxidation reaction may enhance the detoxification of organic pollutants. For example, the dechlorination of PCBs by bimetal nanoparticles (Fe/Pd) will lead to biphenyl formation as one of the final products. Further successful oxidation of biphenyl by the chelate modified Fenton reaction was also demonstrated in our experiments.

8.2 Specific Conclusions Drawn from This Work:

- The successful uses of citrate as a mono-chelate and polyacrylic acid (PAA) as a poly-chelate in the Fenton reaction for pollutant degradation show that the chelating agents are capable of preventing iron precipitation at a neutral pH environment. Our experiments demonstrate that the chelate modified Fenton reaction can successfully be used for detoxification of chlorinated organic compounds (TCP, CCl_4, 2,2′-PCB, and biphenyl). Because of the low activity of metal chelate (Fe^{2+}−citrate and Fe^{3+}−citrate), the overall reaction for the modified Fenton reaction is much slower than that of standard Fenton reaction. Two potential benefits for groundwater remediation bringing by this slow overall reaction are: 1) to utilize the free radicals more effectively because of the very slow motion of groundwater, and avoid the waste of reactants by reducing

unwanted side reactions; 2) to prevent any significant heat generation to cause a local temperature surge and its impact because of the exothermic reaction of the Fenton reaction during groundwater remediation.

- Superoxide radical anion is a strong nucleophile and is capable of degradation of chlorinated organic compounds. The concentration of superoxide radical anion increases significantly because of the neutral pH environment of the chelate modified Fenton reaction, as demonstrated by our kinetic model simulation. CCl_4 was detoxified by both citrate and PAA modified Fenton reactions at a neutral pH environment. On the other hand, the chloride formation of the standard Fenton reaction with the same reactant dosages was below the detection limit, which confirmed our hypothesis about a much higher concentration of superoxide radical anion formation in the chelate modified Fenton reaction system.
- The synthesized PAA-functionalized silica particles and PVDF membrane are shown to be able to detoxify the chlorinated organic compounds (TCE and biphenyl) at a neutral pH environment. The successful functionalized silica particles were proven by the FTIR and TGA analysis. From the TCE dechlorination experimental data, PAA-functionalized silica particles have the same reactive efficiency as the homogenous PAA modified Fenton reaction. On the other hand, the overall reaction rate of pollutant oxidation by using a PAA-functionalized PVDF membrane is lower than that by the PAA-functionalized silica particles because of the mass transfer rate limitation. However, this problem can be addressed by using a convention flow reactor to improve mass transfer rate.

The potential uses of PAA-functionalized silica particles for groundwater remediation and PAA-functionalized PVDF membrane for wastewater treatment indicate that poly-chelate has very broad applications in water remediation.

- Numeric simulation for the chelate modified Fenton reaction was developed by using the chelation chemistry and the rate law of the well-known Fenton reactions. These mathematical calculations based on the kinetic model also help one to understand the mechanism of dechlorination of CCl_4 by superoxide radical anion for the modified Fenton reaction, and these calculations were confirmed by experimental data. The observed rate constants for detoxification of TCP, biphenyl, and CCl_4 were derived from experimental data and kinetic models. The observed reaction rate constant for dechlorination of CCl_4 was compared to the results of other scientists, and this also helped to verify the reactive efficiency of the chelate modified Fenton reaction.
- Reduction technique is a well-known process for water remediation and many researchers did extensive studies by using different reducing agents at different reaction conditions. As an alternative, oxidation technique, especially advanced oxidation processes (AOP), is also a prosperous way for in-situ water remediation because of its easy, fast, and low cost. However, any single method may be not sufficient for a thorough detoxification of contaminants because of the complex remediation environment. Combination of both reduction and oxidation techniques will bring a fast and economic way to solve water remediation problems. For example, PCBs have very limited solubility and present as solids or DNAPL form in the groundwater. Nanosized bimetallic particles can quickly

dechlorinate these PCBs to biphenyl for further oxidation by using a chelate modified Fenton reaction. This is also the main reason to choose biphenyl as a model compound in our detoxification experiments. Further combination experiments can be carried out to improve the overall dechlorination efficiency.

Reference

Ahuja, D. K.; Gavalas, V. G.; Bachas, L. G.; Bhattacharyya, D. Aqueous-phase dechlorination of toxic chloroethylenes by vitamin B_{12} cobalt center: conventional and polypyrrole film-based electrochemical studies. Ind. Eng. Chem. Res. 2004, 43, 1049–1055.

Andreozzi, R.; D' Apuzzo, A.; Marotta, R. A kinetic model for the degradation of benzothiazole by Fe^{3+}-photo-assisted Fenton process in a completely mixed batch reactor. J. Haz. Mater. 2000, B80, 241–257.

Aronstein, B. N.; Paterek, J. R.; Rice, L. E. The effect of chemical pretreatment on the aerobic microbial degradation of PCB congeners in aqueous systems, J. Ind. Microbiology. 1995, 15, 55–59.

Augusti, R.; Dias, A. O.; Rocha, L. L.; Lago, R. M. Kinetics and mechanism of benzene derivative degradation with Fenton's reagent in aqueous medium studied by MIMS. J. Phys. Chem. 1998, A 102, 10723–10727.

Baes, C.F.; Mesmer, R.E. *The hydrolysis of cations*; John Wiley & Sons: New York, 1976.

Basu, S.; Wei, I. W. Advanced chemical oxidation of 2,4,6-trichlorophenol in aqueous phase by fenton's reagent-part I: effects of the amounts of oxidant and catalyst on the treatment reaction. Chem. Eng. Comm. 1998a, 164, 111–137.

Basu, S.; Wei, I. W. Advanced chemical oxidation of 2,4,6-trichlorophenol in aqueous phase by Fenton's reagent-part II: effects of various reaction parameters on the treatment reaction. Chem. Eng. Comm. 1998b, 164, 139–151.

Beltran, F. J.; Encinar, J. M.; Gonzalez, J. F. Industrial wastewater advanced oxidation. Part 2. Ozone combined with hydrogen peroxide or UV radiation. Wat. Res. 1997, 31, 2415–2428.

Benitez, F. J.; Beltran-Heredia, J.; Acero, J. L.; Rubio, F. J. Chemical decomposition of 2,4,6-trichlorophenol by ozone, Fenton's reaction, and UV radiation. Ind. Eng. Chem. Res. 1999, 38, 1341–1349.

Benitez, F. J.; Beltran-Heredia, J.; Acero, J. L.; Rubio, F. J. Oxidation of several chlorophenolic derivatives by UV irradiation and hydroxyl radicals. J. Chem. Technol. Biotechnol. 2001, *76*, 312–320.

Bhattacharyya, D., Hestekin, J.A., Brushaber, P., Cullen, L., Bachas, L.G. and Sikdar, S.K., Novel poly-glutamic acid functionalized Microfiltration membranes for sorption of heavy metals at high capacity, J. Membr. Sci., 1998, 141, 121–135.

Boye, B.; Dieng, M. M.; Brillas, E. Electrochemical Degradation of 2,4,5-Trichlorophenoxyacetic Acid in Aqueous Medium by Peroxi-coagulation. Effect of pH and UV light. Electrochim. Acta 2003a, 48, 781–790.

Boye, B.; Dieng, M. M.; Brillas, E. Anodic oxidation, electro-Fenton and photoelectron-Fenton tgreatments of 2,4,5-trichlorophenoxyacetic acid. J. Electroanal. Chem. 2003b, 557, 135–146.

Cassidy, D.; Hampton, D.; Kohler, S. Combined chemical (ozone) and biological treatment of polychlorinated biphenyls (PCBs) adsorbed to sediments, J. Chem. Technol. Biotechnol. 2002, 77, 663–670.

Chaberek, S.; Martell, A. E. *Organic sequestering agents*; John Wiley & Sons: New York, 1959.

Chen, H.; Zhou, S.; Gu, G.; Wu, L. Study on modification and dispersion of nano-silica. J. Dispersion Sci. Technol. 2005, 26, 27–37.

Chu, W.; Law, C. K. Treatment of Trichlorophenol by Catalytic Oxidation Process. Wat. Res. 2003, 37, 2339–2346

Chen, X.; Schuler, R. H. Directing effects of phenyl substitution in the reaction of OH radical with aromatics: the radiolytic hydroxylation of biphenyl, J. Phys. Chem. 1993, 97 421–425.

Crichton, R. R.; Wilmet, S.; Legssyer, R.; Ward, R. J. Molecular and cellular mechanisms of iron homeostasis and toxicity in mammalian cells. J. Inorg. Biochem. 2002, 91, 9–18.

De Laat, J.; Gallard, H. Catalytic decomposition of hydrogen peroxide by Fe(III) in homogeneous aqueous solution: mechanism and kinetic modeling. Environ. Sci. Technol. 1999, 33, 2726–2732.

Dwyer, F. P.; Mellor, D. P. *Chelating agents and metal chelates*; Academic Press: New York, 1964.

Ei-Morsi, T. M.; Emara, M. M.; Adb El Bary, H. M. H. Abd-EI-Aziz, A.S., Friesen, K.J., Homogeneous degradation of 1,2,9,10-tetrachlorodecane in aqueous solutions using hydrogen peroxide, iron and UV light. Chemosphere 2002, 47, 343–348.

Feng, J.; Lim, T. T. Pathways and kinetics of carbon tetrachloride and chloroform reductions by nano-scale Fe and Fe/Ni particles: comparison with commercial micro-scale Fe and Zn. Chemosphere 2005, 59, 1267–1277.

Fish, R. H.; Oberhausen, K.; Chen, S.; Richardson, J. F.; Pierce, W.; Buchanan, R. M. Biomimetic oxidation studies. 7. Alkane functionalization with MMO structural model, [$Fe_2O(OAc)$(tri((1-methylimidazol-1-yl)methyl)amine)$_2^{3+}$], in the presence of *t*-butyl hydroperoxide and oxygen gas. Catal. Lett. 1993, 18, 357–365.

Galey, J. B.; Dumats, J.; Genard, S.; Destree, O.; Pichaud, P.; Cctroux, P.; Marrot, L.; Beck, I.; Fernandez, B.; Barre, G.; Seite, M.; Hussler, G.; Hocquaux, M. N, N'-bis-(3,4,5-trimethoxybenzyl) ethylenediamine N, N'-diacetic acid as a new iron chelator with potential medicinal applications against oxidative stress. Biochem. Pharmacol. 1996, 51, 103–115.

Gantzer, C. J.; Wackett, L. P. Reductive dechlorination catalysed by bacterial transition metal coenzymes. Environ. Sci. Technol. 1991, 25, 715–722.

Glaze W. H.; Kenneke J. F.; Ferry J. L. Chlorinated byproducts from the TiO2-mediated photo-degradation of trichloroethylene and tetrachlooethylene in water. Environ. Sci. Technol. 1993, 27, 177–184.

Gong, J.; Liu, Y.; Sun, X. O_3 and UV/O_3 oxidation of organic constituents of biotreated municipal wastewater. Wat. Res. In Press, Corrected Proof, available online 26 September 2007.

Hong, C. S.; Wang, Y. B.; Bush, B. Kinetics and products of the TiO_2 photocatalytic degradation of 2-chlorobiphenyl in water. Chemosphere, 1998, 36, 1653–1667.

Huang, K. C.; Hoag, G. E.; Chheda, P.; Woody, B. A.; Dobbs, G. M. Kinetic study of oxidation of trichloroethylene by potassium permanganate. Environ. Eng. Sci. 1999, 16, 265–274.

Huang, K. C.; Hoag, G. E.; Chheda, P.; Woody, B. A.; Dobbs, G. M. Kinetic and mechanism of oxidation of tetrachloroethylene with permanganate. Chemosphere, 2002, 46, 815-825.

Huston, P. L.; Pignatello, J. J. Degradation of selected pesticide active ingredients and commercial formulations in water by the photo-assisted Fenton reaction. Wat. Res. 1999, 33, 1238–1246.

IARC. 1987. Overall Evaluations of Carcinogenicity. IARC Monographs on the Evaluation of Carcinogenic Risk of Chemicals to Humans, Supplement 7. Lyon, France: International Agency for Research on Cancer.

IARC. 1999. Re-evaluation of Some Organic Chemicals, Hydrazine, and Hydrogen Peroxide. IARC Monographs on the Evaluation of Carcinogenic Risk of Chemicals to Humans, vol. 71. Lyon, France: International Agency for Research on Cancer.

Inczedy, J. *Analytical application of complex equilibria;* Ellis Horwood Limited: Chiester, England, 1976.

Jacobsen, F.; Holcman, J.; Sehested, K. Activation parameters of ferryl ion reactions in aqueous acid solutions. Int. J. Chem. Kinet. 1997, 29, 17–24.

Jacobsen, F.; Holcman, J.; Sehested, K. Reactions of ferryl ion with some compounds found in cloud water. Int. J. Chem. Kinet. 1998, 30, 215–221.

Kiwi, J.; Lopez, A.; Nadtochenko, V. Mechanism and kinetics of the OH-radical intervention during Fenton oxidation in the presence of a significant amount of radical scavenger (Cl^-). Environ. Sci. Technol. 2000, 34, 2162–2168.

Königsberger, L.; Königsberger, E.; May, P. M.; Hefter, G. T. Complexation of iron (III) by citrate. Implications for iron speciation in blood plasma. J. Inorg. Biochem. 2000, 78, 175–184.

Kosaka, K.; Yamada, H.; Matsui, S.; Echigo, S.; Shishida, K. Comparison among the methods for hydrogen peroxide measurements to evaluate advanced oxidation processes: application of a spectrophotometric method using copper(II) ion and 2,9-dimethyl-1,10-phenanthroline. Environ. Sci. Technol. 1998, 32, 3821–3824.

Kwan, W. P.; Voelker, B. M. Decomposition of hydrogen peroxide and organic compounds in the presence of dissolved iron and ferrihydrite. Environ. Sci. Technol. 2002, 36, 1467–1476.

Kwan, W. P.; Voelker, B. M. Rates of Hydroxyl Radical Generation and Organic Compound Oxidation in Mineral-catalyzed Fenton-like Systems. Environ. Sci. Technol. 2003, 37, 1150–1158.

Laat, J. D.; Gallard, H. Catalytic decomposition of hydrogen peroxide by Fe(III) in homogeneous aqueous solution: mechanism and kinetic modeling. Environ. Sci. Technol. 1999, 33, 2726–2732.

Leising, R. A.; Brennan, B. A.; Que, L. Jr.; Fox, B. G.; Munck, E. Models for non-heme iron oxygenases: a high-valent iron-oxo intermediate. J. Am. Chem. Soc. 1991, 113, 3988–3990.

Li, Y. C.; Bachas, L. G.; Bhattacharyya, D. Kinetics studies of trichlorophenol destruction by chelate-based Fenton reaction. Environ. Eng. Sci. 2005, 22, 756–771.

Li, Y. C.; Bachas, L. G.; Bhattacharyya, D. Selected Chloro-Organic Detoxifications by Poly-Chelate (poly-acrylic acid) and Citrate-Based Fenton Reaction at Neutral pH Environment. Ind. Eng. Chem. Res. 2007, In Press.

Lin, C. J.; Lo, S. L.; Liou, Y. H. Degradation of aqueous carbon tetrachloride by nanoscale zerovalent copper on a cation resin. Chemosphere 2005, 59, 1299–1307.

Lin, S. S.; Gurol, M. D. Catalytic decomposition of hydrogen peroxide on iron oxide: kinetics, mechanism, and implications. Environ. Sci. Technol. 1998, 32, 1417–1423.

Liu, Y.; Majetich, S. A.; Tilton, R. D.; Sholl, D.; Lowry, G. V. TCE dechlorination rates, pathways, and efficiency of nanoscale iron particles with different properties. Envrion. Sci. & Technol. 2005, 39, 1338–1345.

Lopes, K. B.; Schulman, H. M.; Hermes-Lima, M. Polyphenol tannic acid inhibits hydroxyl radical formation from Fenton reaction by complexing ferrous ions. Biochim. Biophys. Acta 1999, 1472, 142–152.

Lowry, G. V.; Johnson, K. M. Congener-specific dechlorination of dissolved PCBs by microscale and nanoscale zerovalent iron in a water/methanol solution. Environ. Sci. Technol. 2004, 38, 5208–5216.

Luo, N.; Kombo, D. C.; Osman, R. Theoretical studies of hydrogen abstraction from 2-propanol by OH radical. J. Phys. Chem. 1997, A 101, 926–936.

Mackay, D.; Shiu, W. Y.; Ma, K. C.; Lee, S. C. *The Handbook of Physical-Chemical Properties and Environmental Fate for Organic Chemicals.* Taylor & Francis Group: London, England, 2006.

Maithreepala, R. A.; Doong, R. A. Enhanced remediation of carbon tetrachloride by Fe(II)-Fe(III) systems in the presence of copper ions. Water Sci. Technol. 2004, 50, 161–168.

Maltoni, C.; Lefemine, G.; Cotti, G.; Perino. G. Long-term carcinogenicity bioassays on trichloroethylene administered by inhalation to Sprague-Dawley rats and Swiss and B6C3F1 mice. Ann N Y Acad. Sci. 1988, 534, 316–42.

McKinzi, A. M.; Dichristina, T. J. Microbially driven Fenton reaction for transformation of pentachlorophenol. Environ. Sci. Technol. 1999, 33, 1886–1891.

Moharram, M. A. and Khafagi, M. G., Thermal behavior of poly(acrylic acid)–poly(vinyl pyrrolidone) and poly(acrylic acid)–metal–poly(vinyl pyrrolidone) complexes, J. Appl. Poly. Sci., 2006, 102, 4049–4057.

Neyens, E.; Beayens, J. A review of classic Fenton's peroxidation as an advanced oxidation technique. J. Haz. Mater. 2003, B98, 33–50.

Nonnenberg, C.; van der Donk, W. A.; Zipse, H. Reductive dechlorination of trichloroethylene. A computational study. J. Phy. Chem. 2002, A 106, 8708–8715.

Nomiyama, K.; Tanizaki, T.; Arizono, K.; Shinohara, R. Endocrine effects generated by photooxidation of coplanar biphenyls in water using titanium dioxide. Chemosphere, 2007, 66, 1138–1145.

NTP. 1988. Toxicology and Carcinogenesis Studies of Trichloroethylene (CAS No. 79-01-6) in Four Strains of Rats (ACI, August, Marshall, Osborne-Mendel) (Gavage Studies). Technical Report Series No 273. Reaserch Triangle Park, NC: National Toxicology Program

NTP. 1990. Carcinogenesis Studies of Trichloroethylene (Without Epichlorohydrin) (CAS No. 79-01-6) in F344/N Rats and B6C3F1 Mice (Gavage Studies). Technical Report Series No 243. Research Triangle Park, NC: National Toxicology Program.

Ottenbrite, R. M.; Yin, R.; Zengin, H., Suzuki, K.; Siddiqui, J. A. Surface modification of silica particles and silica glass beads (Chapter 11), in Specialty Monomers and Polymers: Synthesis, Properties, and Applications, Havelka, K.O. and McCormick, C.L., eds., *ACS Symposium Series 755,* ACS, 2000; 170-183.

Perez, M.; Torrades, F.; Garcia-Hortal, J. A.; Domenech, X.; Peral, J. Removal of organic contaminants in paper pulp treatment effluents under Fenton and photo-Fenton conditions. Applied Catalysis B: Environmental 2002a, 36, 63–74.

Perez, M.; Torrades, F.; Domenech, X.; Peral, J. Fenton and photo-Fenton oxidation of textile effluents. Wat. Res. 2002b, 36, 2703–2710.

Pignatello, J. J. Dark and photoassisted Fe^{3+}-catalyzed degradation of chlorophenoxy herbicides by hydrogen peroxide. Environ. Sci. Technol. 1992, 26, 944–951.

Pignatello, J.J.; Chapa, G. Degradation of PCBs by Ferric Ion, Hydrogen Peroxide and UV Light. Environ. Toxicol. & Chem. 1994, 13, 423-427.

Pignatello, J. J.; Oliveros, E.; MacKay, A. Advanced oxidation processes for organic contaminant destruction based on the Fenton reaction and related chemistry. Crit. Rev. Environ. Sci. Technol. 2006, 36, 1–84.

Pratt, D. A.; Van der Donk, W. A. On the role of alkylcobalamins in the vitamin B12 - catalyzed reductive dehalogenation of perchloroethylene and trichloroethylene. Chem. Commun. (Cambridge, United Kingdom), 2006, 5, 558–560.

Ravikumar J. X.; Gurol M. D. Chemical oxidation of chlorinated organics by hydrogen peroxide in the presence of sand. Environ. Sci. Technol. 1994, 28, 394–400.

Schrauzer, G. N.; Deutsh, E. Reactions of cobalt (I) supernucleophiles. The alkylation of vitamin B_{12}s, cobaloximes (I), and related compounds. J. Am. Chem. Soc. 1968, 12, 3341–3350.

Sedlak, D. L.; Andren, A. W. Aqueous-phase oxidation of polychlorinated biphenyls by hydroxyl radicals. Environ. Sci. Technol. 1991, 25, 1419–1427.

Sedlak, D. L.; Andren, A. W. The effect of sorption on the oxidation of polychlorinated biphenyls (PCBs) by hydroxyl radical. Wat. Res. 1994, 28, 1207–1215.

Serjeant, E. P.; Dempsey, B. *Ionisation constants of organic acids in aqueous solution*; IUPAC Chemical Data Series-No. 23, Pergamon Press: Oxford, 1979.

Shen, J.; Xi, J.; Zhu, W.; Chen, L.; Qiu, X. A nanocomposite proton exchange membrane based on PVDF, poly(2-acrylamido-2-methyl propylene sulfonic acid), and nano-Al_2O_3 for direct methanol fuel cells. J. Power Sources 2006, 159, 894–899.

Sheu,C.; Richert, S. A.; Cofre, P.; Ross, B. Jr.; Sobkowiak, A.; Sawyer, D. T.; Kanofsky, J. R. Iron-induced activation of hydrogen peroxide for the direct ketonization of methylenic carbon [c-C_6H_{12} → c-C_6H_{10}(O)] and the dioxygenation of acetylenes and arylolefins. J. Am. Chem. Soc. 1990, 112, 1936–1942.

Siegrist, R. L.; Lowe, K. S.; Murdoch, L. C.; Case, T. L. Pickering, D. A. In situ oxidation by fracture emplaced reactive solids. J. Environ. Eng. 1999, 429–440

Smith, B. A.; Teel, A. L.; Watts, R. J. Identification of reactive oxygen species responsible for carbon tetrachloride degradation in modified Fenton's systems. Environ. Sci. Technol. 2004, 38, 5465–5469.

Smith, B. A.; Teel, A. L.; Watts, R. J. Mechanism for the destruction of carbon tetrachloride and chloroform DNAPLs by modified Fenton's reagent. J. Contam. Hydrol. 2006, 85, 229–246.

Stookey, L. L. Ferrozine-a new spectrophotometric reagent for iron. Anal. Chem. 1970, 42, 779–781.

Studart, A. R.; Pandolfelli, V. C.; Tervoort, E.; Gauckler, L. J. Selection of Dispersants for High –alumina Zero-cement Refractory Castables. J. Eur. Ceram. Soc. 2003, 23, 997-1004.

Sun, Y.; Pignatello, J. J. Chemical treatment of pesticide wastes. evaluation of Fe(III) chelates for catalytic hydrogen peroxide oxidation of 2,4-D at circumneutral pH. J. Agric. Food Chem. 1992, 40, 322–327.

Sun, Y., Pignatello, J. J. Photochemical Reactions Involved in the Total Mineralization of 2,4-D by $Fe^{3+}/H_2O_2/UV$. Environ. Sci. Technol. 1993a, 27, 304–310.

Sun, Y.; Pignatello, J. J. Organic intermediates in the degradation of 2,4-dichlorophenoxyacetic acid by Fe^{3+}/H_2O_2 and $Fe^{3+}/H_2O_2/UV$. J. Agric. Food. Chem. 1993b, 41, 1139–1142.

Sun, Y.; Pignatello, J. J. Activation of hydrogen peroxide by iron (III) chelates for abiotic degradation of herbicides and insecticides in water. J. Agric. Food Chem. 1993c, 41, 308–312.

Tang, W. Z.; Huang, C.P. 2,4-Dichlorophenol oxidation kinetics by Fenton's reagent. Environ. Technol. 1996, 17, 1371–1378.

Tarr, M.A. Fenton and modified Fenton methods for pollutant degradation. In Environ. Sci. Pollut. Control Ser. 2003, 26, 165–200.

Teel, A. L.; Warberg, C. R.; Atkinson, D. A.; Watts, R. J. Comparison of Mineral and Soluble Iron Fenton's Catalysts for the Treatment of Trichloroethylene. Wat. Res. 2001, 35, 977–984.

Teel, A. L.; Watts, R. J. Degradation of Carbon Tetrachloride by Modified Fenton's Reagent. J. Haz. Mater. 2002, B94, 179–189.

Truax, C. T. 1993. Investigation of the in situ potassium permanganate oxidation of residue DNAPLs located below the groundwater table. M.S. Thesis, University of Waterloo, Ontario, Canada.

Vella, P. A.; Veronda, B. Oxidation of trichloroethylene: a comparison of potassium permanganate and fenton's reagent. Chemical Oxidation: technology for the nineties. In: Proceedings of the Third International Symposium, PA, 1992, 62–73.

Voelker, B. M.; Sulzberger, B. Effects of Fulvic Acid on Fe(II) Oxidation by Hydrogen Peroxide. Environ. Sci. Technol. 1996, 30, 1106–1114.

Walling, C. Fenton reagent revisited. Acc. Chem. Res. 1975, 8, 125–131.

Watts, R. J.; Teel, A. L. Chemistry of modified Fenton's reagent (catalyzed H_2O_2 propagations-CHP) for in situ soil and groundwater remediation. J. Environ. Eng. 2005, 131, 612–622.

Watts, R. J.; Teel, A. L. Treatment of contaminated soils and groundwater using ISCO. Pract. Periodical Hazard., Toxic, Radioact. Waste Manage. 2006, 10, 2–9.

Willey, J. D.; Whitehead, R. F.; Kieber, R. J.; Hardison, D. R. Oxidation of Fe(II) in rainwater. Environ. Sci. Technol. 2005, 39, 2579–2585.

Winterbourn, C. C. Toxicity of iron and hydrogen peroxide: the Fenton reaction. Toxicol. Lett. 1995, 82/83, 969–974.

Xu, J.; Bhattacharyya, D. Membrane-based bimetallic nanoparticles for environmental remediation: synthesis and reactive properties. Environ. Prog. 2005, 24, 358–366.

Xu, J.; Bhattacharyya, D. Fe/Pd nanoparticle immobilization in microfiltration membrane pores: synthesis, characterization and application in dechlorination of polychlorinated biphenyls. Ind. Eng. Chem. Res. 2007, 46, 2348-2359.

Yin, R.; Ottenbrite, R. M.; Siddiqui, J. A. Grafting of poly(acrylic acid) onto nonporous glass beads surface. Polym. Adv. Technol. 1997, 8, 761–766.

Ying, L., Yu, W.H., Kang, E.T., Neoh, K.G., Functional and surface-active membranes from poly (vinylidene fluoride)-graft-poly (acrylic acid) prepared via RAFT-mediated graft copolymerization, Langmuir, 2004, 20, 6032–6040.

Zengin, H.; Hu, B.; Siddiqui, J. A.; Ottenbrite, R. M. Effects of surface modification of glass beads with poly(acrylic acid). Des. Monomers Polym. 2002, 5, 173–182.

Zepp, R. G.; Faust, B. C.; Holgne, J. Hydroxyl radical formation in aqueous reactions (pH 3-8) of iron (II) with hydrogen peroxide: the photo-Fenton reaction. Environ. Sci. Technol. 1992, 26, 313–319.

Zhang, W.X., Wang, C.B., Lien, H.L. Treatment of chlorinated organic contaminants with nanoscale bimetallic particles. Catalysis Today. 1998, 40, 387–395.

Appendix A: Nomenclature

Variables and constants

$[2,2'\text{-PCB}]_0$	concentration of 2,2′-PCB at time, t = 0, mM
$[\text{Biphenyl}]_0$	concentration of biphenyl at time, t = 0, mM
$[Cl]_{max}$	maximum concentration of chloride, for TCP: $[Cl]_{max} = 3 \times [TCP]_0$, mM for CCl_4: $[Cl]_{max} = 4 \times [CCl_4]_0$, mM
$[CCl_4]_0$	cocentration of CCl_4 at time, t = 0, mM
$[Fe^{2+}]_0$	the concentration of free ferrous ions at time, t = 0, mM
$[Fe^{3+}]_0$	the concentration of free ferric ions at time, t = 0, mM
$[Fe(II)]_0$	the concentration of total ferrous ions at time, t = 0, mM
$[Fe(III)]_0$	the concentration of total ferric ions at time, t = 0, mM
[Fe(II)L]	the concentration of Fe^{2+}-chelate, mM
[Fe(III)L]	the concentration of Fe^{3+}-chelate, mM
$[H_2O_2]_0$	concentration of hydrogen peroxide at time, t = 0, mM
$k_{biphenyl}'$	observed reaction rate constant of biphenyl detoxification
k_i	reaction rate constants listed in Table 5.1 (i = 1, 2, 3, …, 16), $M^{-1}\ s^{-1}$
$(k_{TCP})'$	observed reaction rate constant of TCP dechlorination
r_i	reaction rates listed in Table 5.1 (i = 1, 2, 3, …, 16), $M\ s^{-1}$
t	reaction time, min
$[TCE]_0$	concentration of TCE at time, t = 0, mM
$[TCP]_0$	concentration of TCP at time, t = 0, mM

Abbreviations and Chemical Symbols

2,2′-PCB	2,2′-dichloro biphenyl
AA	atomic absorption
BSTFA	N,o-Bis (Trimethylsilyl) trifluoroacetamide
CCl_3	chloroform
CCl_4	carbon tetrachloride
Cl	free chloride
DIUF	deionized ultra-filtered
DMP	2,9-dimethyl-1,10-phenanthroline
DNAPLs	dense non-aqueous phase liquids
EDB	1,2-dibromoethane
EDTA	ethylenediaminetetraacetic acid
ERTL	Environmental Research and Training Laboratory
EPA	Environmental Protection Agency
Fe	iron
Fe(II)L	complex formed between Fe(II) and the chelate
Fe(III)L	complex formed between Fe(III) and the chelate
Ferrozine	3-(2-pyridyl)-5,6-diphenyl-1,2,4,-triazine-4′,4″-disulfonic acid sodium salt
$HO_2\bullet$	perhydroxyl radical
GC/FID	Gas Chromatography-Flame Ionization Detector
GC/MS	gas chromatography/mass spectroscopy
ICS:	ion chromatography system
MPTS:	methacryloxypropyltrimethoxysilane
NIEHS:	National Institute of Environmental Health Sciences

$O_2\bullet^-$	superoxide radical anion
OH●	free hydroxyl radical
PAA:	polyacrylic acid
PCBs:	polychlorinated biphenyls
PCE	perchloroethylene
PVDF:	polyvinylidene fluoride
TCE:	trichloroethylene
TCP:	2,4,6-trichlorophenol
TGA	thermo-gravimetric analysis
TMPTA	1,1,1-trimethylolpropane triacrylate
UV/vis	Ultraviolet-Visible Spectrophotometry

Appendix B: MATLAB Programs

1) MATLAB program to determine citric acid species distribution

```
clear

K1 = 10^16;
K2 = 10^6.1;
K3 = 10^10.5;
K4 = 10^13.5;

Lt = 2e-4;
a = 1.5;

for i = 1:61
    pH = a + (i-1)*0.1;
    H = 10^(-pH);
    x(i,1) = pH;
    y(i) = Lt/(1 + K1*H + K1*K2*H^2 + K1*K3*H^3 + K1*K4*H^4);
    L(i) = y(i)
     HL(i,1) = K1*H*y(i);
    H2L(i,1) = K1*K2*H^2*y(i);
    H3L(i,1) = K1*K3*H^3*y(i);
    H4L(i,1) = K1*K4*H^4*y(i);
end

semilogy(x,L,'*',x,HL,'-',x,H2L,'^',x,H3L,'--',x,H4L,'o')
set(gcf,'Color',[1 1 1])
xlabel('pH','FontSize',18,'FontWeight','bold')
ylabel('[species], M','FontSize',18,'FontWeight','bold')
axis([1.5 7.5 1e-30 1])
```

2) MATLAB program to determine the iron species distribution

```
K1=10^(-9.5);
K2=10^(-20.5);
```

```
K3=10^(-3.05);
K4=10^(-6.31);
K5= 8e-4;
Khl=10^16;
Kh2l=10^22.1;
Kh3l=10^26.5;
Kh4l=10^29.5;
Kml=10^15.5;
Kmhl=10^19.1;
Kmh2l=10^24.2;
Knl=10^25;          %       Fe^3+ + L            --->Fe(III)L
Knhl=10^27.8;
Knh2l=10^28.4;
pH = 7;
H = 10^(-pH);
KKhl = 1+Khl*H+Kh2l*H^2+Kh3l*H^3+Kh4l*H^4;
KKml = Kml+Kmhl*H+Kmh2l*H^2;
KKnl = Knl+Knhl*H+Knh2l*H^2;
KKm  = 1+K1/H+K2/H^2;
KKn  = 1+K3/H+K4/H^2;

tt = 2e-4;
Q = [tt KKhl KKml KKnl KKm KKn K5 H];

a = 0;
for i = 1:1000
    MT = a + (i-1)*2e-7;
    NT = tt - MT;
    [M,N] = myfun1(MT,Q);
    xx(i) = MT;
    y1(i) = KKm*M;
    y2(i) = KKn*N + K5*N^2/H^2;
end

semilogy(xx,y1,'-',xx,y2,'--','lineWidth',4);
set(gcf,'Color',[1 1 1])
xlabel('Fe(II)_t_o_t_a_l, M','FontSize',18,'FontWeight','bold')
ylabel('species Distribution','FontSize',18,'FontWeight','bold')
```

The program-myfun1 used by the main program above:

```
function [m,n,l] = myfun1(x,q)

TT = q(1);
KKhl = q(2);
KKml = q(3);
KKnl = q(4);
KKm  = q(5);
KKn  = q(6);
```

```
K5 = q(7);
H = q(8);
MT = x;
NT = TT - MT;
LMT = MT;
LNT = NT;
M = 1/2/KKm/KKml*(MT*KKml-KKm*KKhl-
KKml*LMT+(MT^2*KKml^2+2*KKm*KKml*MT*KKhl-
2*MT*KKml^2*LMT+KKm^2*KKhl^2+2*KKm*KKhl*KKml*LMT+KKml^2*LMT^2)^(1/2));
LM= LMT/(KKhl+KKml*M);
N = 1/2/KKn/KKnl*(NT*KKnl-KKn*KKhl-
KKnl*LNT+(NT^2*KKnl^2+2*KKn*KKnl*NT*KKhl-
2*NT*KKnl^2*LNT+KKn^2*KKhl^2+2*KKn*KKhl*KKnl*LNT+KKnl^2*LNT^2)^(1/2));
LN = LNT/(KKhl+KKnl*N);
N1 = 1/2/K5*(-H*KKn-
H*KKnl*LN+(H^2*KKn^2+2*H^2*KKn*KKnl*LN+H^2*KKnl^2*LN^2+4*K5*NT)^(1/2))*
H;
a = abs(N1-N);
if a > 1e-20;
    N = N1;
    LN = LNT/(KKhl+KKnl*N);
    N1 = 1/2/K5*(-H*KKn-
H*KKnl*LN+(H^2*KKn^2+2*H^2*KKn*KKnl*LN+H^2*KKnl^2*LN^2+4*K5*NT)^(1/2))*
H;
    a = abs(N1-N);
    N = N1;
end
LN = LNT/(KKhl+KKnl*N);
b = abs(LM-LN);

while b > 1e-20
    L = TT/(KKhl+KKml*M+KKnl*N);
    M = MT/(KKm+KKml*L);
    N = NT/(KKn+KKnl*L);
    LL = TT/(KKhl+KKml*M+KKnl*N);
    b = abs(LL-L);
    L = LL;
end
m = M;
n = N;
l = LL;
```

3) MATLAB program to determine H_2O_2 decomposition for the standard and citrate modified Fenton reaction

```
clear
```

```
k1=63;         %       Fe(II) +H2O2 --->Fe(III) +OH* +OH^-
k2=2e-3;       %       Fe(III) +H2O2         --->Fe(II) +HO2* +H^+;
k3=3.2e+8;     %       OH* +Fe(II)           --->Fe(III) +OH^-;
k4=1.2e+6;     %       HO2* +Fe(II) +H^+     ---> Fe(III) +H2O2;
k5=2e+3;       %       HO2* +Fe(III)         --->FE(II) +O2 +H^+;
k6=3.3e+7;     %       OH* +H2O2             --->HO2* +H2O;
k7=3.1;        %       HO2* +H2O2            --->H2O +OH* +O2;
k8=8.3e+5;     %       HO2* +HO2*            --->H2O2 +O2;
k9=5.2e+9;     %       OH* +OH*              --->H2O2;
k10=1.58e+5;   %       HO2*                  --->H^+ +O2*^-;
k11=1e+10;     %       O2*^- + H^+           --->HO2*;
k12=5e+7;      %       O2*^- + Fe(III)       --->Fe(II) +O2;
k13=1e+7;      %       O2*^- + Fe(II) +2H^+  --->Fe(III) +H2O2;
k14=9.7e+7;    %       HO2* +O2*+H2O         --->H2O2 +O2 +OH^- ;
k15=7.1e+9;    %       OH* +HO2*             --->H2O +O2;
k16=1.01e+10; %        OH* +O2*              --->OH- +O2;

K1=10^(-9.5);
K2=10^(-20.5);
K3=10^(-3.05);
K4=10^(-6.31);
K5=10^(-2.95);

Khl=10^16;
Kh2l=10^22.1;
Kh3l=10^26.5;
Kh4l=10^29.5;
Kml=10^15.5;
Kmhl=10^19.1;
Kmh2l=10^24.2;
Knl=10^25;
Knhl=10^27.8;
Knh2l=10^28.4;
pH = 7;
H = 10^(-pH);
KKhl = 1+Khl*H+Kh2l*H^2+Kh3l*H^3+Kh4l*H^4;
KKml = Kml+Kmhl*H+Kmh2l*H^2;
KKnl = Knl+Knhl*H+Knh2l*H^2;
KKm  = 1+K1/H+K2/H^2;
KKn  = 1+K3/H+K4/H^2;

tt = 2e-4;
MT = 2e-4;
NT = 0;
Q = [tt KKhl KKml KKnl KKm KKn K5 H];
[M,N] = myfun1(MT,Q);
L = tt/(KKhl+KKml*M+KKnl*N);
a = KKm*M;
b = 5e-4;
c = 0;
d = 0;
e = 0;
f = 0;

q = [k1 k2 k3 k4 k5 k6 k7 k8 k9 k10 k11 k12 k13 k14 k15 k16 H];
```

```
options = odeset('RelTol',1e-9,'AbsTol',1e-55);
[T,Y] = ode15s(@rigid0,[0 0.001],[a b c d e f],options,q);
TT = T;
x1 = Y(:,1);
x2 = Y(:,2);
x3 = Y(:,3);
x4 = Y(:,4);
x5 = Y(:,5);
x6 = Y(:,6);
n = length(x1);
aa = a - x1(n);
b = x2(n);
c = x3(n);
e = x5(n);
f = x6(n);
bb = x4(n)-d;
ee = aa - bb
for  i = 1:2199
     t1 = linspace(0.0011,1200,1200);
     t2 = linspace(1200.1,86400,1000);
     t = [t1 t2];
     tspan = [t(i) t(i+1)];
     mt(i,1) = MT;
     nt(i,1) = NT;
     MT = mt(i) - aa;
     NT = nt(i) + bb;
     if MT > 0
         [m,n] = myfun1(MT,Q);
         M(i+1,1) = m;
         N(i+1,1) = n;
         L(i+1,1) = tt/(KKhl+KKml*m+KKnl*n);
         a = KKm*m;
         ML(i+1,1) = KKml*m*L(i+1,1);
         FeII(i,1) = a;
         d = KKn*n;
         NL(i+1,1) = KKnl*n*L(i+1,1);
         FeIII(i,1) = d;
         [T,Y] = ode15s(@rigid0,tspan,[a b c d e f],options,q);
         TT = [TT;T];
         x1 = [x1;Y(:,1)];
         x2 = [x2;Y(:,2)];
         x3 = [x3;Y(:,3)];
         x4 = [x4;Y(:,4)];
         x5 = [x5;Y(:,5)];
         x6 = [x6;Y(:,6)];
         l = length(T);
         o(i) = l;
         b = Y(l,2);
         c = Y(l,3);
         e = Y(l,5);
         f = Y(l,6);
         aa = a - Y(l,1);
         bb = Y(l,4)-d;
         ee(i+1) = aa - bb
     end
end
```

```
pH = 2.5;
H = 10^(-pH);
q = [k1 k2 k3 k4 k5 k6 k7 k8 k9 k10 k11 k12 k13 k14 k15 k16 H];
[T1 Y1] = ode15s(@rigid0,[0 86400],[2e-4 5e-4 0 0 0 0],options,q);
plot(TT/60,x2/5e-4,'-',T1/60,Y1(:,2)/5e-4,'--')
set(gcf,'Color',[1 1 1])
xlabel('Time, mins')
ylabel('[H_2O_2]/[H_2O_2]_0')
axis([-Inf Inf 1e-14 1e-8])
```

The program-myfun1 used by the main program above:

```
function [m,n,l] = myfun1(x,q)

TT = q(1);
KKhl = q(2);
KKml = q(3);
KKnl = q(4);
KKm  = q(5);
KKn  = q(6);
K5 = q(7);
H = q(8);
MT = x;
NT = TT - MT;
LMT = MT;
LNT = NT;
M = 1/2/KKm/KKml*(MT*KKml-KKm*KKhl-
KKml*LMT+(MT^2*KKml^2+2*KKm*KKml*MT*KKhl-
2*MT*KKml^2*LMT+KKm^2*KKhl^2+2*KKm*KKhl*KKml*LMT+KKml^2*LMT^2)^(1/2));
LM= LMT/(KKhl+KKml*M);
N = 1/2/KKn/KKnl*(NT*KKnl-KKn*KKhl-
KKnl*LNT+(NT^2*KKnl^2+2*KKn*KKnl*NT*KKhl-
2*NT*KKnl^2*LNT+KKn^2*KKhl^2+2*KKn*KKhl*KKnl*LNT+KKnl^2*LNT^2)^(1/2));
LN = LNT/(KKhl+KKnl*N);
N1 = 1/2/K5*(-H*KKn-
H*KKnl*LN+(H^2*KKn^2+2*H^2*KKn*KKnl*LN+H^2*KKnl^2*LN^2+4*K5*NT)^(1/2))*
H;
a = abs(N1-N);
if a > 1e-20;
    N = N1;
    LN = LNT/(KKhl+KKnl*N);
    N1 = 1/2/K5*(-H*KKn-
H*KKnl*LN+(H^2*KKn^2+2*H^2*KKn*KKnl*LN+H^2*KKnl^2*LN^2+4*K5*NT)^(1/2))*
H;
    a = abs(N1-N);
    N = N1;
end
```

```
LN = LNT/(KKhl+KKnl*N);
b = abs(LM-LN);

while b > 1e-20
    L = TT/(KKhl+KKml*M+KKnl*N);
    M = MT/(KKm+KKml*L);
    N = NT/(KKn+KKnl*L);
    LL = TT/(KKhl+KKml*M+KKnl*N);
    b = abs(LL-L);
    L = LL;
end
m = M;
n = N;
l = LL;
```

The program-rigid0 used by the main program above:

```
function dy = rigid0(t,y,q)


dy = zeros(6,1);    % a column vector

k1=q(1);
k2=q(2);
k3=q(3);
k4=q(4);
k5=q(5);
k6=q(6);
k7=q(7);
k8=q(8);
k9=q(9);
k10=q(10);
k11=q(11);
k12=q(12);
k13=q(13);
k14=q(14);
k15=q(15);
k16=q(16);
H=q(17);

%y(1)=Fe(2+), y(2)=H2O2, y(3)=OH*, y(4)=Fe(3+), y(5)=HO2*, y(6)=O2*;

dy(1) = -k1*y(1)*y(2)+k2*y(4)*y(2)-k3*y(3)*y(1)-
k4*y(5)*y(1)+k5*y(5)*y(4)+k12*y(6)*y(4)-k13*y(6)*y(1);
dy(2) = -k1*y(1)*y(2)-k2*y(4)*y(2)-k6*y(3)*y(2)-
k7*y(5)*y(2)+k8*y(5)*y(5)+k9*y(3)*y(3)+k13*y(6)*y(1)+k14*y(5)*y(6);
dy(3) =  k1*y(1)*y(2)-k3*y(3)*y(1)-k6*y(3)*y(2)+k7*y(5)*y(2)-
k9*y(3)*y(3)-k15*y(3)*y(5)-k16*y(3)*y(6);
```

```
dy(4) =  -(-k1*y(1)*y(2)+k2*y(4)*y(2)-k3*y(3)*y(1)-
k4*y(5)*y(1)+k5*y(5)*y(4)+k12*y(6)*y(4)-k13*y(6)*y(1));
dy(5) =  k2*y(4)*y(2)-k4*y(5)*y(1)-k5*y(5)*y(4)+k6*y(3)*y(2)-
k7*y(5)*y(2)-k8*y(5)*y(5)-k10*y(5)+k11*H*y(6)-k14*y(5)*y(6)-
k15*y(3)*y(5);
dy(6) =  k10*y(5)-k11*H*y(6)-k12*y(6)*y(4)-k13*y(6)*y(1)-k14*y(5)*y(6)-

k16*y(3)*y(6);
```

Vita

The author, Mr. YongChao Li, was born in Wuhan, Hubei province, China, in January, 1970. He graduated from Zhejiang University with a Bachelor of Science degree in chemical engineering in 1991. He joined the Ph.D. program in Chemical and Materials Engineering at the University of Kentucky, Lexington in Spring 2002.

Refereed journal articles and proceedings

- **Li, Y. C.**; Bachas, L. G.; Bhattacharyya, D. "Chelate-based modified Fenton reaction for destruction of chlorinated organic compounds near neutral pH environment", Annual SBRP Meeting conducted by the NIEHS, Hanover, NH, November 9-12, 2003.
- **Li, Y. C.**; Bachas, L. G.; Bhattacharyya, D. "Oxidation of trichlorophenol by chelate modified Fenton reaction", Annual Meeting of the American Institute of Chemical Engineers (AIChE), Austin, TX, November 7-12, 2004.
- **Li, Y. C.**; Bachas, L. G.; Bhattacharyya, D. Kinetics studies of trichlorophenol destruction by chelate-based Fenton reaction. Environ. Eng. Sci. 2005, 22, 756–771.
- **Li, Y. C.;** Bachas, L. G.; Bhattacharyya, D. Chlorinated organic compounds destruction by modified Fenton reaction involving iron-chelate" Annual SBRP Meeting conducted by the NIEHS, New York, January 11-13, 2006.

- **Li, Y. C.**; Bachas, L. G.; Bhattacharyya, D. Selected chloro-organic detoxifications by poly-chelate (poly-acrylic acid) and citrate-based Fenton reaction at neutral pH environment. Ind. Eng. Chem. Res. ASAP, October, 2007.